

Enclosure C  
L-14-241

Generic Letter 95-05 Tube Intersection Burst Test, Leakage Test, and Morphology  
Conclusions  
(87 Pages Follow)

# **Interim Report: Examination of Steam Generator Tubes Removed from Beaver Valley Unit 2**

Prepared for the  
FirstEnergy Nuclear Operating Company

### LEGAL NOTICE

This report was prepared as an account of work performed by Westinghouse Electric Company LLC. Neither Westinghouse Electric Company LLC, nor any person acting on its behalf:

- A. Makes any warranty or representation, express or implied including the warranties of fitness for a particular purpose or merchantability, with respect to the accuracy, completeness, or usefulness of the information contained in this report, or that the use of any information, apparatus, method, or process disclosed in this report may not infringe privately owned rights; or
- B. Assumes any liabilities with respect to the use of, or for damages resulting from the use of, any information, apparatus, method, or process disclosed in this report.

**SG-CCOE-14-1**  
**Revision 0**

Prepared for the FirstEnergy Nuclear Operating Company

**Interim Report: Examination of  
Steam Generator Tubes  
Removed from Beaver Valley Unit 2**

Author's Name Thomas P. Magee	Signature / Date <u>TPM (*)</u>	For Pages All
Verifier's Name Jonna M. Partezana	Signature / Date <u>JMP (*)</u>	For Pages All
Manager Name Lauren A. Tosatto	Signature / Date <u>LAT (*)</u>	For Pages All

*\* Electronically Approved Records Are Authenticated in the Electronic Document Management System*

Westinghouse Electric Company LLC  
1000 Westinghouse Drive  
Cranberry Township, PA 16066

© 2014 Westinghouse Electric Company LLC  
All Rights Reserved



## RECORD OF REVISIONS

Revision	Date	Revision Description
0	July 2014	Original issue

## TABLE OF CONTENTS

Record of Revisions .....	iv
Table of Contents .....	v
List of Tables .....	vi
List of Figures .....	vii
1.0 Introduction .....	1-1
1.1 Background .....	1-1
1.2 Steam Generator Description .....	1-2
1.3 Description of the Beaver Valley Unit 2 Tubes Pulled for Examination .....	1-2
2.0 Sectioning for Leak and Burst Testing .....	2-1
3.0 Leak Screening .....	3-1
3.1 Purpose .....	3-1
3.2 Sample Preparation .....	3-1
3.3 Procedure .....	3-1
3.4 Results .....	3-2
4.0 Burst Test .....	4-1
4.1 Purpose .....	4-1
4.2 Sample Preparation .....	4-1
4.3 Burst Test Procedure .....	4-1
4.4 Burst Test Results .....	4-2
4.5 Post-Burst Observations .....	4-2
5.0 Post-Burst Sectioning .....	5-1
6.0 SEM Fractography .....	6-1
6.1 Sample Preparation .....	6-1
6.2 Procedure .....	6-1
6.3 Fractography Depth Profiles .....	6-1
6.4 Crack Surface Characterization .....	6-2
7.0 Metallography of Cracks .....	7-1
7.1 Procedure .....	7-1
7.2 R19C38 02H .....	7-1
7.3 R24C41 02H .....	7-1
7.4 R24C41 03H .....	7-2
7.5 R24C41 04H .....	7-2
8.0 Conclusions .....	8-1
9.0 References .....	9-1

---

## LIST OF TABLES

Table 1-1:	Support Plate Elevations .....	1-4
Table 1-2:	As-Received Lengths .....	1-5
Table 2-1:	Leak and Burst Test Samples.....	2-1
Table 3-1:	Leak Screening Results.....	3-3
Table 4-1:	Measurements Before Leak / Burst Testing.....	4-4
Table 4-2:	Burst Results and Post-Burst Measurements .....	4-5
Table 6-1:	Summary of Burst Opening Depth Profiles .....	6-3
Table 7-1:	Defect Metallography Samples.....	7-4

## LIST OF FIGURES

Figure 1-1:	Orientation System Used in the Examination.....	1-6
Figure 2-1:	R19C38 Segment 3 Sectioning Diagram .....	2-2
Figure 2-2:	R19C38 Segment 4 Sectioning Diagram .....	2-3
Figure 2-3:	R24C41 Segment 3 Sectioning Diagram .....	2-4
Figure 2-4:	R24C41 Segment 5 Sectioning Diagram .....	2-5
Figure 2-5:	R24C41 Segment 6 Sectioning Diagram .....	2-6
Figure 2-6:	R24C41 Segment 7 Sectioning Diagram .....	2-7
Figure 4-1:	Burst Test Support Simulation.....	4-6
Figure 4-2:	Burst Pressurization of R19C38-3B (02H).....	4-7
Figure 4-3:	Burst Pressurization of R19C38-4B (Freespan) .....	4-8
Figure 4-4:	Burst Pressurization of R24C41-3B (02H).....	4-9
Figure 4-5:	Burst Pressurization of R24C41-5B (03H).....	4-10
Figure 4-6:	Burst Pressurization of R24C41-6B (04H).....	4-11
Figure 4-7:	Burst Pressurization of R24C41-7B (Freespan) .....	4-12
Figure 4-8:	Burst Opening at R19C38-3B (02H) .....	4-13
Figure 4-9:	Burst Opening at R19C38-4B (Freespan).....	4-14
Figure 4-10:	Burst Opening at R24C41-3B (Burst in Freespan, Outside of 02H) .....	4-15
Figure 4-11:	Burst Opening at R24C41-5B (Burst in Freespan, Outside of 03H) .....	4-16
Figure 4-12:	Burst Opening at R24C41-6B (04H) .....	4-17
Figure 4-13:	Burst Opening at R24C41-7B (Freespan).....	4-18
Figure 4-14:	Post-Burst Observations on R19C38-3B (02H Region).....	4-19
Figure 4-15:	Short Cracks Near the Bottom of the 02H TSP of R19C38 (0° Orientation)....	4-20
Figure 4-16:	Short Cracks Near the Top of the 02H TSP of R19C38 (0° Orientation) .....	4-20
Figure 4-17:	Short Cracks Near the Bottom of the 02H TSP of R19C38 (200° Orientation).....	4-21
Figure 4-18:	Post-Burst Observations on R24C41-3B (02H Region).....	4-22
Figure 4-19:	Shallow Corrosion Partially Obscured by Surface Deposits, Near the 0° Orientation of R24C41 02H.....	4-23
Figure 4-20:	Post-Burst Observations on R24C41-5B (03H Region) .....	4-24
Figure 4-21:	Shallow Axial Cracks (Marked with Arrows) Near Center of R24C41 03H TSP Region (180° Orientation).....	4-25
Figure 4-22:	Shallow Non-axial Cracks at Top of R24C41 03H TSP Region (0° Orientation).....	4-25
Figure 4-23:	Post-Burst Observations on R24C41-6B (04H Region) .....	4-26
Figure 4-24:	Larger Axial Cracks Near the Centerline of R24C41 04H TSP Region, Between 335°-360° .....	4-27
Figure 4-25:	Larger Axial Cracks Near the Centerline of R24C41 04H TSP Region, Between 315°-340° .....	4-27
Figure 4-26:	Example of Shallow Cracks Located Adjacent to the Burst Opening Of R24C41-6B (04H) at the 90° Orientation .....	4-28
Figure 5-1:	Post-Burst Sectioning of R19C38-3B.....	5-2
Figure 5-2:	Post-Burst Sectioning of R19C38-4B.....	5-3
Figure 5-3:	Post-Burst Sectioning of R24C41-3B.....	5-4
Figure 5-4:	Post-Burst Sectioning of R24C41-5B.....	5-5

Figure 5-5:	Post-Burst Sectioning of R24C41-6B .....	5-6
Figure 5-6:	Post-Burst Sectioning of R24C41-7B .....	5-7
Figure 6-1:	SEM Photomontage of R19C38-3B (02H) Burst Opening.....	6-4
Figure 6-2:	SEM Photomontage of R24C41-6B (04H) Burst Opening.....	6-5
Figure 6-3:	R19C38-3B (02H) Burst Opening Depth Profile.....	6-6
Figure 6-4:	R24C41-6B (04H) Burst Opening Depth Profile.....	6-7
Figure 6-5:	Example of R19C38-3B Burst Opening Fracture Surface (Near Top End of Crack) .....	6-8
Figure 6-6:	Example of R19C38-3B Burst Opening Fracture Surface (Center of Crack).....	6-9
Figure 6-7:	OD Surface of R19C38 02H, Adjacent to Burst Opening (Axial Direction is Horizontal) .....	6-10
Figure 6-8:	Example of R24C41-6B Burst Opening Fracture Surface.....	6-11
Figure 6-9:	OD Surface of R24C41 04H, Adjacent to Burst Opening (Axial Direction is Horizontal) .....	6-12
Figure 7-1:	R19C38 02H - Overall View of Transverse Section .....	7-5
Figure 7-2:	R19C38 02H Cracks at 200° .....	7-6
Figure 7-3:	R19C38 02H Crack at 340° .....	7-6
Figure 7-4:	R24C41 02H - Overall View of Transverse Section .....	7-7
Figure 7-5:	R24C41 02H Cracks at 20° .....	7-8
Figure 7-6:	R24C41 02H Cracks at 160° .....	7-8
Figure 7-7:	R24C41 02H Cracks at 340° .....	7-9
Figure 7-8:	R24C41 03H - Overall View of Transverse Section .....	7-10
Figure 7-9:	R24C41 03H Cracks at 180° .....	7-10
Figure 7-10:	R24C41 04H - Overall View of Transverse Section .....	7-11
Figure 7-11:	R24C41 04H Cracks at 80° .....	7-12
Figure 7-12:	R24C41 04H Cracks at 40° .....	7-12
Figure 7-13:	R24C41 04H Cracks at 350° .....	7-13
Figure 7-14:	R24C41 04H Cracks at 335° .....	7-13
Figure 7-15:	R24C41 04H Cracks at 315° .....	7-14
Figure 7-16:	R24C41 04H Cracks at 350°, 20 mils Further Down the TSP from Figure 7-13 .....	7-14

## 1.0 INTRODUCTION

### 1.1 Background

The U.S. Nuclear Regulatory Commission (NRC) issued Generic Letter 95-05 (GL 95-05) (Reference 1) to give guidance to licensees who may wish to request a license amendment to the plant's technical specifications in order to implement alternate steam generator tube repair criteria (ARC) that is applicable specifically to outside diameter stress corrosion cracking (ODSCC) at the tube-to-tube support plate intersections in Westinghouse-designed steam generators (SGs) containing drilled-hole tube support plates (TSPs) and alloy 600 steam generator tubing.

For outages prior to EOC-16, the alternate repair criterion per GL 95-05 had been approved for Beaver Valley Power Station Unit 2 (BVPS2), but was not implemented. FirstEnergy Nuclear Operating Company (FENOC) had not implemented the criterion due to the low number of bobbin indications at TSP intersections that were confirmed by +Point™<sup>1</sup> to contain axial outside diameter stress corrosion cracking (ODSCC). The 2R16 initial inspection plan did not include application of GL 95-05; however, the criterion was implemented at 2R16 due to an increase in the number of Distorted Support Indications (DSIs) that were confirmed to contain axial ODSCC.

The 2R17 outage (Spring 2014) represents the second application of the GL 95-05 voltage-based repair criteria, and implementation of its requirements, to the Beaver Valley Unit 2 SGs. The analysis of the 2R17 outage data is reported in Reference 2.

Implementation of the GL 95-05 ARC includes a program of tube removal for testing and examination. The purpose of this program is to:

- (1) confirm axial ODSCC as the dominant degradation mechanism,
- (2) monitor the degradation mechanism over time,
- (3) provide additional data to enhance the burst pressure, probability of leakage, and conditional leak rate correlations described in GL 95-05, and
- (4) assess inspection capability.

During the 2R17 outage, FENOC removed two tubes for laboratory examination, each containing a TSP location with confirmed axial ODSCC. These tubes were sent to the Westinghouse Churchill Site (WCS) to complete the laboratory examination.

Reporting requirements for the laboratory examination in GL 95-05 are as follows:

*The results of metallurgical examinations performed for tube intersections removed from the SG. If it is not practical to provide all the results within 90 days, as a minimum, the burst test, leakage test and morphology conclusions should be provided within 90 days. The remaining information should be submitted when it becomes available.*

---

<sup>1</sup> +Point™ is a trademark of Zetec, Inc.

The purpose of this interim report is to provide the burst test, leakage test and morphology results and conclusions to satisfy the 90-day GL 95-05 reporting requirement.

## **1.2 Steam Generator Description**

Beaver Valley Unit 2, operated by FENOC, is a three loop Westinghouse designed pressurized water reactor located in Shippingport, PA. The plant commenced commercial operation in August 1987.

The Westinghouse Model 51M steam generators contain 3376 heat transfer tubes per steam generator. The tubes are mill-annealed NiCrFe Alloy 600 (hereafter Alloy 600) with a nominal 0.875 inch OD and 0.050 inch wall thickness. The tubes are mounted in 21.25 inches thick low alloy steel tubesheets. The tubes are supported by seven 0.75-inch thick carbon steel tube support plates (TSP). Most tubes also pass through one 0.75-inch thick carbon steel flow distribution baffle (FDB), which is referred to as TSP#1.

Table 1-1 provides a summary of the TSP elevations (Reference 3).

## **1.3 Description of the Beaver Valley Unit 2 Tubes Pulled for Examination**

Two tubes were selected by FENOC for removal and laboratory examination, based on the 2R17 outage eddy current examination results and GL 95-05 requirements. Both tube selections were in the "C" steam generator (SG-C).

The tube at Row 19, Column 38 (R19C38) had a 0.62 volt bobbin coil Distorted Support Indication (DSI) at hot leg TSP#2 (02H) location. This indication was confirmed by +Point.

The tube at Row 24, Column 41 (R24C41) had a 0.47 volt bobbin coil DSI at its 04H location that was confirmed by +Point. It also had a 1.19 volt DSI at its 02H location that was not confirmed by +Point.

Segments from the two tubes were pulled from the hot leg primary side of the tubesheet of SG-C. Tube R19C38 was cut below 03H, pulled through the tubesheet and cut into four segments. Tube R24C41 was cut below 05H, pulled through the tubesheet and cut into seven segments.

Table 1-2 provides a summary of the segments that were delivered to the WCS laboratories. Reference 4 acknowledges the receipt of the segments. Each segment was provided in its own individual plastic tube, labelled so as to indicate the row, column and section (segment) number. The orientation within the steam generator was also marked.

As each segment was pulled through the tubesheet, it was cut at about a 45° angle so as to aid in tracing the azimuthal orientation from segment-to-segment. A small notch was made at the bottom of most segments to indicate which end of each segment was the bottom and to indicate an azimuthal orientation reference. For the segments from R19C38, the notch is on the side of the tube that was closest to the periphery. For the segments from R24C41, the notch is on the side of the tube that was closest to the manway.

For the laboratory examination, the orientation system was based on this bottom end notch. Segments that did not have a notch were given an identifying mark on the bottom end of the segment, at the same azimuthal orientation as on an adjacent segment. The notch was used as the 0° azimuthal reference point; all other azimuthal orientations progressed in the clockwise direction while viewing the tube from the bottom end. See Figure 1-1 for a sketch of the orientation system used in the laboratory. This orientation system was transferred to sections that were cut from these segments by making a similar mark, where possible.

In comparison with tubes pulled from other plants, the condition of all of the Beaver Valley Unit 2 pulled tube segments from SG-C was good. There were relatively few fresh outer surface scratches/scrapes on the outer surfaces. No significant bends or diameter reductions were detected from the pulling operation.



Table 1-1: Support Plate Elevations

Location	Distance Above Tube Mouth (inches)
Tubesheet Primary Side / Cladding Surface	0
Tube End (recessed for tube-to-tubesheet weld)	0.04
Cladding-to-Tubesheet Interface (nominal, cladding thickness $\geq 0.15$ inch)	0.25
Top-of-Tubesheet (tubesheet thickness = 21.34 / 21.22 inches)	21.47
Center of TSP #1 (FDB)	41.55
Center of TSP #2	71.6
Center of TSP #3	122.1
Center of TSP #4	172.6
Center of TSP #5	223.1
Center of TSP #6	273.6
Center of TSP #7	324.1
Center of TSP #8	374.6

Table 1-2: As-Received Lengths

Tube	Segment	Region	Length (in)
R19C38	1	Tubesheet and Top of Tubesheet	25.9
	2	FDB (01H)	31.8
	3	TSP (02H)	25.7
	4	All Freespan	32.4
R24C41	1	Tubesheet and Top of Tubesheet	24.5
	2	FDB (01H)	31.2
	3	TSP (02H)	27.7
	4	All Freespan	33.9
	5	TSP (03H)	32.9
	6	TSP (04H)	32.7
	7	All Freespan	35.6

top elevation for this segment=>

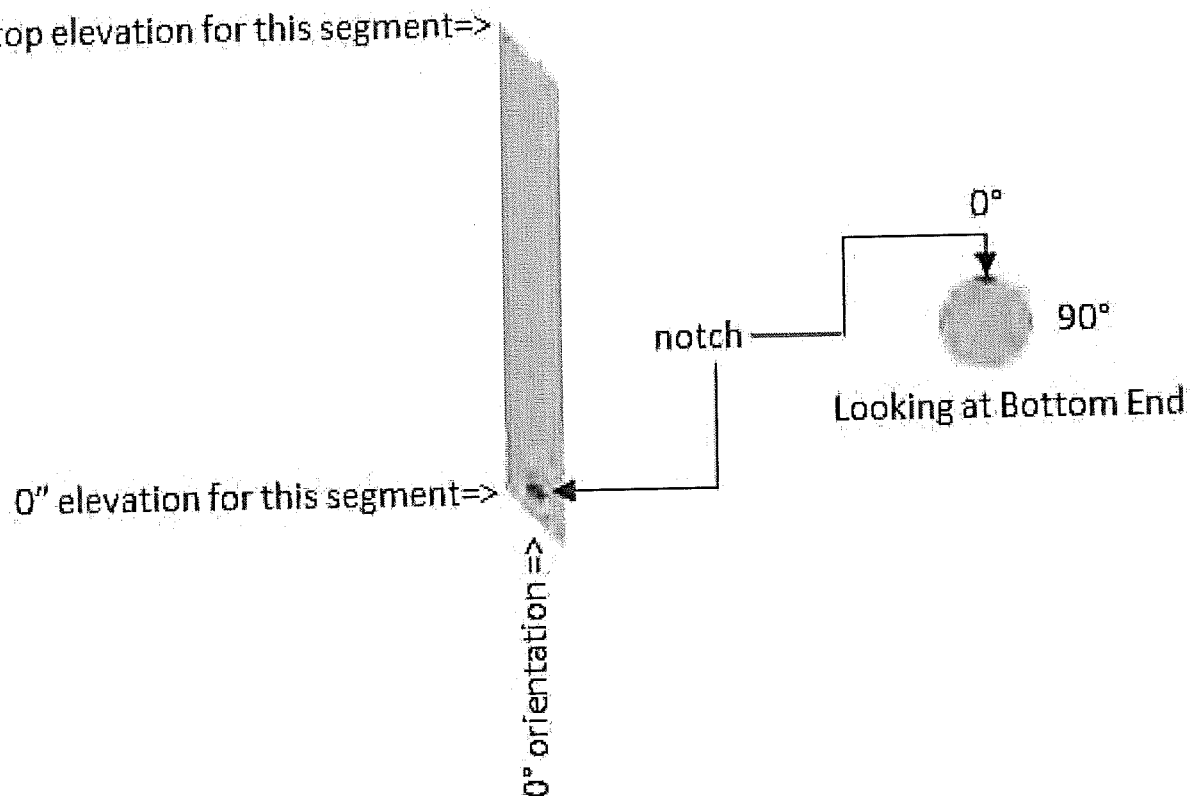


Figure 1-1: Orientation System Used in the Examination

## 2.0 SECTIONING FOR LEAK AND BURST TESTING

A total of six samples were cut from the tube segments for leak and burst testing. Samples having a TSP region were cut, as best as possible, to center the TSP region along its length. The samples are summarized in Table 2-1 below, and the corresponding sectioning diagrams are provided in Figure 2-1 through Figure 2-6. The locations of TSP regions are shown as a darker color on applicable diagrams. The orientation notch that was applied to the tube segments during the pulling operation is shown as a small oval near the bottom of the segment. This orientation was transferred to other sections as they were cut from the parent tube, and is shown as a white mark.

Sections were stored in individual containers, each labelled with the appropriate row, column and section number. Traceability was maintained in accordance with appropriate WCS work instructions (Reference 5).

The ends of each sample were deburred prior to testing.

Table 2-1: Leak and Burst Test Samples

Tube	Segment	Region	Confirmed ECT Indication	Sectioning Diagram	Section Tested	Leak Screen	Burst Test
R19C38	3	TSP (02H)	x	Figure 2-1	R19C38-3B	x	x
	4	Freespan		Figure 2-2	R19C38-4B		x
R24C41	3	TSP (02H)		Figure 2-3	R24C41-3B		x
	5	TSP (03H)		Figure 2-4	R24C41-5B		x
	6	TSP (04H)	x	Figure 2-5	R24C41-6B	x	x
	7	Freespan		Figure 2-6	R24C41-7B		x

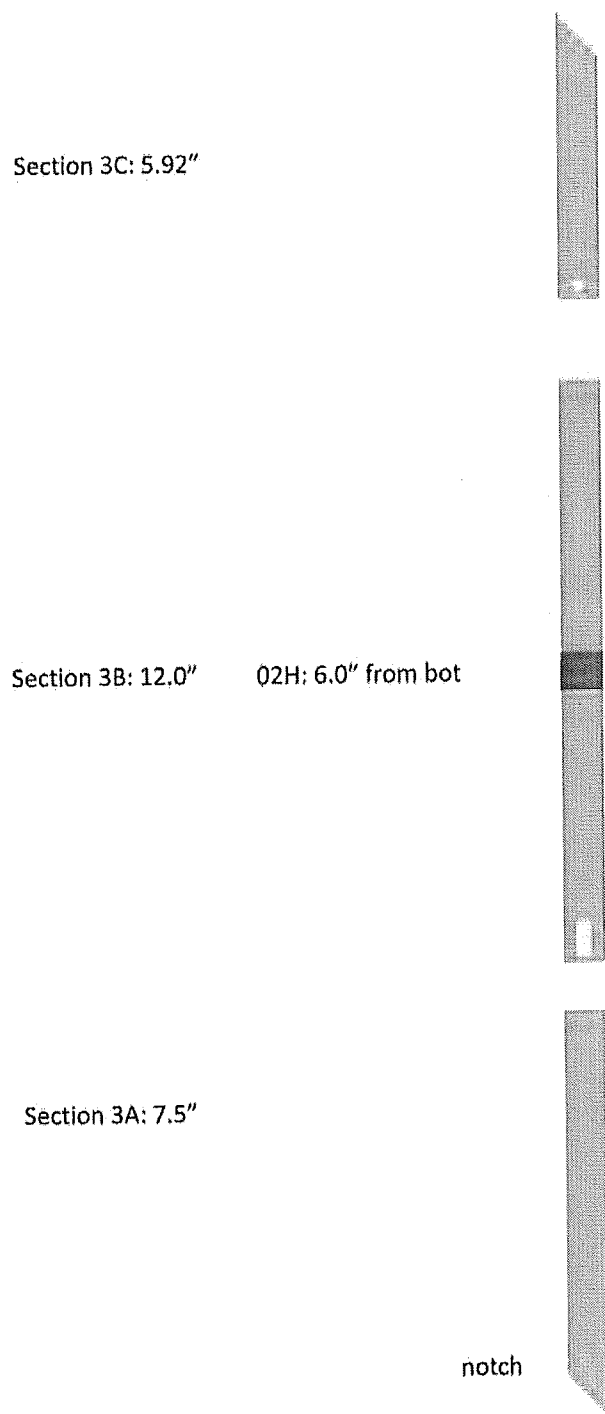


Figure 2-1: R19C38 Segment 3 Sectioning Diagram

R19C38 – 4D: 1"

R19C38 – 4C: 12"

R19C38 – 4B: 12"

R19C38 – 4A: 7.2"



Figure 2-2: R19C38 Segment 4 Sectioning Diagram

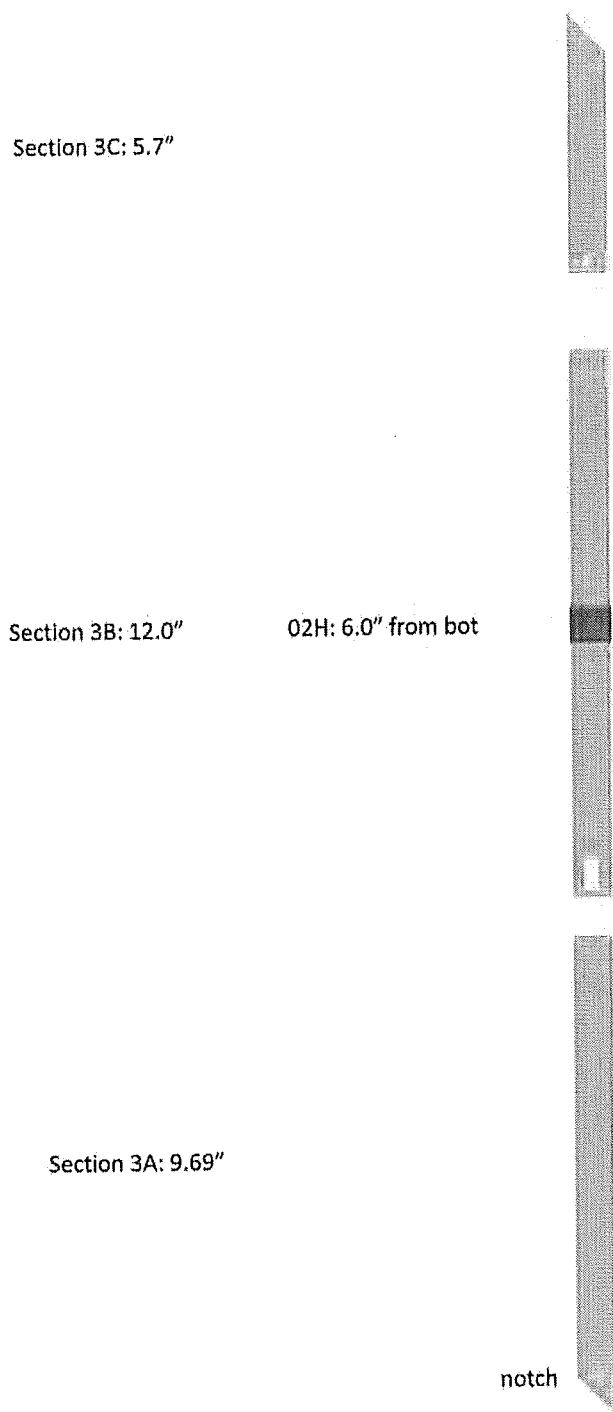


Figure 2-3: R24C41 Segment 3 Sectioning Diagram

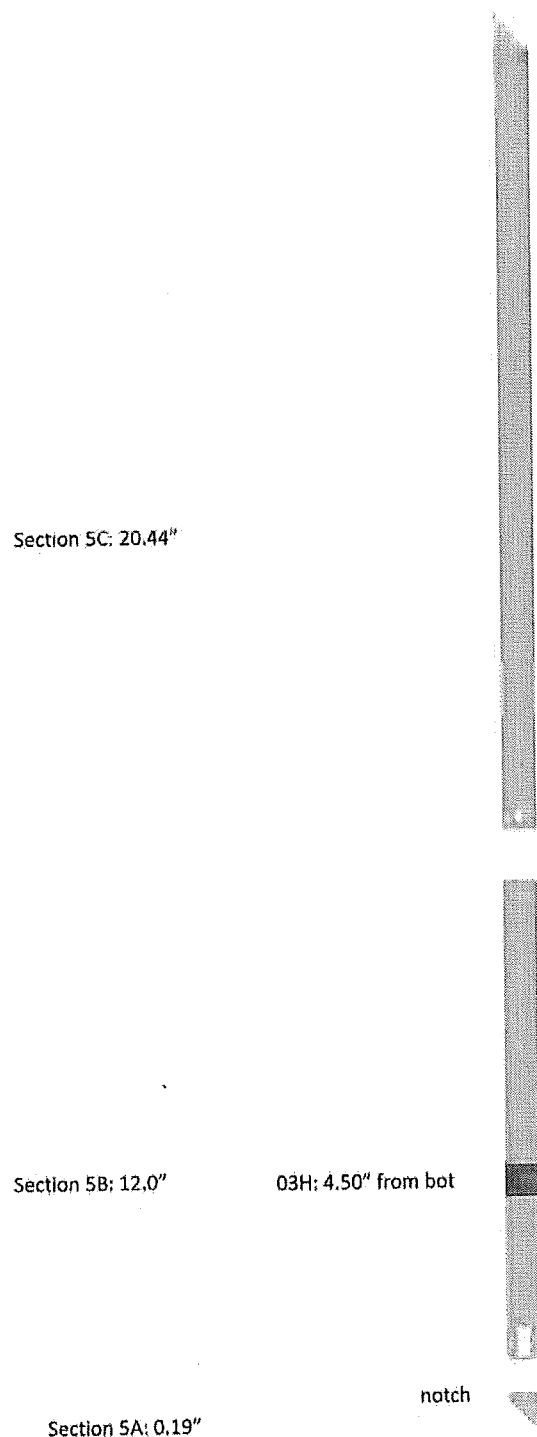


Figure 2-4: R24C41 Segment 5 Sectioning Diagram



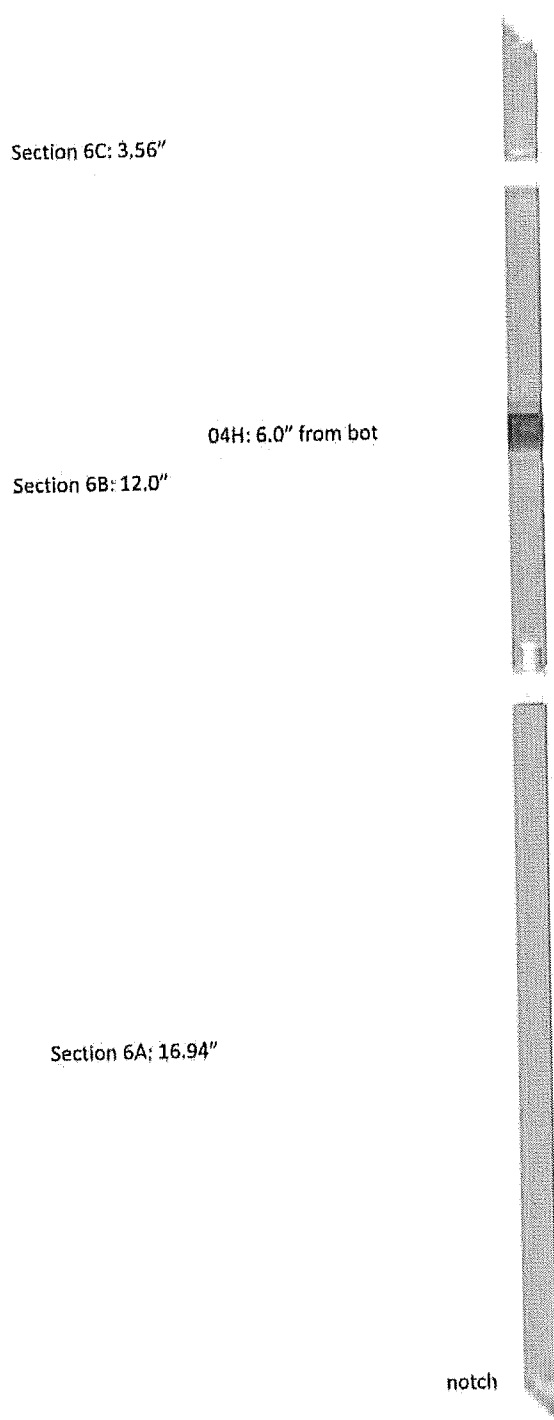


Figure 2-5: R24C41 Segment 6 Sectioning Diagram

R24C41 – 7D: 1"

R24C41 – 7C: 12"

R24C41 – 7B: 12"

R24C41 – 7A: 10.5"



Figure 2-6: R24C41 Segment 7 Sectioning Diagram

### **3.0 LEAK SCREENING**

#### **3.1 Purpose**

To determine if a leak path had developed through the tube wall, each of the two TSP regions with confirmed crack-like eddy current indications were screened for leakage. Leak screening differs from leak rate testing in that there is no measurement of a leak rate. A screening test does not provide a leak rate (other than zero); it provides a result of “leak” or “no leak” condition at each pressure tested. Leak screening, rather than leak rate testing, eliminates the requirements associated with measuring small leak rates. If leakage was identified, leak rate measurements would be conducted.

Each TSP region was pressurized to the pressures identified for in situ testing in the Degradation Assessment (Reference 6) using room temperature water. An assessment was made if the sample was leaking based on visual observations and the loss of internal pressure. The leak screening was performed without internal bladders or fixtures that simulate the constraints of TSP intersections.

#### **3.2 Sample Preparation**

In preparation for leak screening, and subsequent burst testing, the two TSP regions (02H from R19C38-3B and 04H from R24C41-6B) were sectioned into 12 inch long samples, with the TSP region centered as well as possible across the length (see Table 2-1 and Figure 2-1 through Figure 2-6). The ends of the samples were deburred after cutting.

The outer diameters (OD) and wall thicknesses of each sample were measured after cutting. These are presented in Table 4-1.

In addition, a dummy piece was leak screened to check for proper operation of the equipment and for any leakage in the test lines. All equipment was found to be working properly and all sources of leakage from the test lines were sealed. The results of the dummy sample are not included in this report.

Swagelok fittings were then affixed to the tube ends and each tube was pre-filled with deionized water. One end of each sample had a fitting that allowed pressurized room temperature water to pass into the sample from a 1/8 inch diameter supply line.

#### **3.3 Procedure**

Leak screening was conducted in accordance with the appropriate WCS work instructions (Reference 7). These work instructions are in compliance with EPRI Guidelines (Reference 8).

Each sample was connected to pressurization equipment, which included a calibrated pressure transducer used to measure the internal pressure of the tube, a valve to isolate the pressure inside the tube and a data acquisition system for recording the pressure transducer reading vs. time.

Axial flaw leak test pressures included a temperature adjustment factor of 1.10 and 50 psi was added for measurement uncertainty. Target test pressures were rounded up to the nearest increment of 25 psi. Three target test pressures were used: normal operating pressure differential (1700 psig), an intermediate test pressure (2250 psig), and steam line break (SLB) condition (2875 psig).

Each sample was pressurized to the target pressure of 1700 psig, held for five (5.0) minutes, pressurized to the second target pressure of 2250 psig, held for five (5.0) minutes, then pressurized to the final target pressure of 2875 psig. The hold times do not include a one-minute hold to allow the test system to stabilize after the pressure had been increased.

During each hold period, each sample was periodically observed for signs of leakage. Tissue paper was pressed against the sample to aid in this observation. Also, the loss of internal pressure was observed as a second criterion. A loss of 100 psi (maximum) was allowed during the hold period to account for system stabilization.

### **3.4 Results**

Neither sample showed any sign of leakage by either the visual observation or the pressure loss criteria at any pressure. The results are summarized in Table 3-1.

As neither sample with a confirmed eddy current indication leaked during room temperature testing, it was deemed unnecessary to test the samples at an elevated temperature.

Table 3-1: Leak Screening Results

Sample	Region	Target Pressure (psig)	Start Pressure (psig)	End Pressure (psig)	Leakage Observed
R19C38-3B	02H	1700	1799	1789	no
		2250	2253	2243	no
		2875	2905	2892	no
R24C41-6B	04H	1700	1743	1719	no
		2250	2335	2315	no
		2875	3070	3040	no

## **4.0 BURST TEST**

### **4.1 Purpose**

The primary purpose of the burst testing was to determine if the degraded tube sections exceeded the NEI 97-06 requirements on burst strength (Reference 9), implemented by EPRI Tube Integrity Assessment Guidelines (Reference 10). The most limiting requirement is that the tube must sustain three times normal operating pressure differential (3NOP) without burst. 3NOP is approximately 4446 psid for Beaver Valley Unit 2 at temperature, or 4950 psid for room temperature testing (Reference 6).

### **4.2 Sample Preparation**

In preparation for burst testing, all four TSP regions were sectioned into 12 inch long samples, with the TSP region centered as well as possible across the length. In addition, a freespan section from each tube was also selected to establish a baseline, for a total of six burst test samples (see Table 2-1). The ends of the samples were deburred after cutting.

The outer diameters (OD) and wall thicknesses of each sample were measured after cutting. These are presented in Table 4-1.

In addition, a dummy piece was burst tested to check for proper operation of the equipment. All equipment was found to be working properly. The results of the dummy sample are not included in this report.

Swagelok fittings were then affixed to the tube ends and each tube was pre-filled with deionized water. One end of each sample had a fitting that allowed pressurized room temperature water to pass into the sample from a 1/8 inch diameter supply line.

### **4.3 Burst Test Procedure**

Room temperature burst tests were performed in accordance with the Reference 11 procedure and the Reference 8 EPRI Guidelines. The pressurized water for the burst test was supplied by a piston delivery system. Pressure was increased and supplied to the sample with a single, controlled stroke of the piston. A feedback loop was used to establish a relatively constant pressurization rate of 20-500 psi/second. The internal pressure of the specimen was recorded digitally through a data acquisition system and a redundant data acquisition system.

The Reference 8 guidelines and the Reference 11 procedure allow an internal bladder and backing foil to achieve a successful burst test elevated pressure when there is a pre-identified leak path from the tube. Since none of the samples had a leak path and all eddy current signals were relatively small, an internal bladder or foil was judged to be unnecessary and not used.

The TSP regions were laterally restrained by a support system designed to simulate the conditions in the Beaver Valley Unit 2 steam generators under accident conditions. Figure 4-1 shows a sketch of the support system. An unpressurized extension was attached to the top end of

each sample by a welded cap that both sealed the top end and added several feet to its length. The top end of the extension passed through a  $\frac{3}{4}$  inch wide support plate simulation while the attached test sample passed through another  $\frac{3}{4}$  inch wide support plate simulation. The tube-to-support clearance was obtained from the Reference 12 document. The support plate simulations were spaced a fixed 50.5 inches apart (see Table 1-1). The centerline of the TSP region on each section was positioned two (2.0) inches above the centerline of the support plate simulation to conservatively approximate the displacement encountered by the bowing of the tubesheet with tubes that are not locked into their supports during accident conditions. The specimen was pressurized through a Swagelok fitting that connected the bottom of the specimen with the pressurization equipment.

The freespan samples were not tested with the support system.

Once each sample was connected to the pressurization equipment, it was pressurized to burst, without hold points, at a rate of 20-500 psi/second. Section 2.2 of the EPRI Guidelines (Reference 8) provides the acceptance criteria for a burst test.

#### 4.4 Burst Test Results

Figure 4-2 through Figure 4-7 provides the burst pressurization data for all of the burst tests. Table 4-2 summarizes the burst test results. All burst pressures were significantly greater than the 3NOP criteria of 4950 psig and thus meet NEI 97-06 (Reference 9) and EPRI Guideline (Reference 10) criteria.

The 02H region of R19C38 and the 04H region of R24C41 both burst within the TSP region, both at 9678 psig. The other four samples burst in a freespan region at pressures equal to or above 10,733 psig. All bursts were axially-orientated.

#### 4.5 Post-Burst Observations

Table 4-2 presents a summary of the post-test measurements made on the burst test samples.

Figure 4-8 through Figure 4-13 present photos of the burst openings. Tearing was confirmed at all burst tips, by microscope, for all six samples, thus (in accordance with Reference 8 criteria) each burst test was considered to be a valid burst test. The 02H region of R19C38 and the 04H region of R24C41 (Figure 4-8 and Figure 4-12, respectively) show secondary cracks outside of the burst opening; the freespan bursts of the other four samples showed no evidence of any cracks.

Each burst test sample was viewed under a stereomicroscope around its entire circumference in the vicinity of the burst. No corrosion or cracks were observed in the vicinity of any freespan burst.

Each burst test sample with a TSP location was also viewed under a stereomicroscope around its entire circumference in the vicinity of the TSP region. Cracks were observed in all four TSP regions of various depths and numbers. Cellular cracking was not observed. One TSP region had

marginally-discernable OD corrosion that was difficult to distinguish as a region of short axial cracks or intergranular attack (IGA). Cracking was not found outside of a TSP region.

Each TSP region was viewed under a stereomicroscope (up to 20X magnification) to identify the location of cracks, corrosion or other features. These were mapped out to show location and extent, such as that shown in Figure 4-14. The features were photographed to provide qualitative documentation of the feature. In this section, each photo is oriented with the axial direction as horizontal and the bottom side of the view to the left side of the photo.

The 02H TSP region of tube R19C38 burst in the TSP region. The center of the burst was skewed about 0.2 inches above the TSP centerline and the burst opening extended above and below the TSP region. The burst occurred at the 350° orientation. There were several regions of short (<0.15 inch) axial cracks around the circumference, most of which were located near the burst opening. These are shown in the Figure 4-14 diagram. Some of these short cracks can be seen near the burst opening as shown in Figure 4-8; others are shown in Figure 4-15, Figure 4-16 and Figure 4-17.

The 02H TSP region of tube R24C41 did not have a burst. There was a region of marginally-discernable (shallow) corrosion that was partially obscured by surface deposits, and was either a patch of short axial cracks or IGA. It also had another region with shallow corrosion that was discernable as axial cracks. These are shown in the Figure 4-18 diagram and in the Figure 4-19 photo.

The 03H TSP region of tube R24C41 did not have a burst. There were two regions with shallow cracks. These are shown in the Figure 4-20 diagram. The photo in Figure 4-21 shows the shallow axial cracks located near the 180° orientation, as indicated by the two arrows. Figure 4-22 shows the shallow cracks at the top of the TSP region near the 0° orientation. These cracks are neither axial nor circumferential, which may be attributable to their short length and shallow depth.

The 04H TSP region of tube R24C41 burst in the TSP region. The center of the burst was aligned with the TSP centerline and the burst opening extended above and below the TSP region. The burst occurred at the 90° orientation. There were several regions of small axial cracks around the circumference, most of which were located near the centerline of the TSP region. There was another region of larger axial cracks, located between 315° and 360°, all within the center third (0.25-inch long) portion of the TSP length. These are shown in the Figure 4-23 diagram. Figure 4-24 and Figure 4-25 show the region of the larger cracks. These cracks are significantly oriented in the axial direction. Figure 4-12 shows some cracking adjacent to the burst opening; Figure 4-26 shows a closer view of these cracks.



Table 4-1: Measurements Before Leak / Burst Testing

Tube	R19C38	R19C38	R24C41	R24C41	R24C41	R24C41
Section	3B	4B	3B	5B	6B	7B
Region	02H	Freespan	02H	03H	04H	Freespan
Length (in)	12	12	12	12	12	12
Location of OD Measurements	02H	midspan	02H	03H	04H	midspan
OD (0°-180°) (in)	0.876	0.876	0.873	0.879	0.880	0.873
OD (90°-270°) (in)	0.876	0.876	0.869	0.880	0.876	0.874
Location of Wall Thicknesses	bottom	bottom	bottom	bottom	bottom	bottom
0° (in)	0.056	0.056	0.054	0.056	0.057	0.052
90° (in)	0.060	0.058	0.055	0.056	0.057	0.056
180° (in)	0.057	0.053	0.055	0.057	0.056	0.055
270° (in)	0.054	0.055	0.057	0.055	0.057	0.057

OD and wall thickness measurements may include deposit thickness.

Table 4-2: Burst Results and Post-Burst Measurements

Tube	R19C38	R19C38	R24C41	R24C41	R24C41	R24C41
Section	3B	4B	3B	5B	6B	7B
Region	02H	Freespan	02H	03H	04H	Freespan
Burst Pressure (psig)	9,678	10,983	10,741	10,733	9,678	10,770
Burst Orientation	axial	axial	axial	axial	axial	axial
Avg. Pressurization Rate (psi/sec)	100	99	98	99	99	97
Location of Burst	02H	freespan	freespan	freespan	04H	freespan
Center of Burst, inches above bottom	6.20	4.91	8.20	7.73	6.00	5.29
Azimuthal Location of Burst	350°	310°	315°	220°	90°	240°
Length of Burst Opening (in)	1.20	1.91	1.42	1.83	1.28	1.82
Width of Burst Opening (in)	0.33	0.38	0.32	0.36	0.33	0.41
Maximum Diameter (in)	1.180	1.249	1.309	1.265	1.102	1.285
Diameter, 90° from Maximum (in)	1.066	1.103	1.154	1.129	1.076	1.137

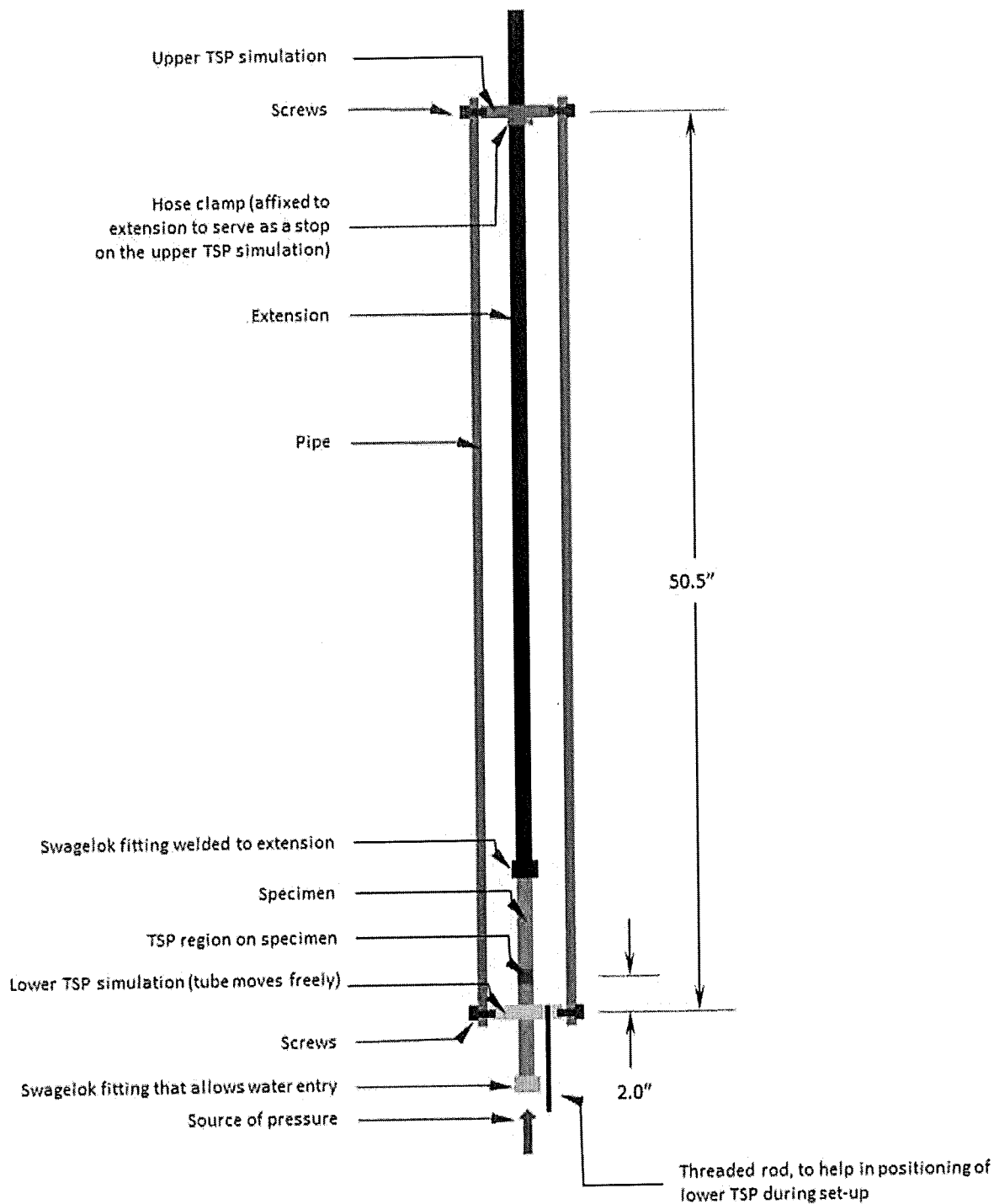


Figure 4-1: Burst Test Support Simulation

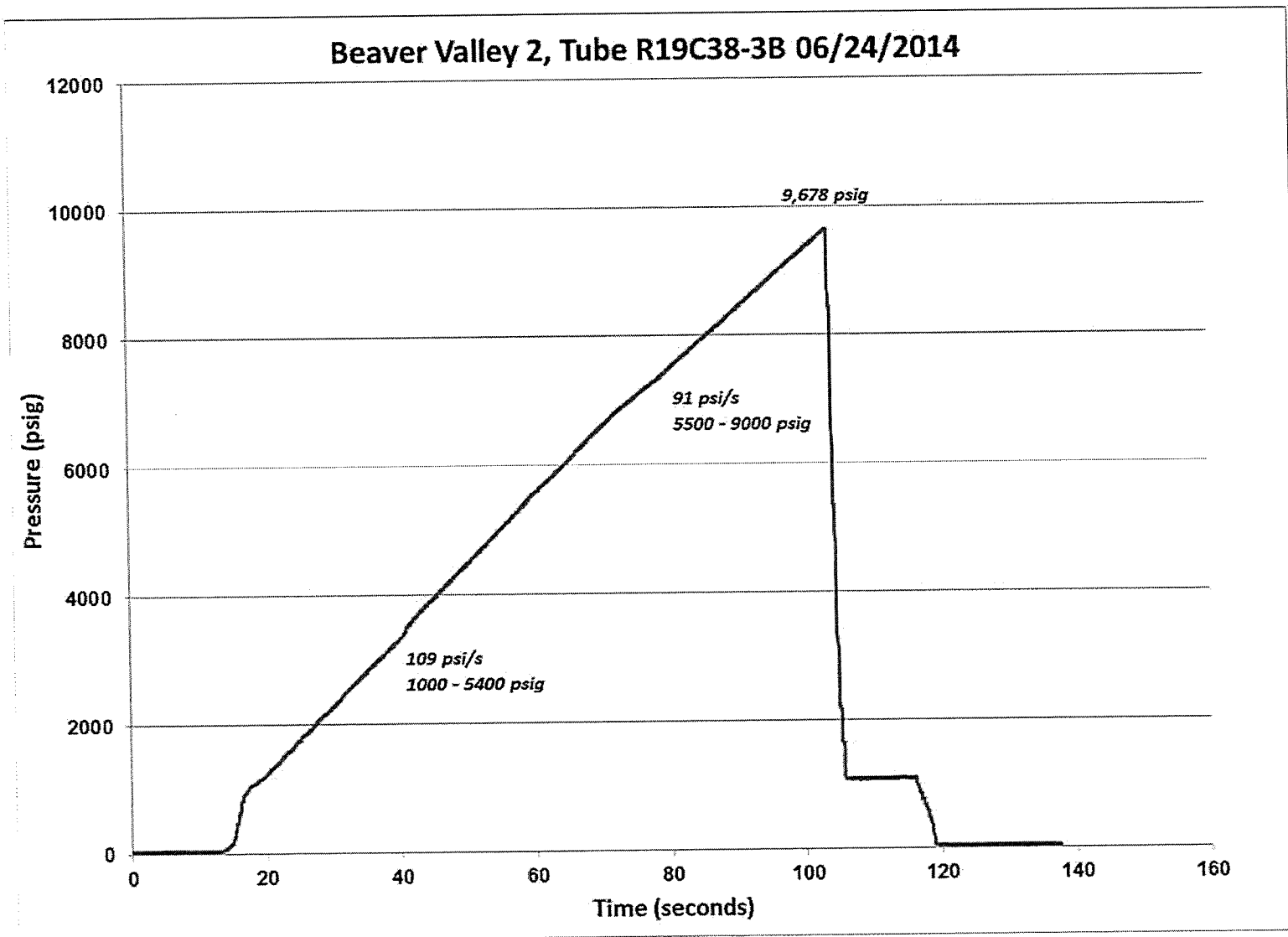


Figure 4-2: Burst Pressurization of R19C38-3B (02H)

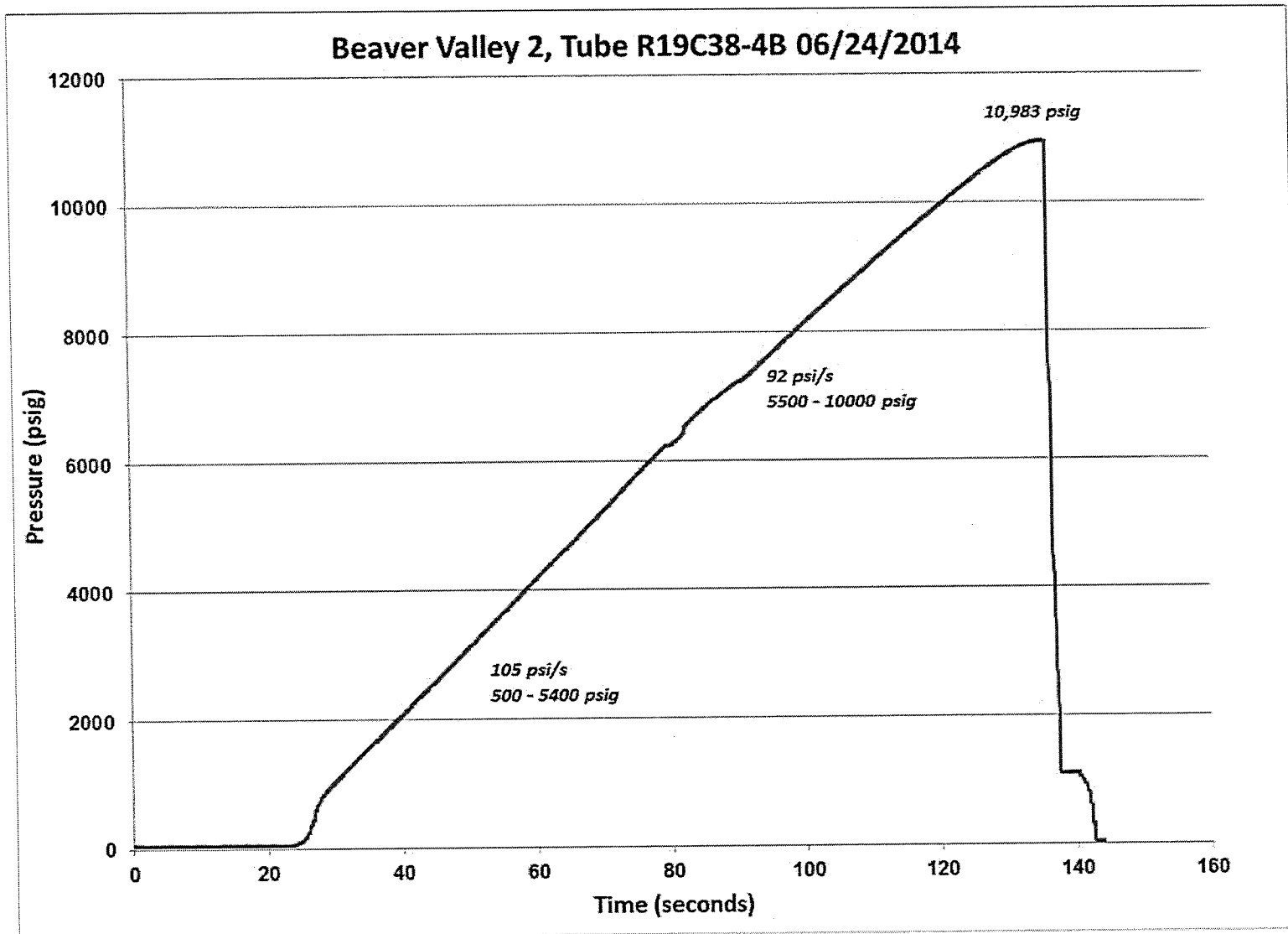


Figure 4-3: Burst Pressurization of R19C38-4B (Freespan)

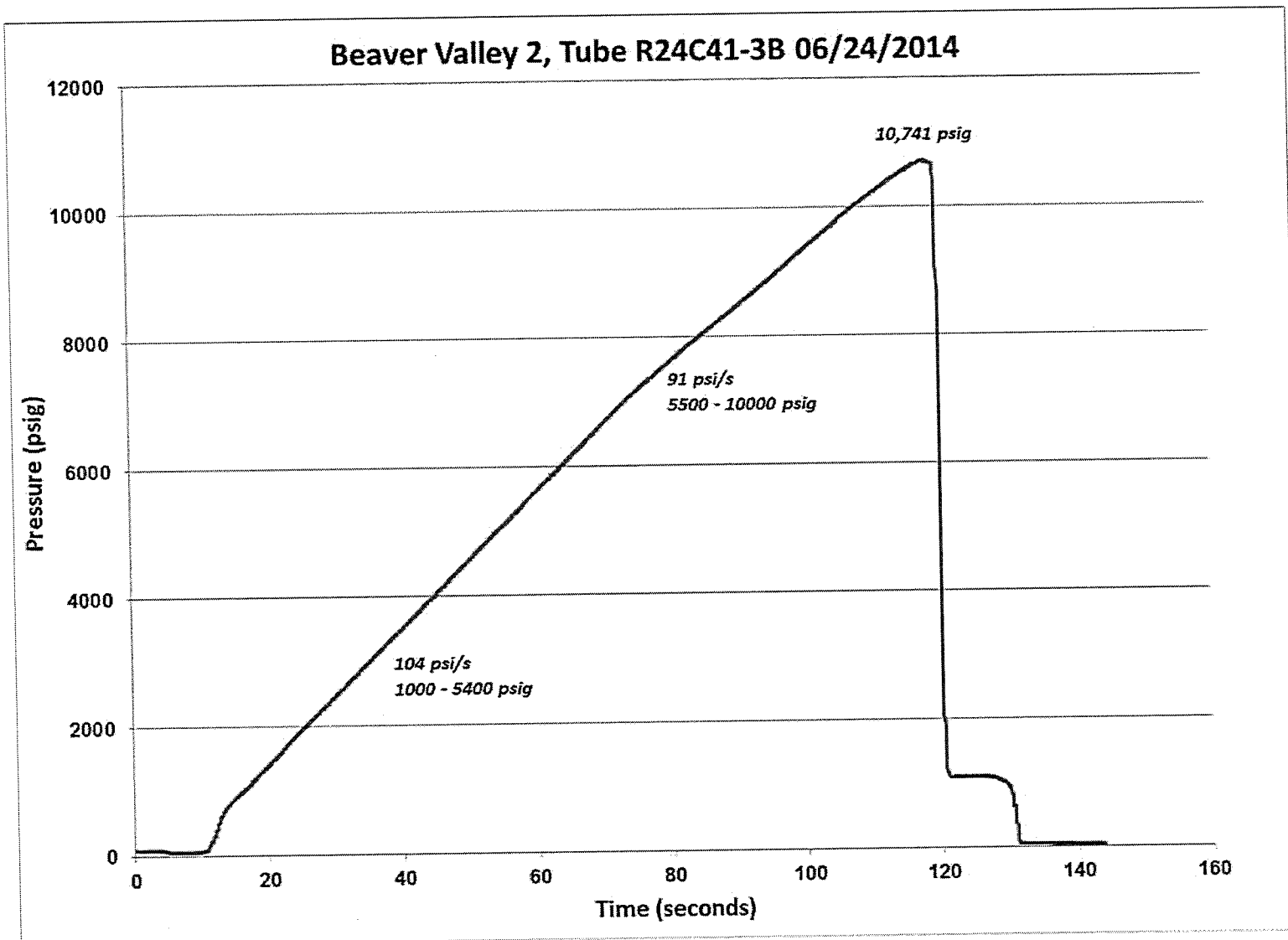


Figure 4-4: Burst Pressurization of R24C41-3B (02H)

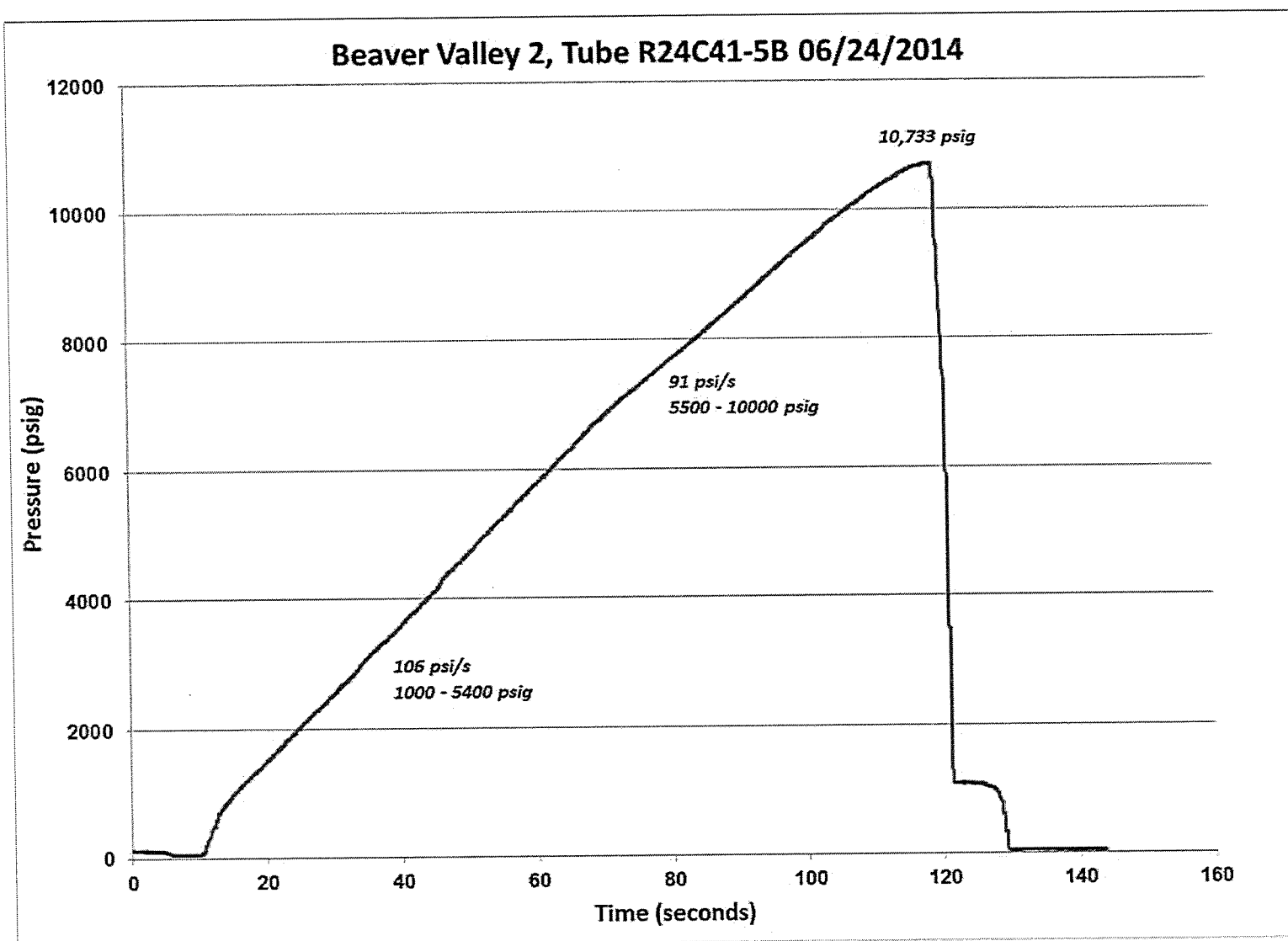


Figure 4-5: Burst Pressurization of R24C41-5B (03H)

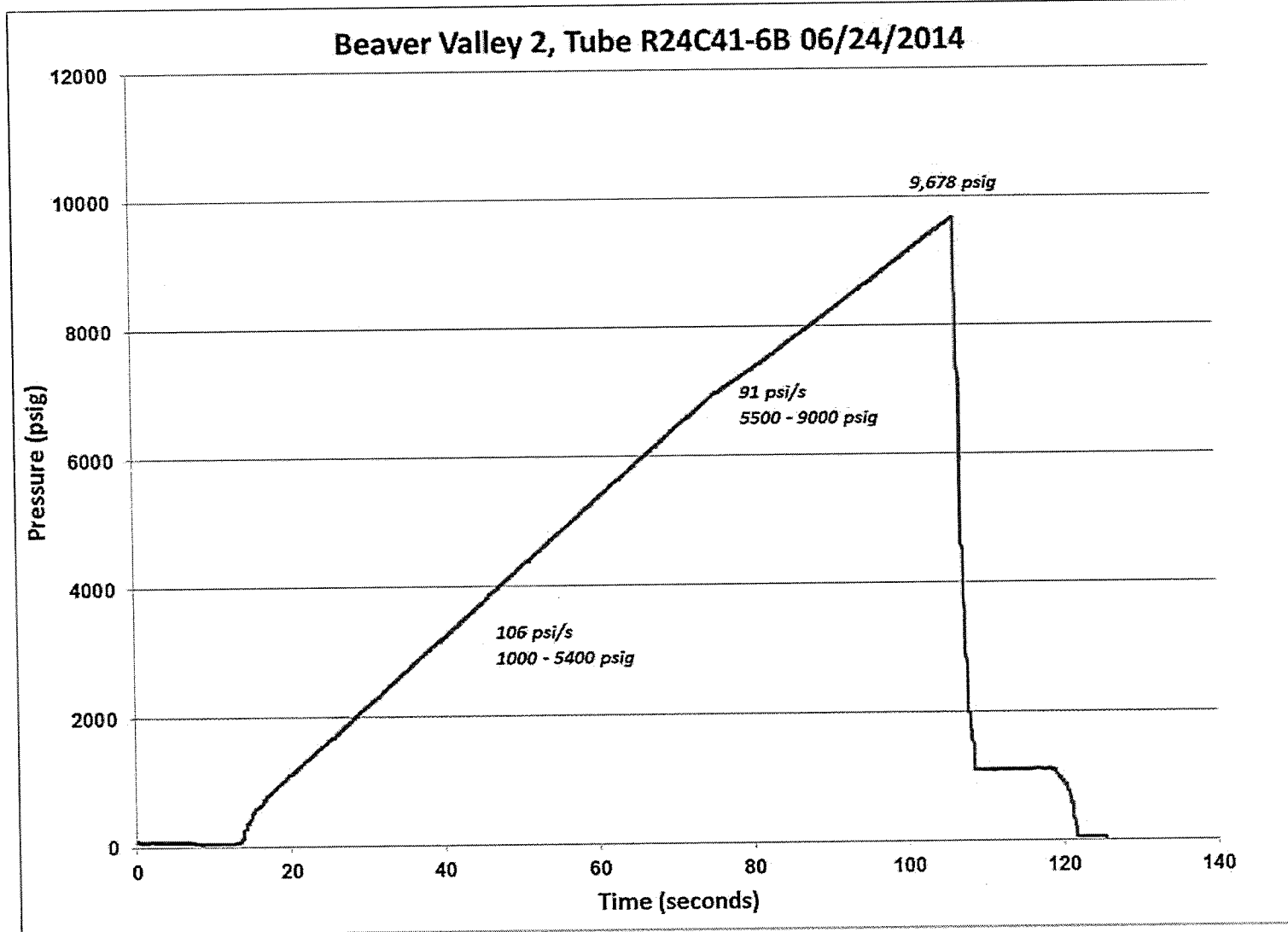


Figure 4-6: Burst Pressurization of R24C41-6B (04H)



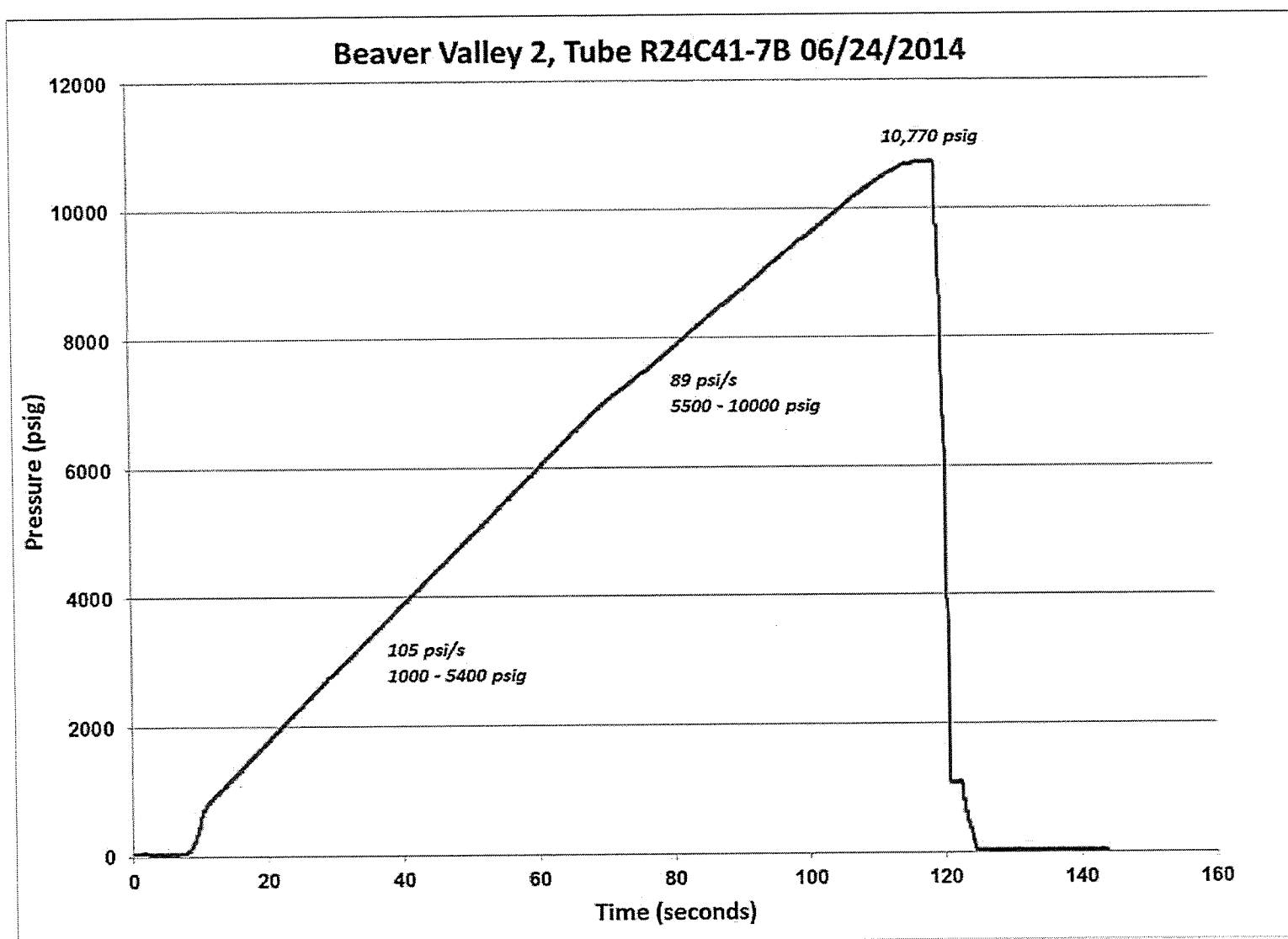


Figure 4-7: Burst Pressurization of R24C41-7B (Freespan)

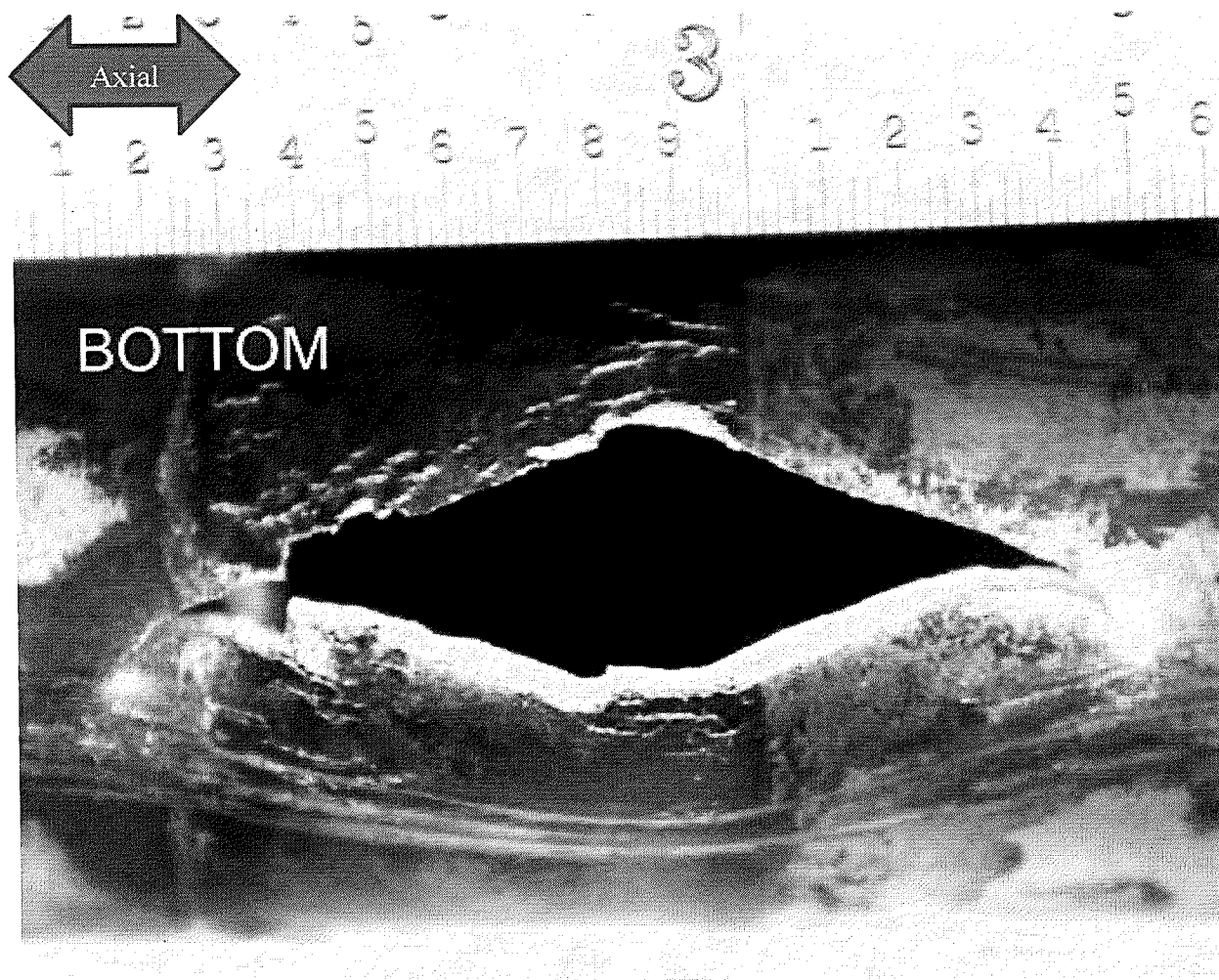


Figure 4-8: Burst Opening at R19C38-3B (02H)

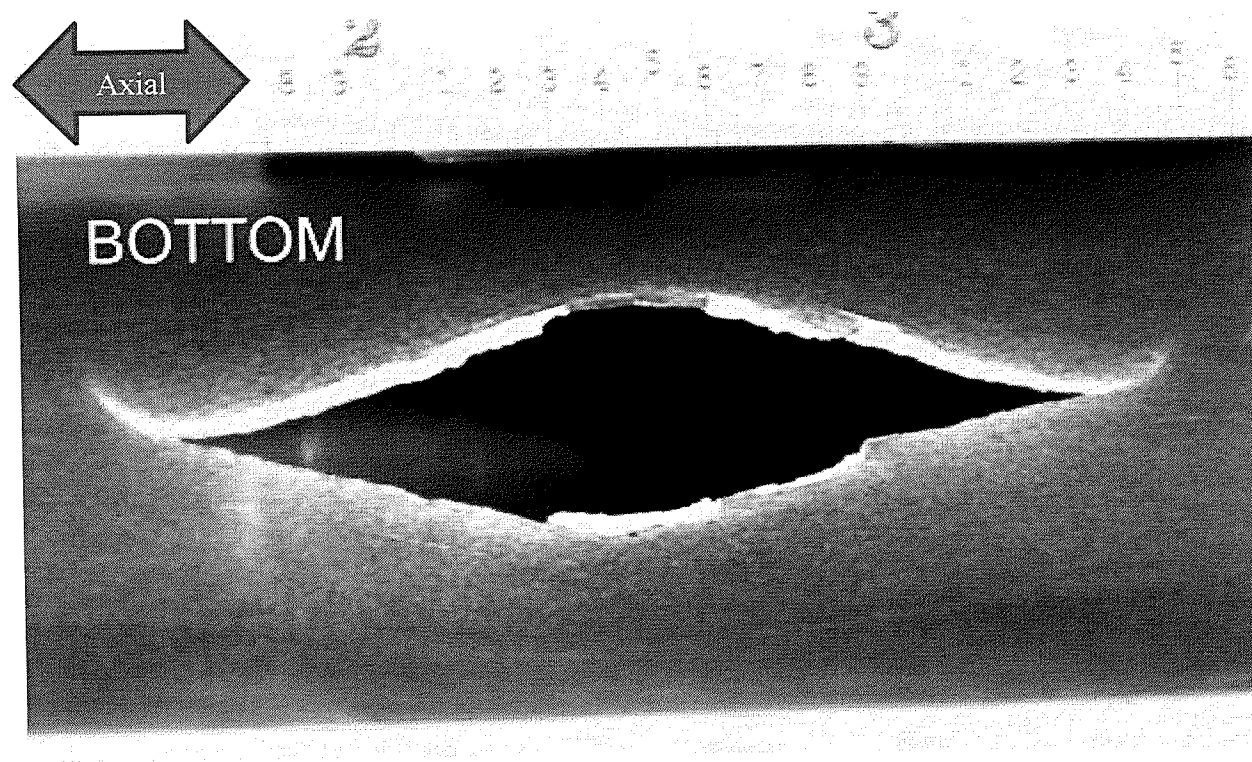


Figure 4-9: Burst Opening at R19C38-4B (Freespan)

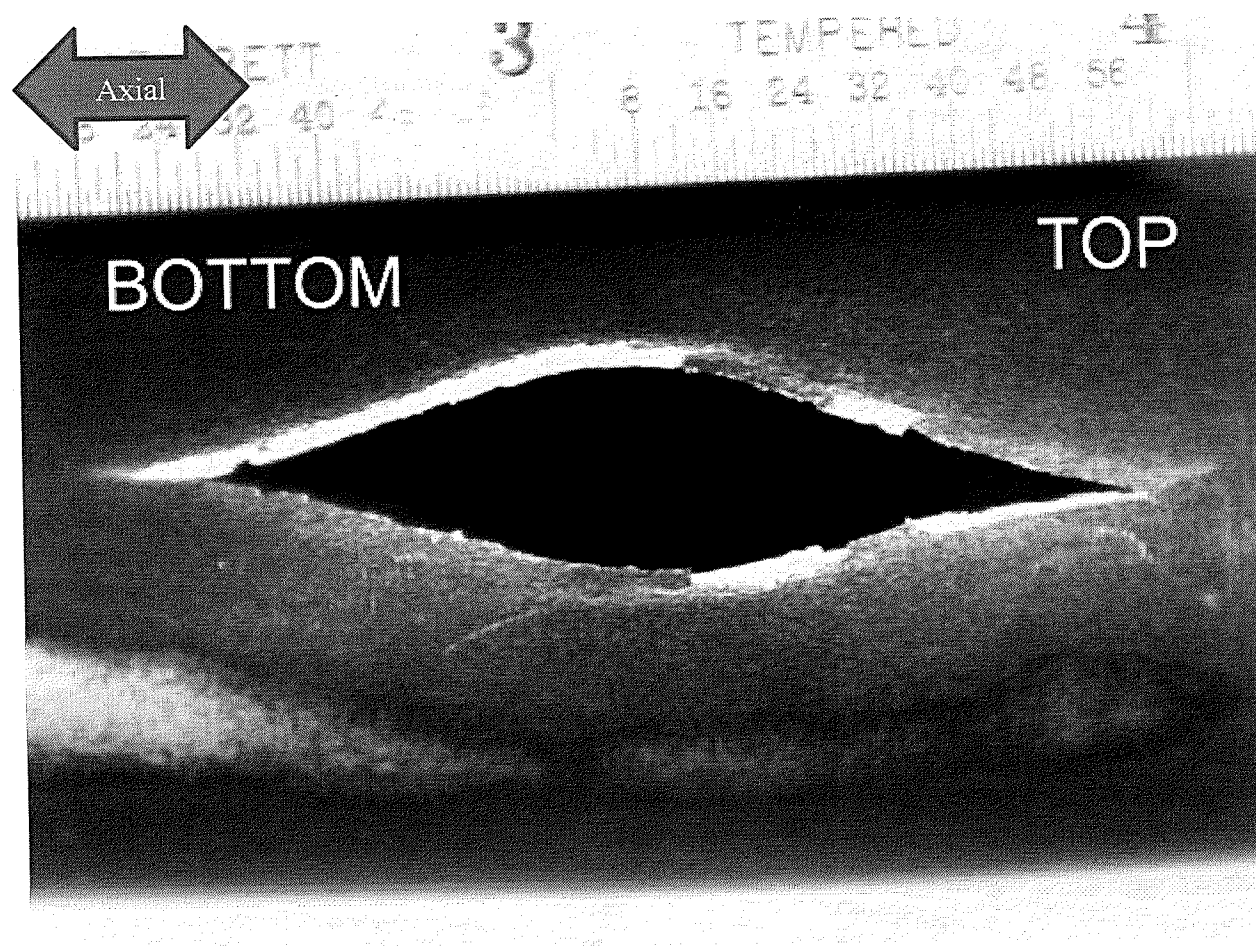


Figure 4-10: Burst Opening at R24C41-3B (Burst in Freespan, Outside of 02H)

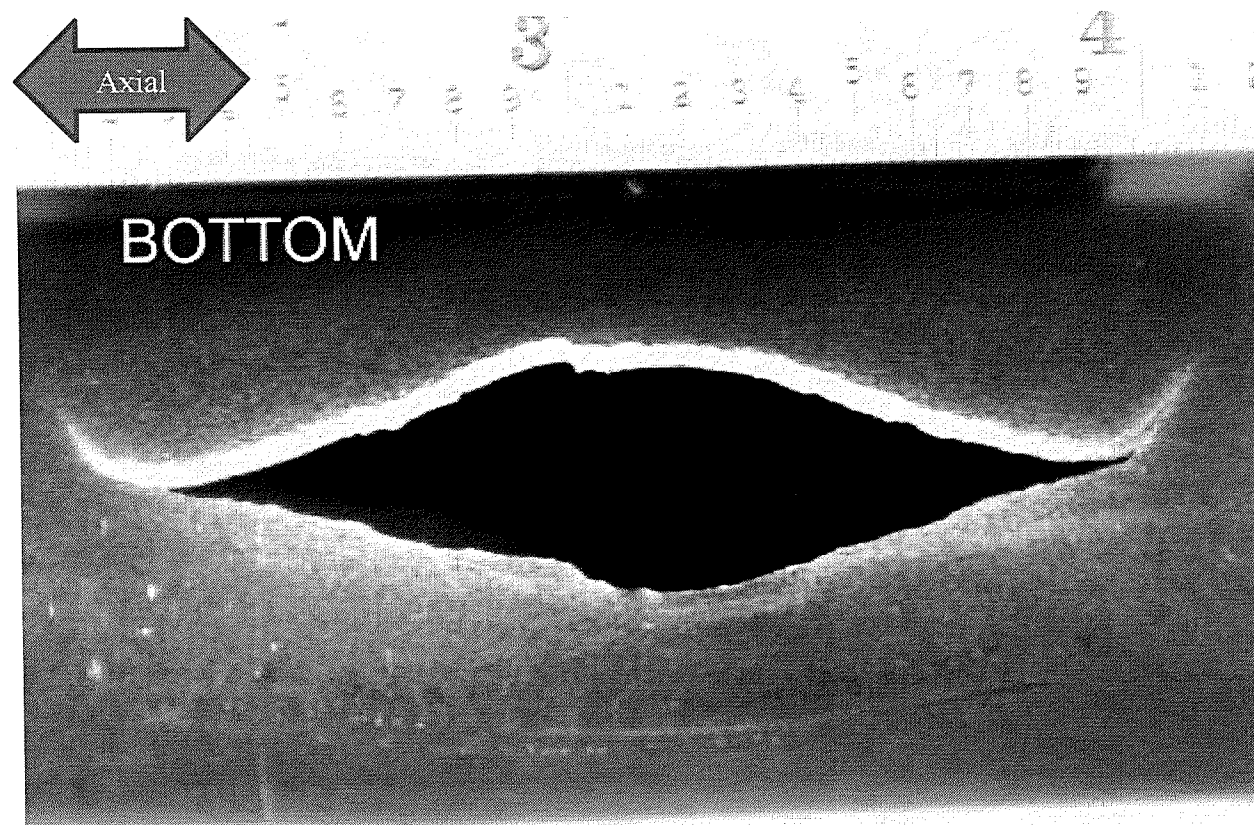


Figure 4-11: Burst Opening at R24C41-5B (Burst in Freespan, Outside of 03H)

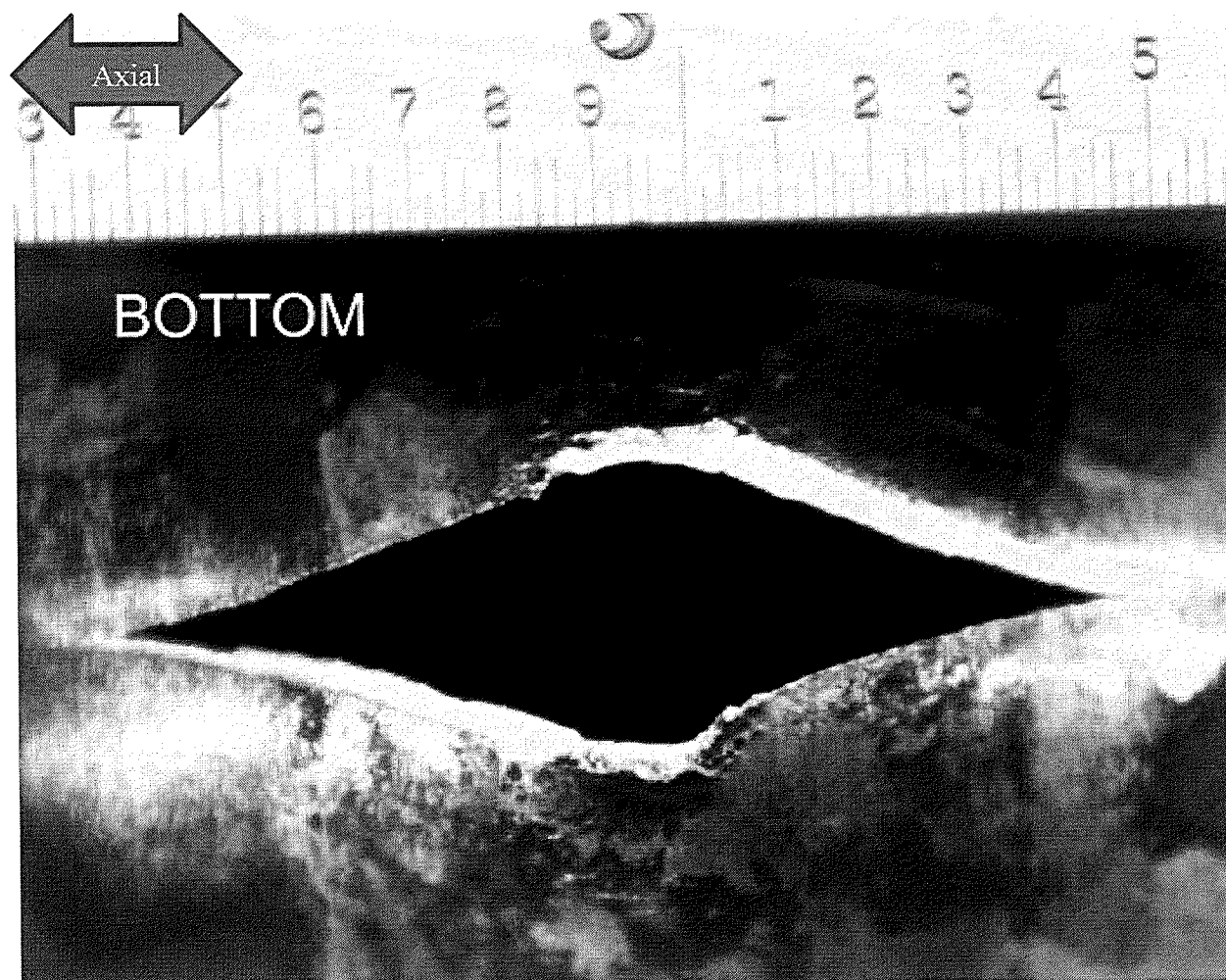


Figure 4-12: Burst Opening at R24C41-6B (04H)

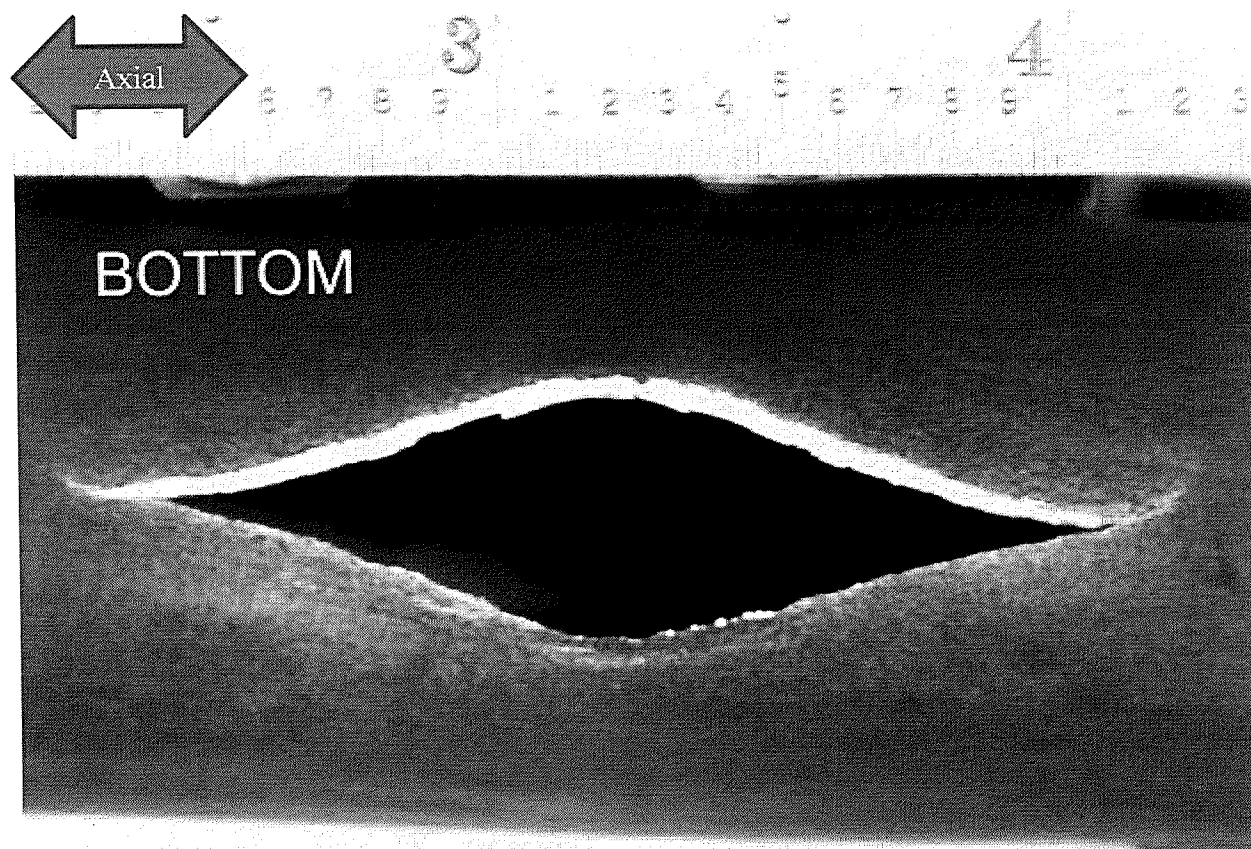


Figure 4-13: Burst Opening at R24C41-7B (Freespan)

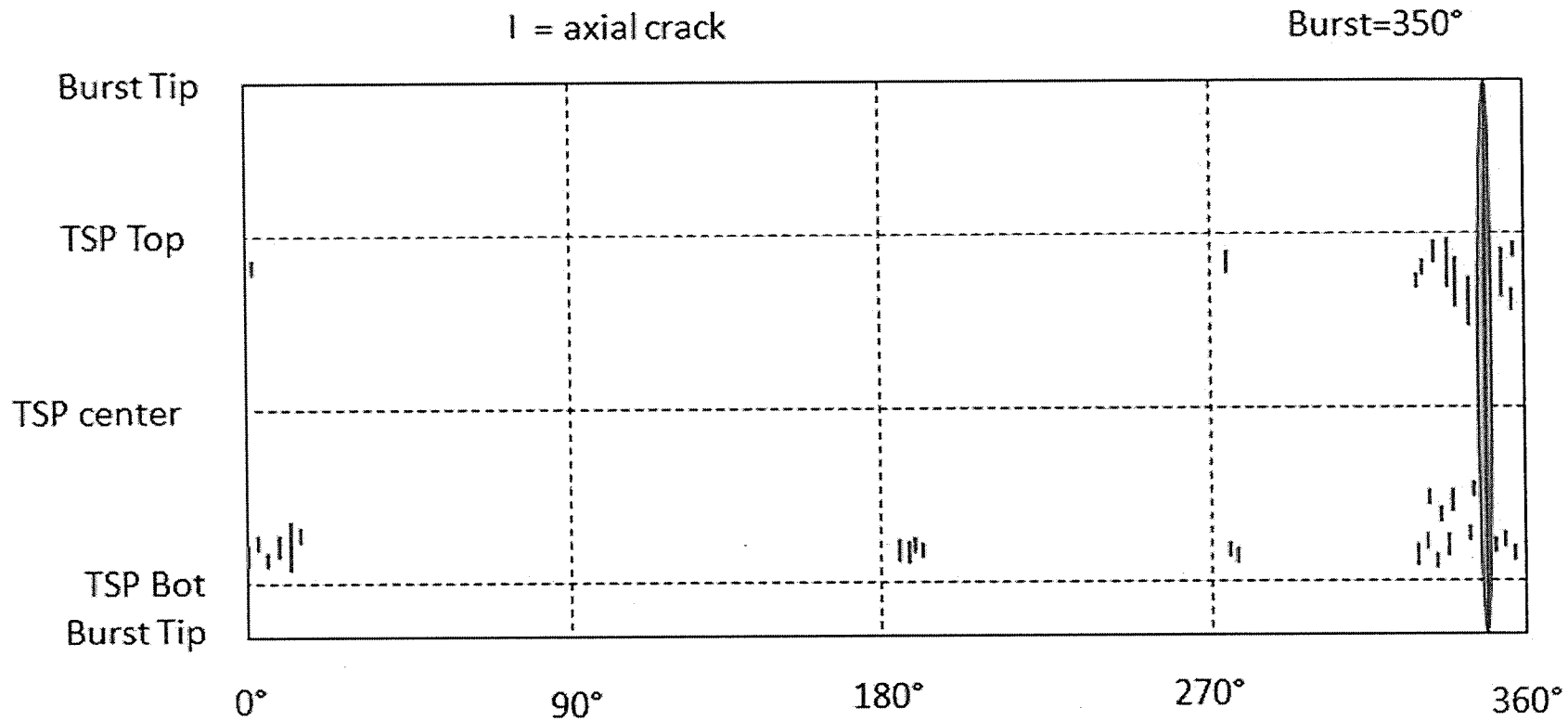


Figure 4-14: Post-Burst Observations on R19C38-3B (02H Region)



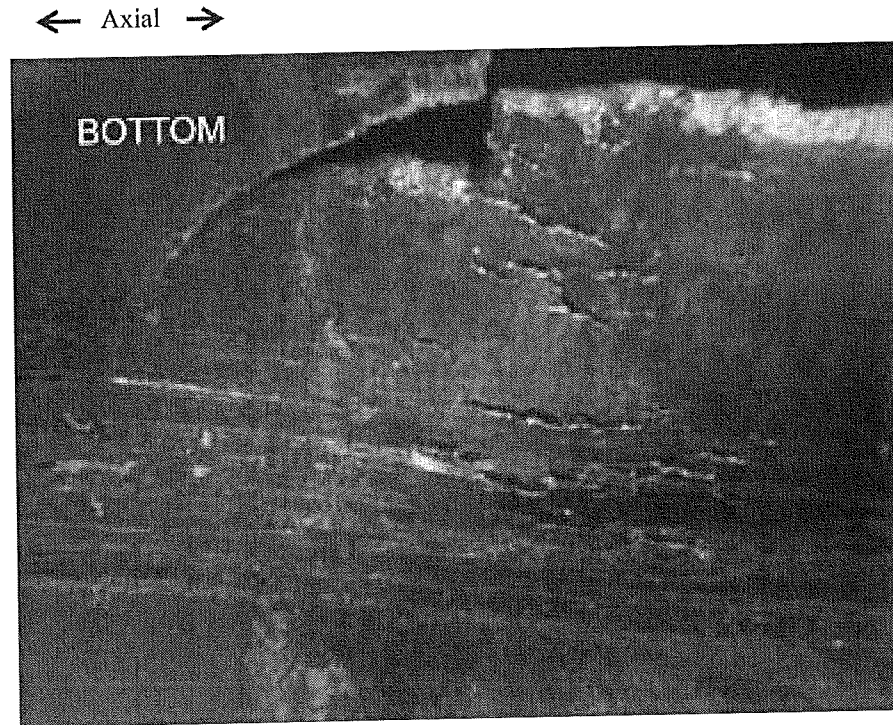


Figure 4-15: Short Cracks Near the Bottom of the 02H TSP of R19C38 (0° Orientation)

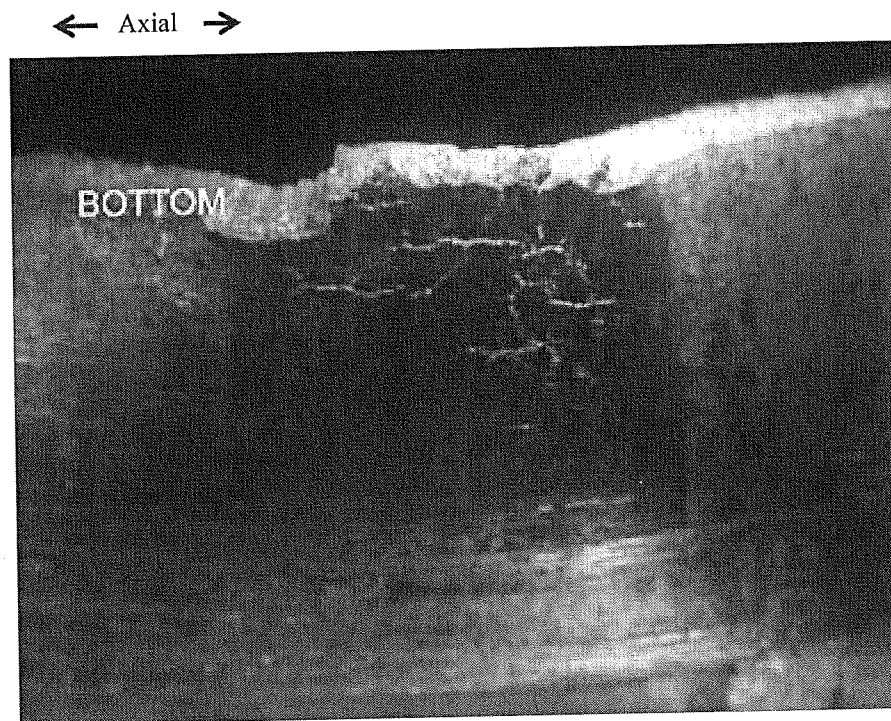


Figure 4-16: Short Cracks Near the Top of the 02H TSP of R19C38 (0° Orientation)

← Axial →

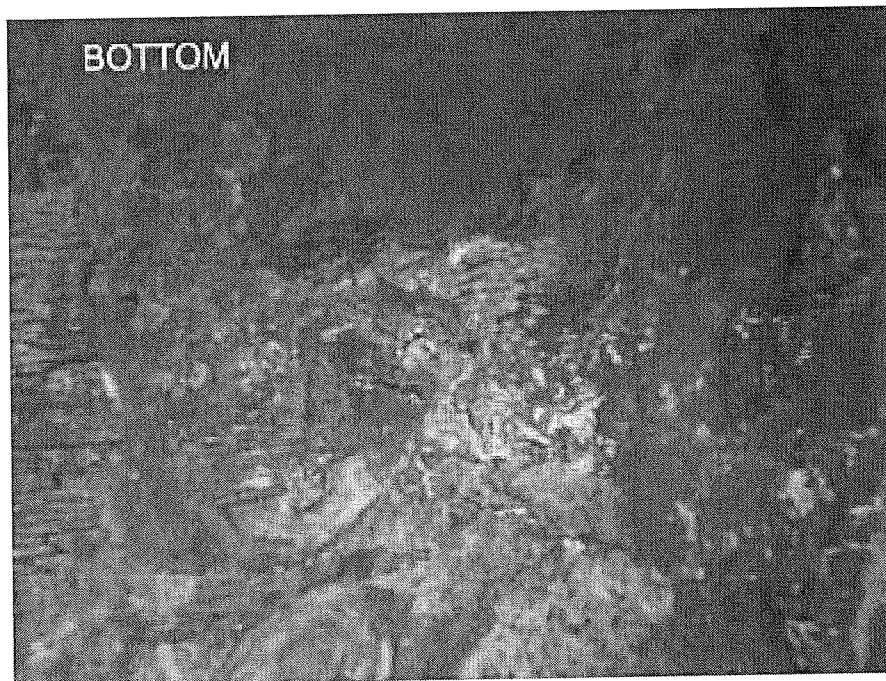


Figure 4-17: Short Cracks Near the Bottom of the 02H TSP of R19C38 (200° Orientation)

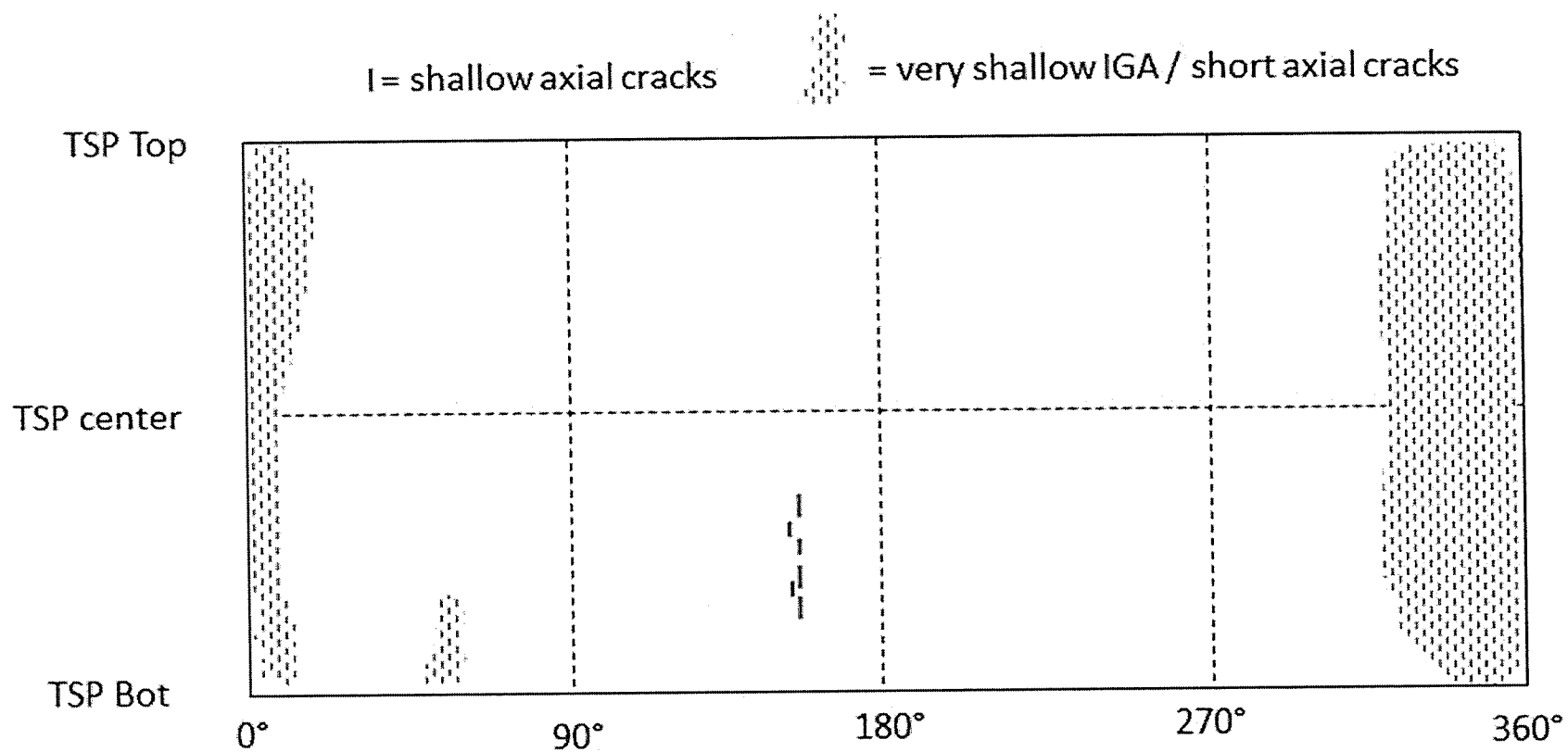


Figure 4-18: Post-Burst Observations on R24C41-3B (02H Region)



Figure 4-19: Shallow Corrosion Partially Obscured by Surface Deposits, Near the 0° Orientation of R24C41 02H

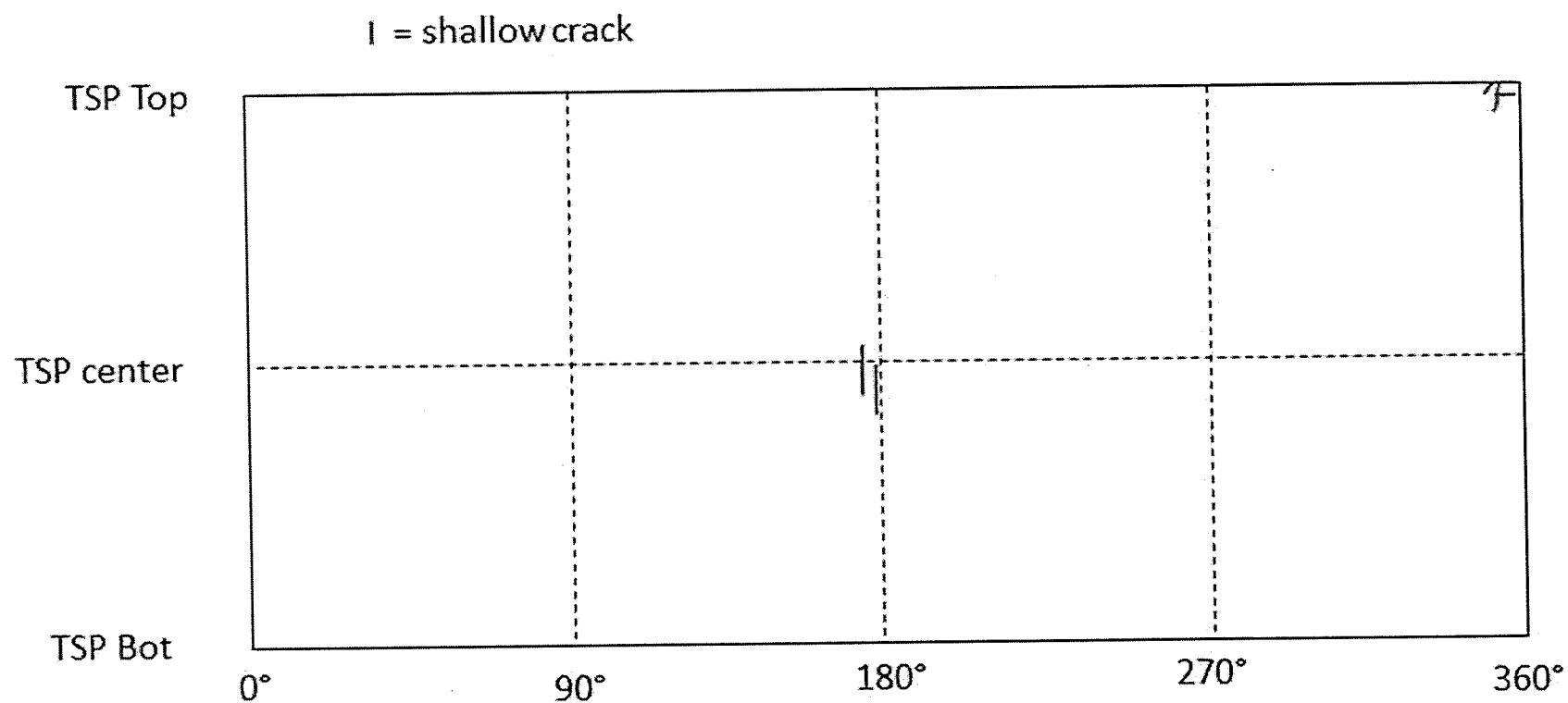


Figure 4-20: Post-Burst Observations on R24C41-5B (03H Region)

← Axial →

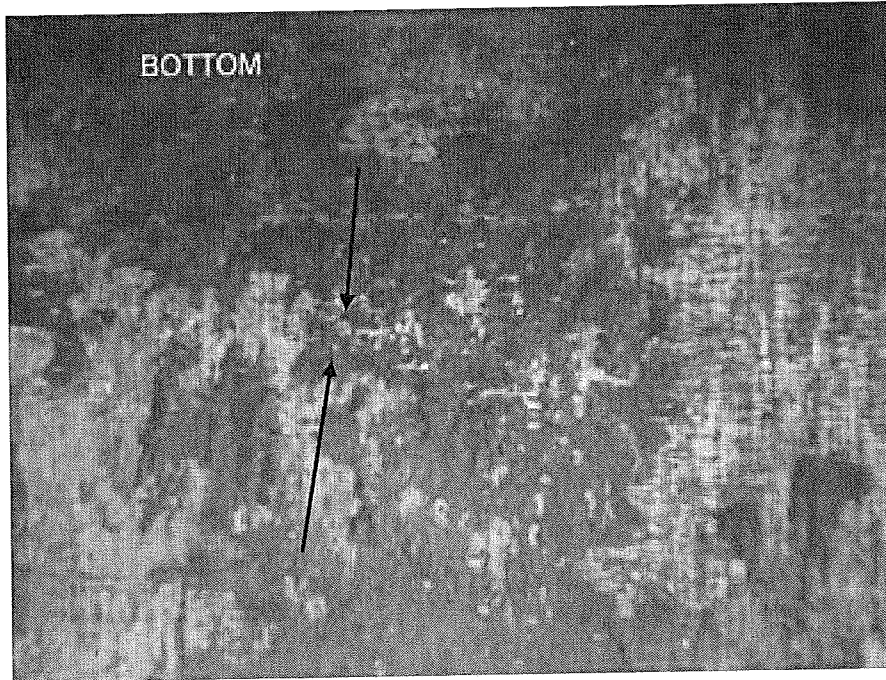


Figure 4-21: Shallow Axial Cracks (Marked with Arrows) Near Center of R24C41 03H TSP Region (180° Orientation)

← Axial →

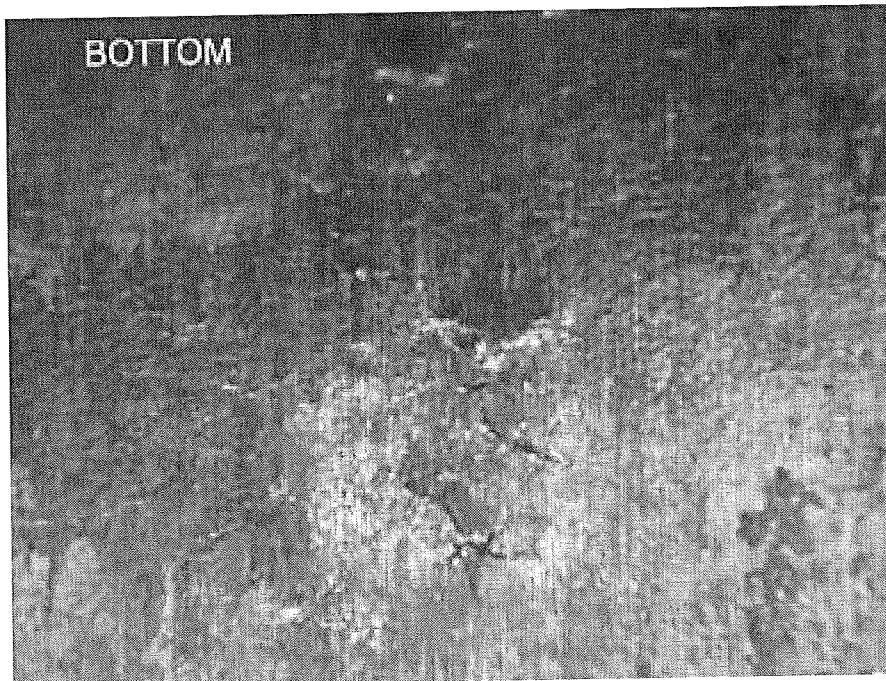


Figure 4-22: Shallow Non-axial Cracks at Top of R24C41 03H TSP Region (0° Orientation)

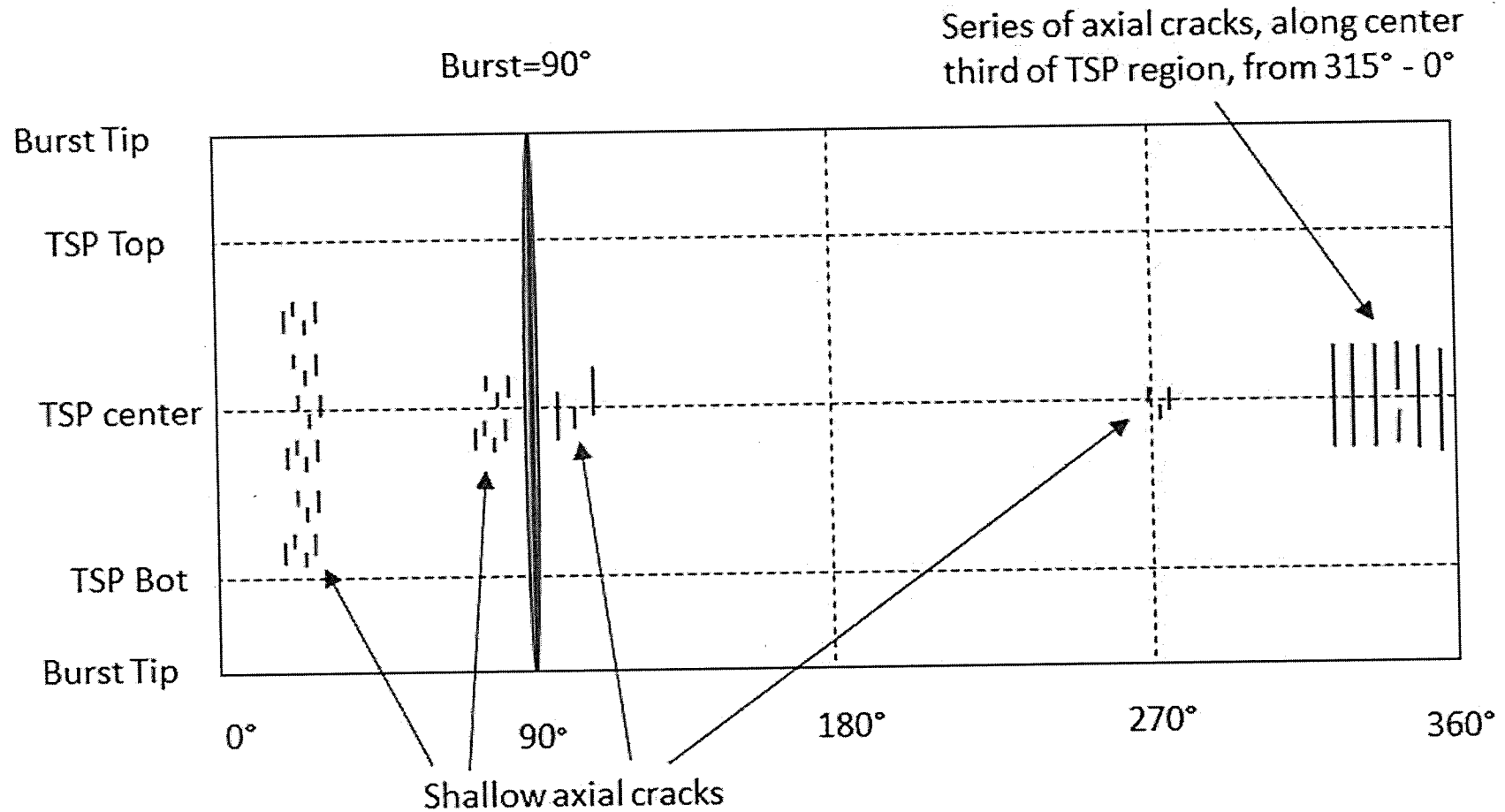


Figure 4-23: Post-Burst Observations on R24C41-6B (04H Region)



← Axial →

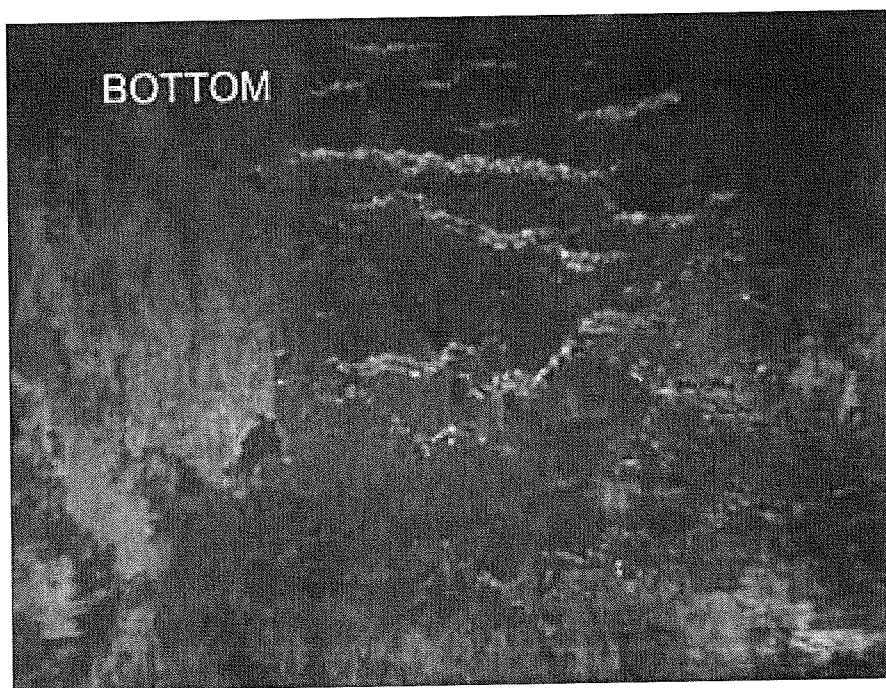


Figure 4-24: Larger Axial Cracks Near the Centerline of R24C41 04H TSP Region, Between 335°-360°

← Axial →

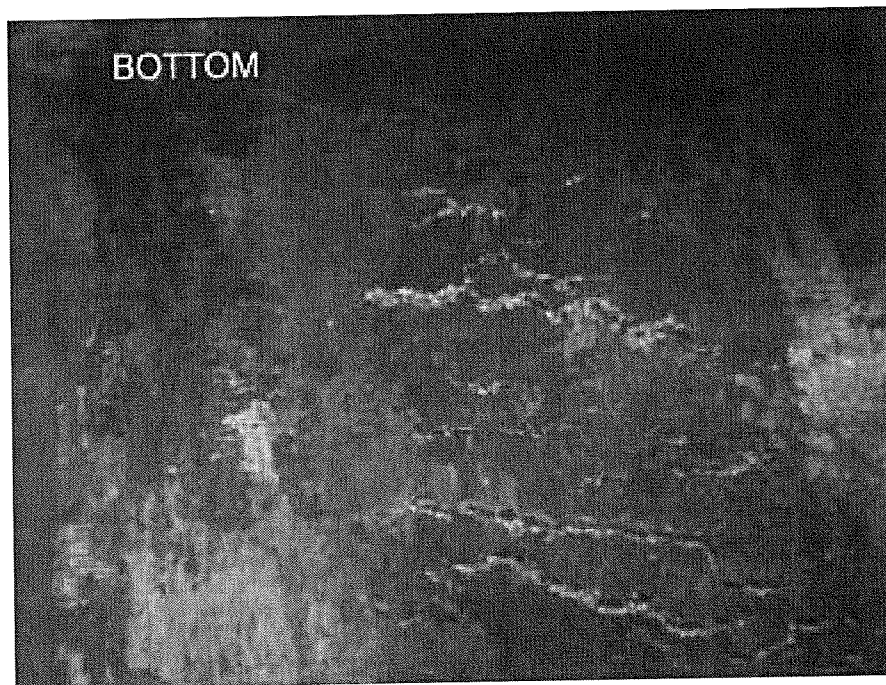


Figure 4-25: Larger Axial Cracks Near the Centerline of R24C41 04H TSP Region, Between 315°-340°



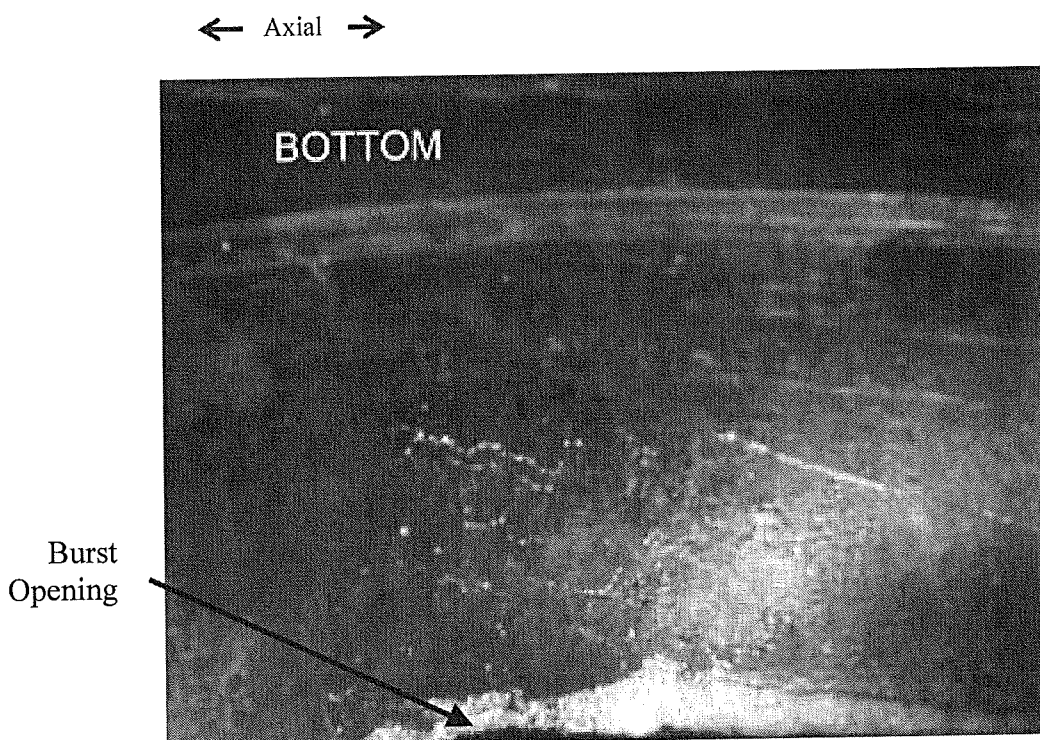


Figure 4-26: Example of Shallow Cracks Located Adjacent to the Burst Opening Of R24C41-6B (04H) at the 90° Orientation

## 5.0 POST-BURST SECTIONING

Following the completion of the burst tests, samples were sectioned for Scanning Electron Microscope (SEM) fractography and defect metallography. Figure 5-1 through Figure 5-6 provide sketches of how each sample was sectioned. In each diagram, the circled “A” and “B”, and the adjacent dotted line, represent the cuts that were made within the section. These cuts were made in order of the “A” cut first and the “B” cut second (where applicable).

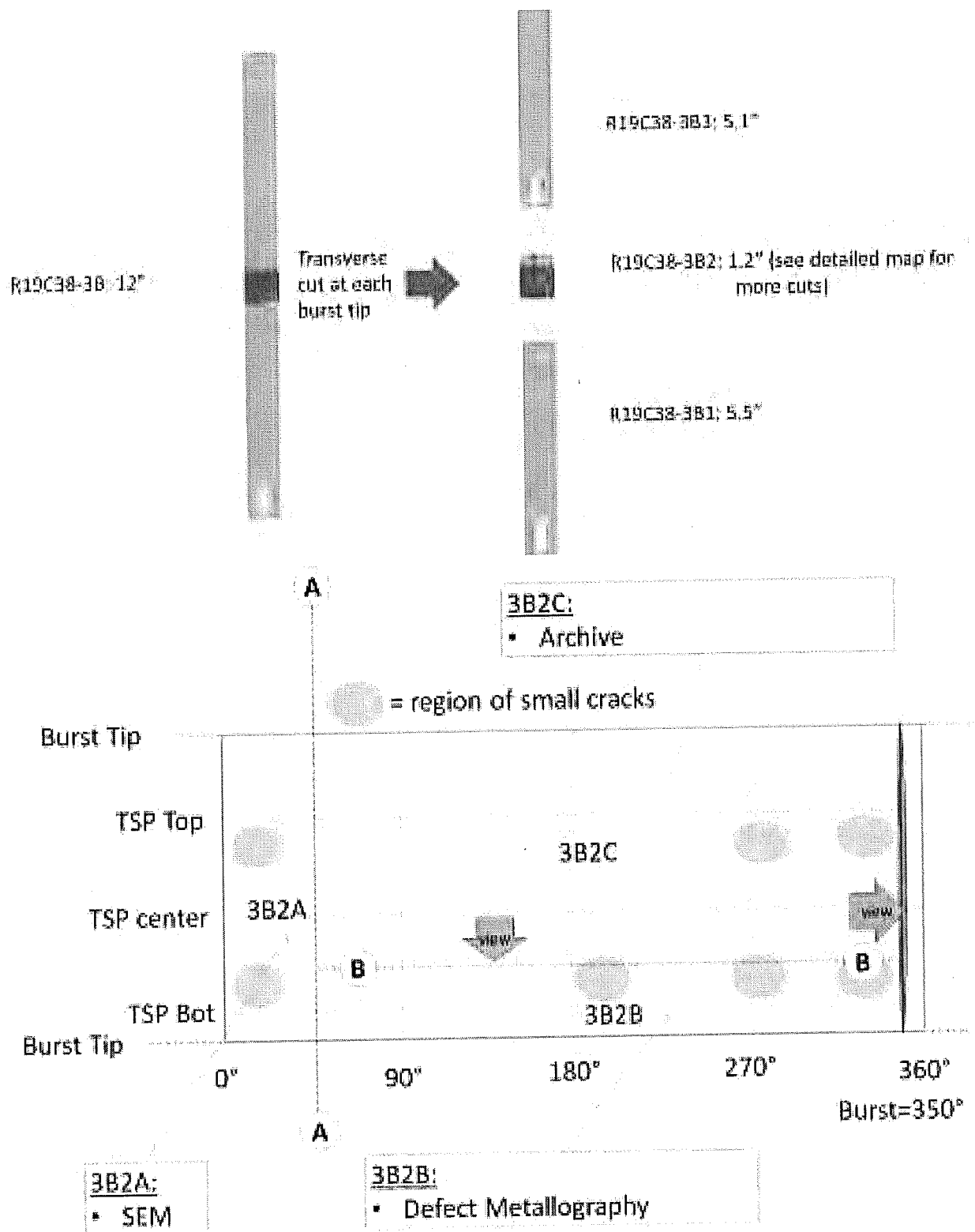


Figure 5-1: Post-Burst Sectioning of R19C38-3B

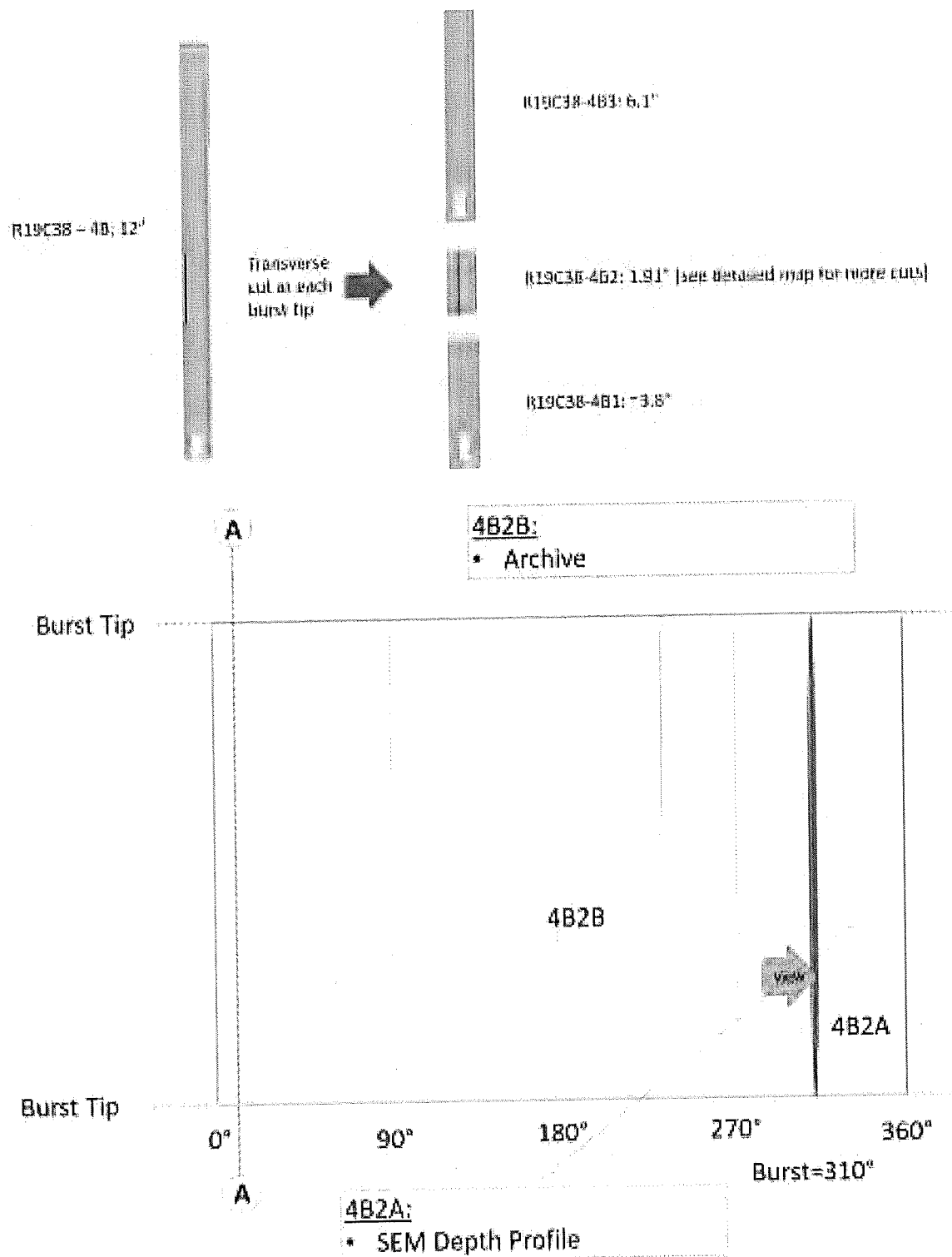


Figure 5-2: Post-Burst Sectioning of R19C38-4B

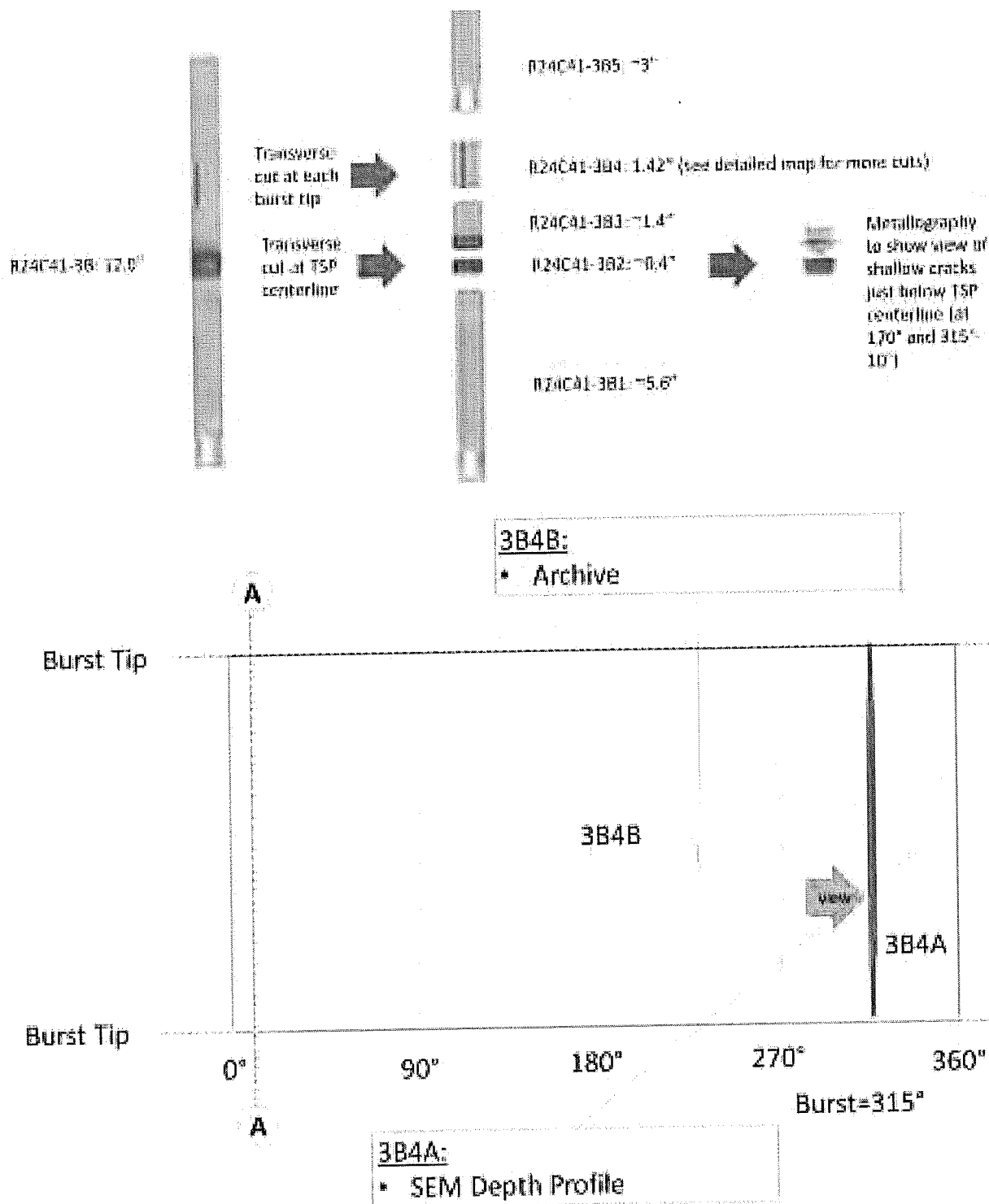


Figure 5-3: Post-Burst Sectioning of R24C41-3B

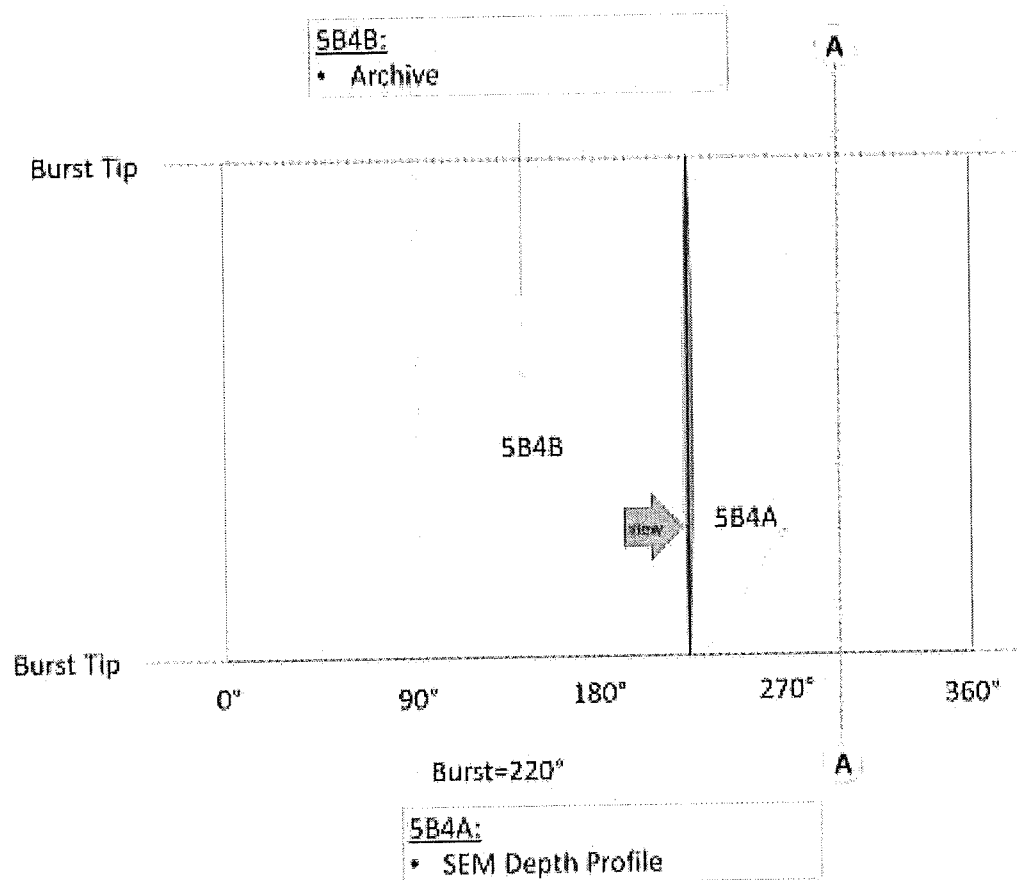
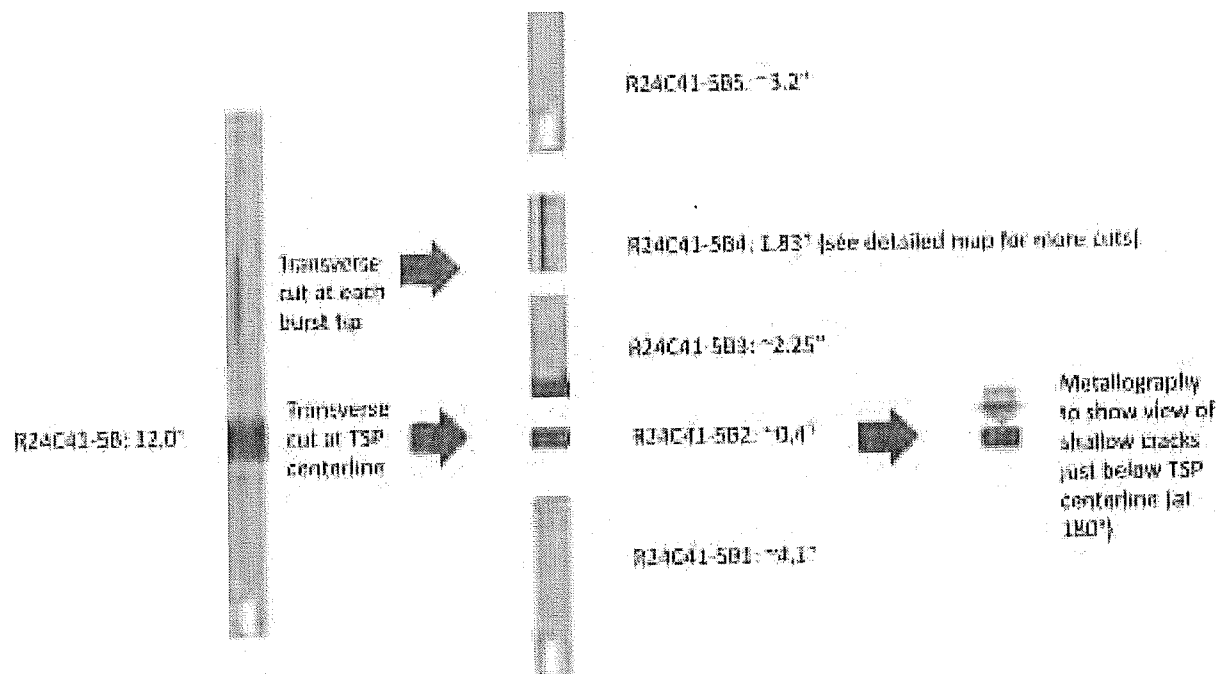


Figure 5-4: Post-Burst Sectioning of R24C41-5B

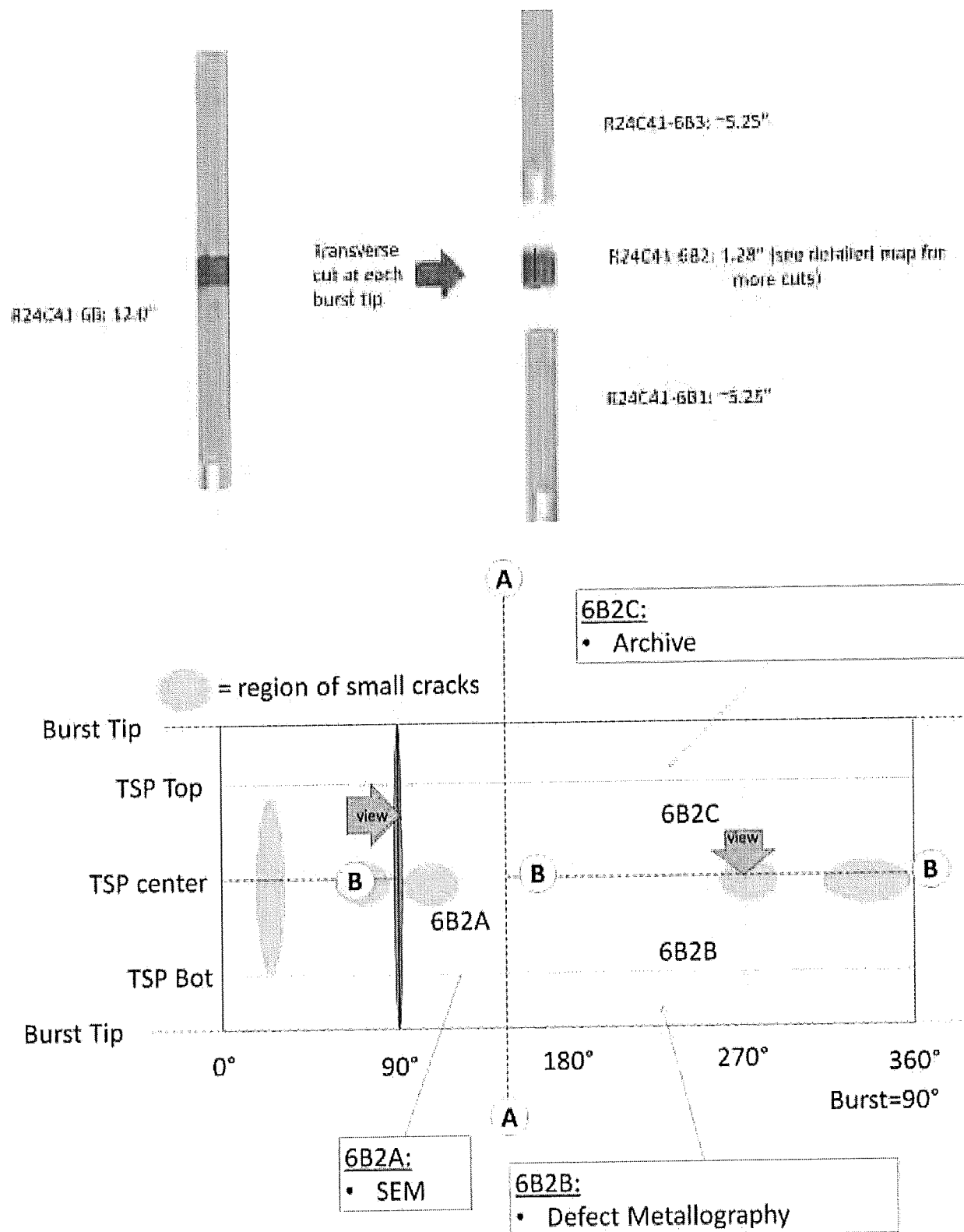


Figure 5-5: Post-Burst Sectioning of R24C41-6B

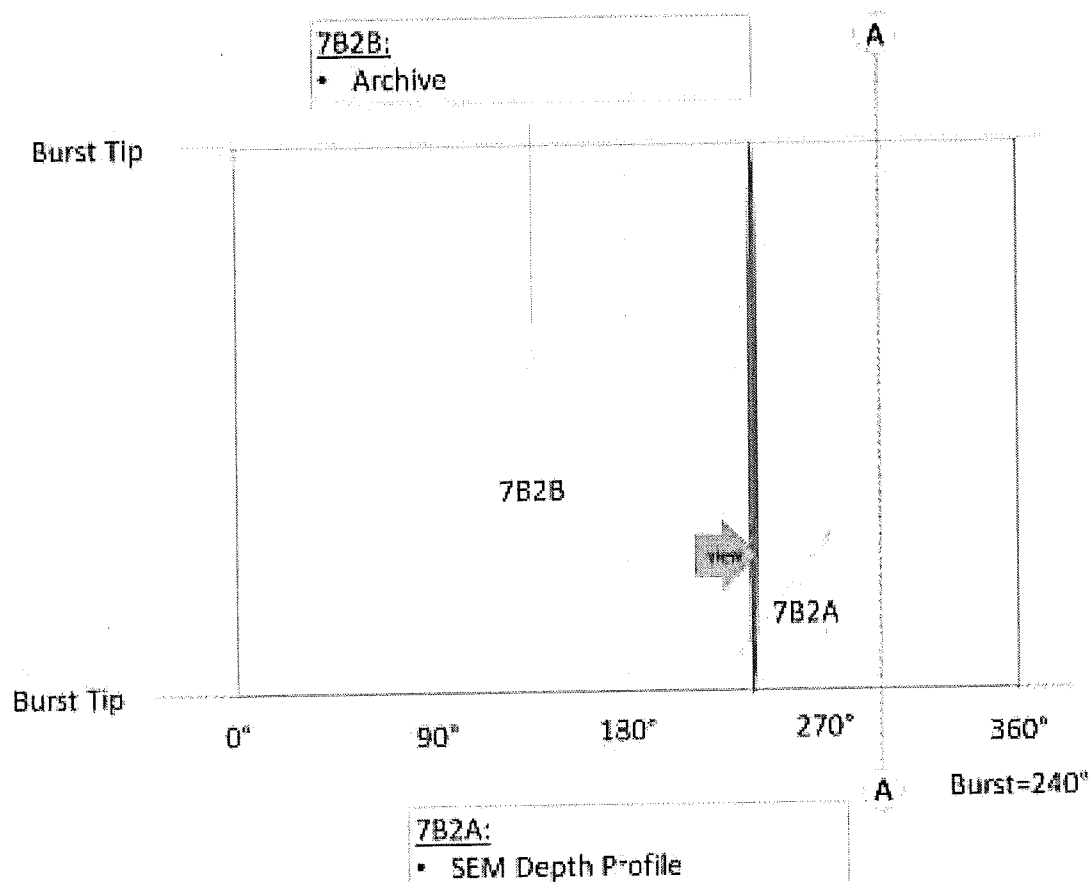
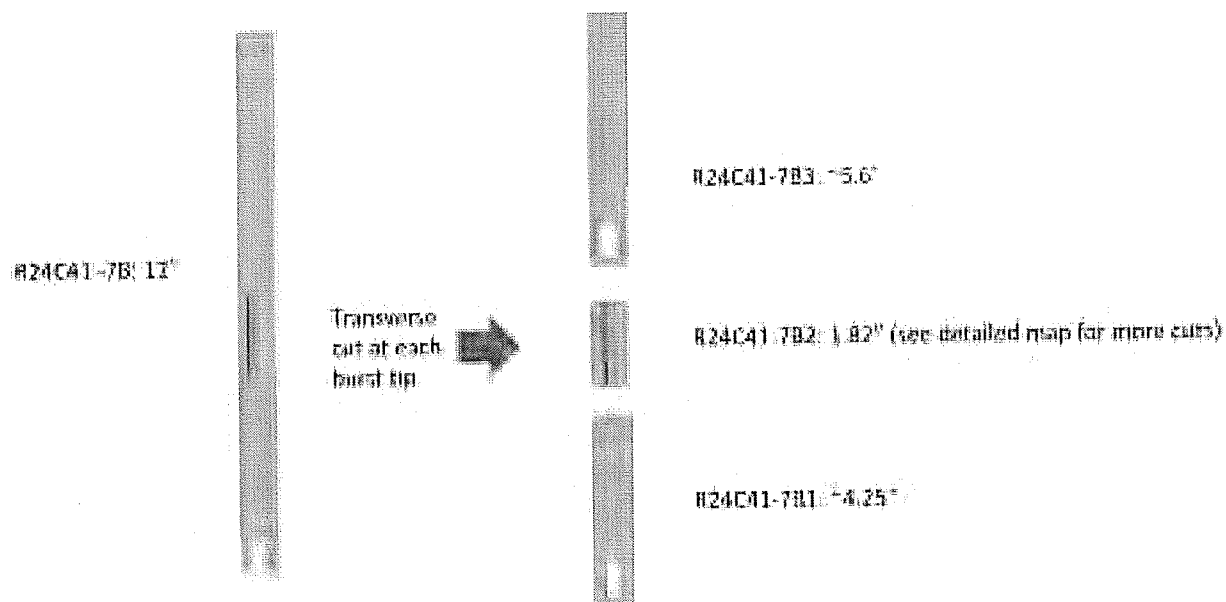


Figure 5-6: Post-Burst Sectioning of R24C41-7B



## **6.0 SEM FRACTOGRAPHY**

### **6.1 Sample Preparation**

A ½-inch wide sample was cut from the right side of each burst opening, as was depicted in the diagrams of Section 5.0. The cuts were made so as to include both tips of the burst opening. Each sample examined by Scanning Electron Microscopy (SEM) was blown with a jet of dry oil-free air to minimize non-conductive particulates from the fracture surfaces that would otherwise collect an electrical charge (and thus hinder the view) during the SEM examination.

### **6.2 Procedure**

Observations made during the SEM examination were documented with micrographs. A TESCAN LYRA Scanning Electron Microscope was used for the fractography examination. Operation of the SEM followed the manufacturer's instruction. ASTM has not published procedures for fractography examinations. However, surfaces examined by SEM in accordance with accepted scientific principles and EPRI guidelines can be compared with fractographs presented in various fractography textbooks, such as "Metals Handbook, Volume 12, Fractography," 9<sup>th</sup> Edition, American Society of Metals, 1985.

SEM fractographs were taken of the entire fracture surface of each burst opening. These fractographs were then aligned end to end to complete a photomontage of each crack surface. The photomontage was obtained using the back-scattered electron SEM detector. The depth of the corrosion was measured at selected intervals, providing a set of depth vs. axial location measurements. The depths were converted to percent throughwall (%TW) values by dividing the depth measurement by the nominal wall thickness of 50 mils.

Fractographs were taken of selected locations at higher magnifications to characterize the crack morphology. Crack characterization was performed using the secondary electron SEM detector.

### **6.3 Fractography Depth Profiles**

The four burst openings that occurred in regions of freespan tubing were confirmed to have no corrosion. The remaining two burst openings that occurred on the TSP regions in section R19C38-3B (02H) and R24C41-6B (04H) both had corrosion within each TSP region. No corrosion was observed outside of a TSP region.

Each burst opening was cut from its tube so as to include both the upper burst tip and the lower burst tip in the same sample. Figure 6-1 and Figure 6-2 show low magnification views of the burst opening fractography photomontages for R19C38-3B (02H) and R24C41-6B (04H), respectively. Because of the length of each image, the photomontage was split in two with some overlap. The top of the burst opening is shown in the upper end of the left photomontage and the bottom of the burst opening is shown in the lower end of the right photomontage.

The depth profiles of the cracks in these two burst openings are shown in Figure 6-3 and Figure 6-4, respectively. Crack depth measurements were taken along the axial direction of the burst

opening, starting at the lowest elevation of the burst opening (bottom of the sample, located at the bottom tip of the burst opening) and proceeding up the tube, in the axial direction, to the upper tip of the burst opening. Figure 6-1 shows how one crack depth measurement was obtained at the indicated distance from the bottom of the sample.

Table 6-1 provides a summary of the depth profiles for the burst openings. R19C38-3B (02H) had the deepest corrosion, at 49.9%TW. The burst opening of R24C41-6B (04H) had a maximum depth of corrosion of 48.6%TW.

#### 6.4 Crack Surface Characterization

Figure 6-5 presents an example of the crack surface of the R19C38-3B burst opening. The surfaces having the rock candy appearance is intergranular cracking - the part of the tube wall that occurred during in-service operation. The dimpled surface is ductile tearing - the part of the tube wall that failed during the burst test. Figure 6-6 presents another region of the fracture surface with intergranular cracking. These surfaces are typical of the burst opening.

Figure 6-7 shows the OD surface of R19C38 02H near the burst opening. In this view, the axial direction is horizontal. This fractograph montage shows several secondary axial cracks with some minor branching and a small patch of intergranular attack (IGA). All of the secondary cracks are intergranular. This surface is typical of axial OD initiated stress corrosion cracking (ODSCC).

Figure 6-8 shows an area on the crack surface of the R24C41-6B burst opening. The fracture surface consists of intergranular cracking (the rock candy topography) and ductile tearing. The figure shows a higher magnification view of the intergranular fracture surface. This example is typical of the burst opening fracture surface.

Figure 6-9 shows the OD surface of R24C41 04H near the burst opening. In this view, the axial direction is horizontal. This fractograph montage shows several secondary axial cracks and some patches of shallow intergranular attack (IGA). This surface is typical of axial ODSCC.

The corrosion observed on all surfaces was intergranular; there was no evidence of transgranular cracking.

Table 6-1: Summary of Burst Opening Depth Profiles

Section	Region of Burst	Crack Length (in)	Maximum Depth (%TW)
R19C38-3B	02H	0.702	49.9
R19C38-4B	Freespan	0	0
R24C41-3B	Freespan	0	0
R24C41-5B	Freespan	0	0
R24C41-6B	04H	0.270	48.6
R24C41-7B	Freespan	0	0

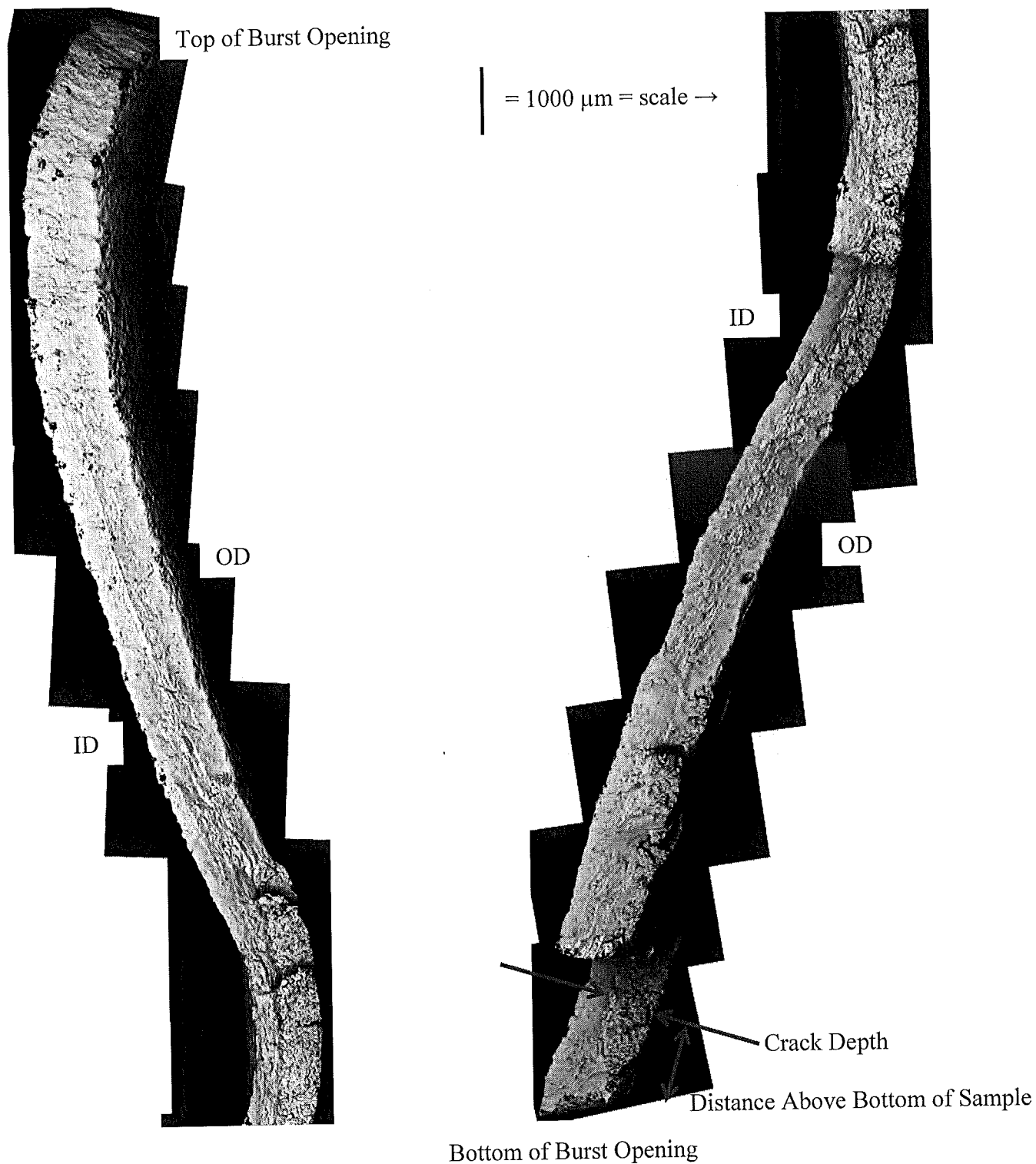
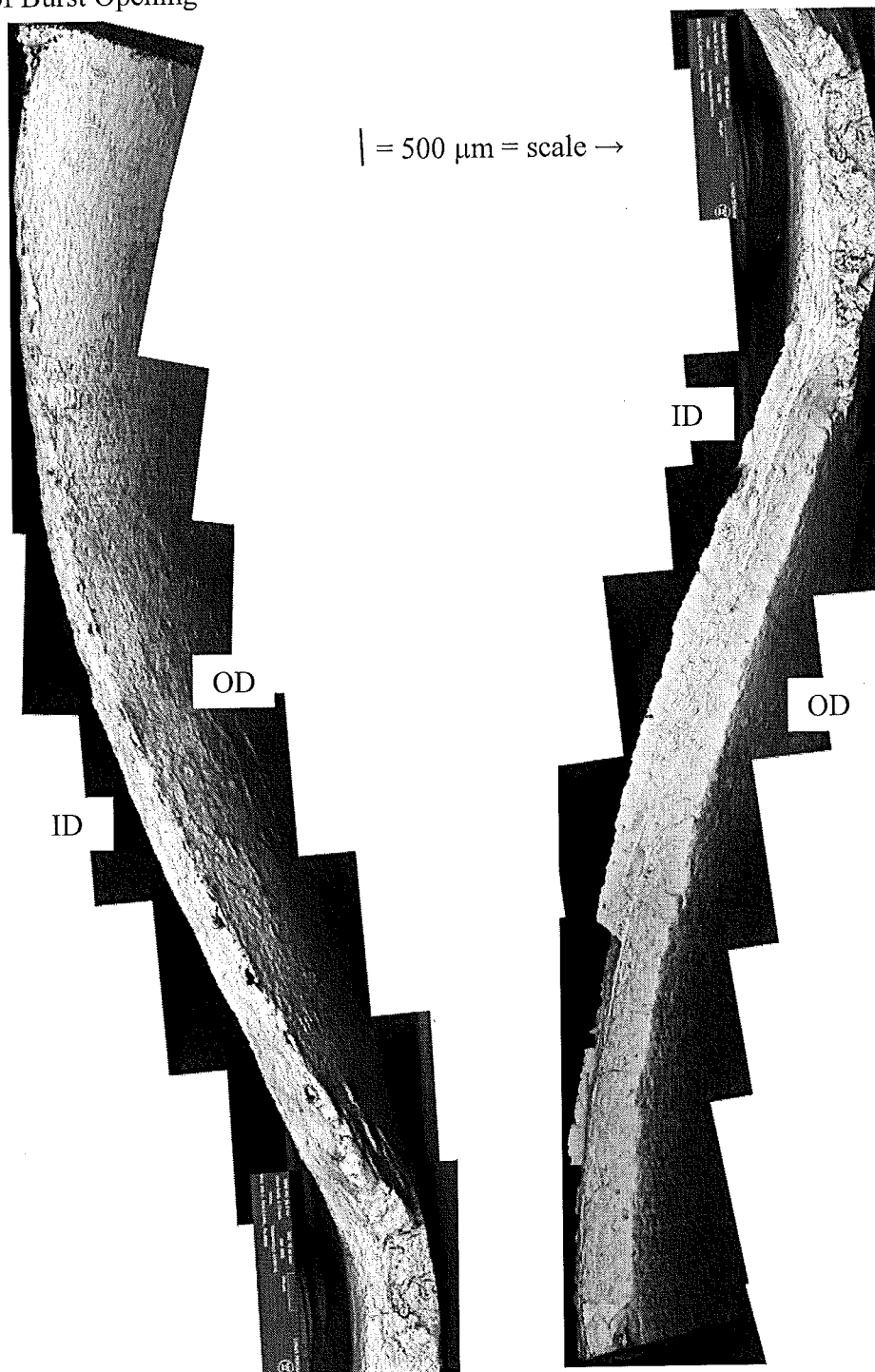


Figure 6-1: SEM Photomontage of R19C38-3B (02H) Burst Opening

Top of Burst Opening



Bottom of Burst Opening

Figure 6-2: SEM Photomontage of R24C41-6B (04H) Burst Opening

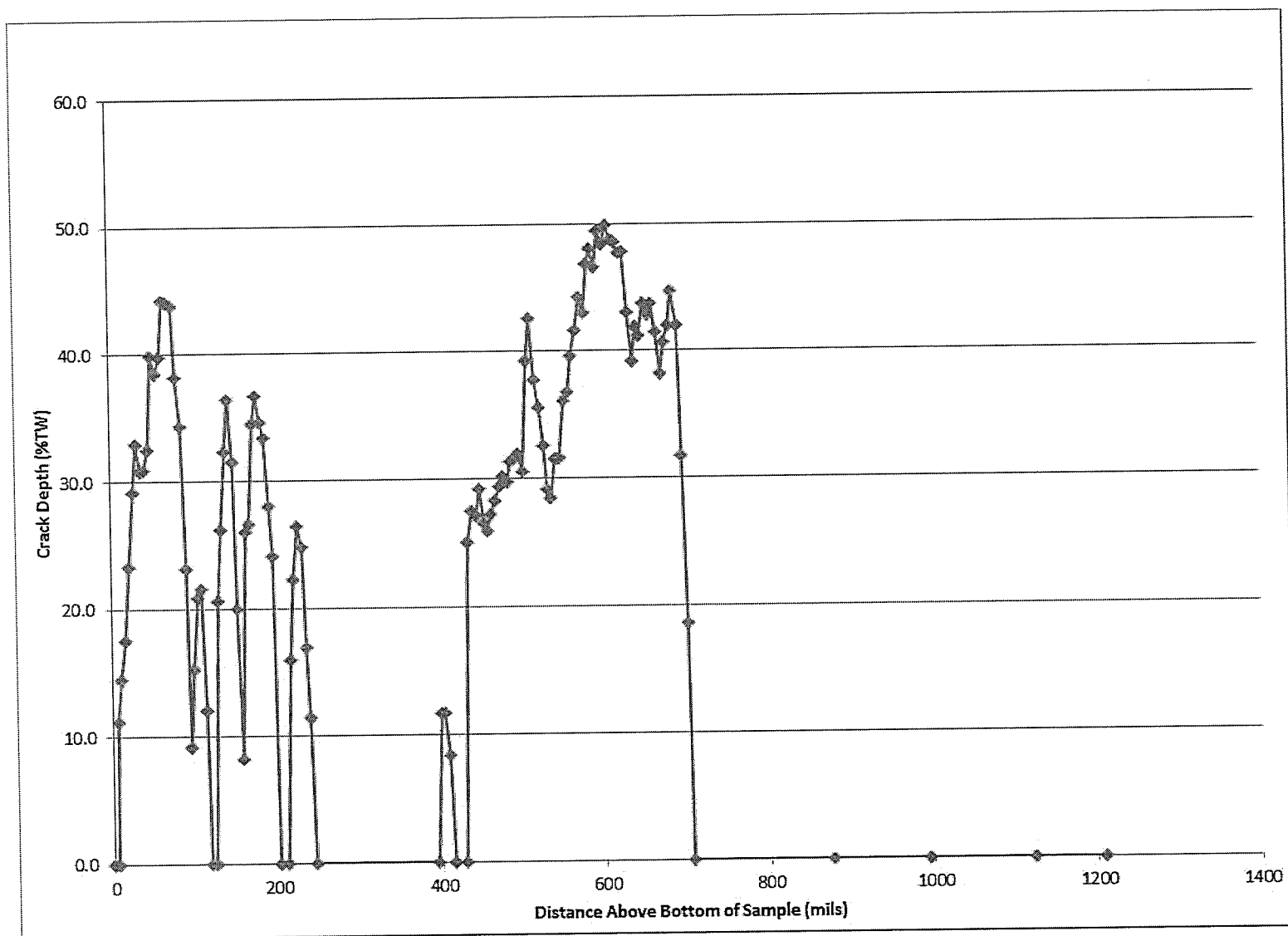


Figure 6-3: R19C38-3B (02H) Burst Opening Depth Profile

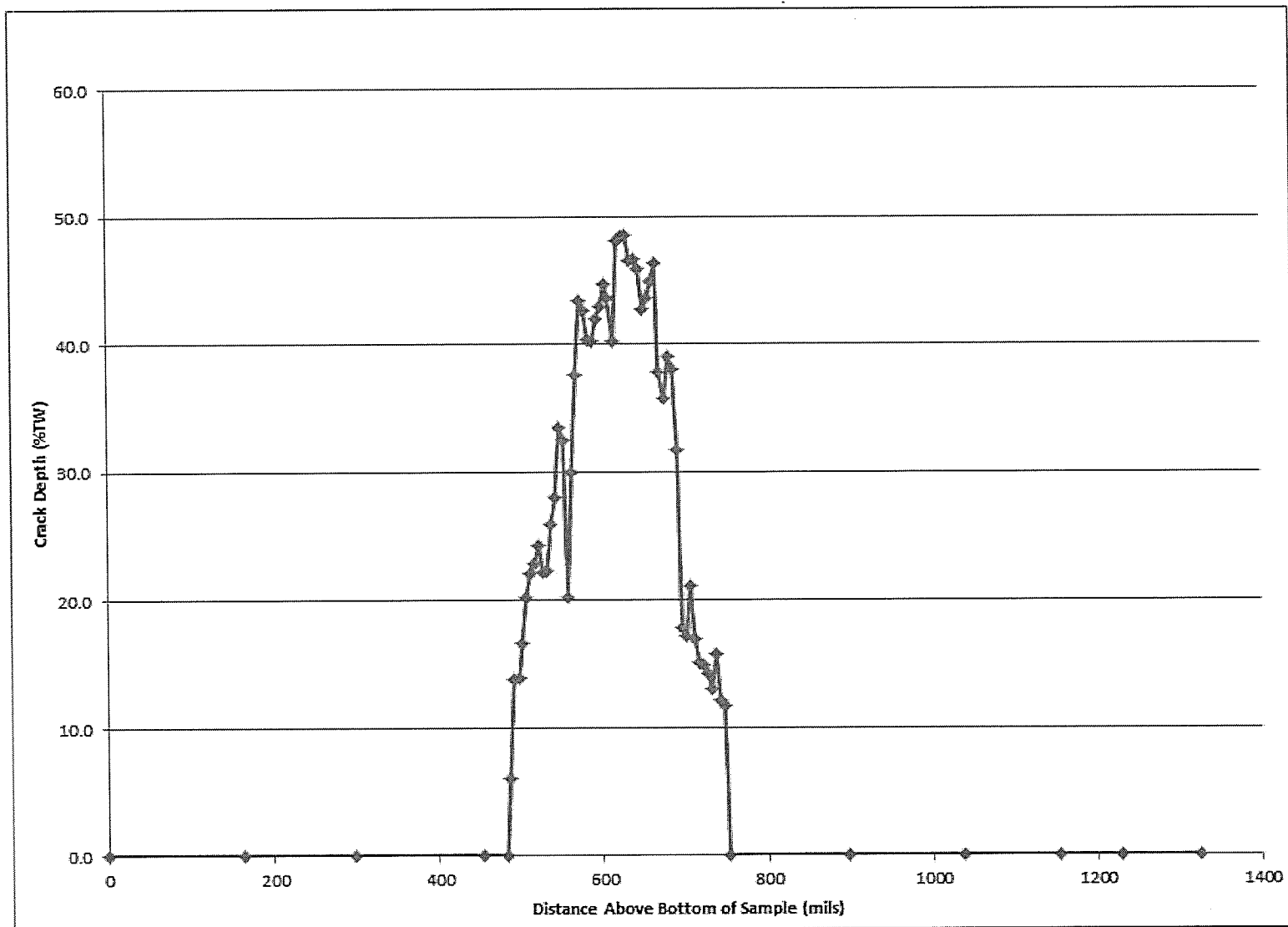
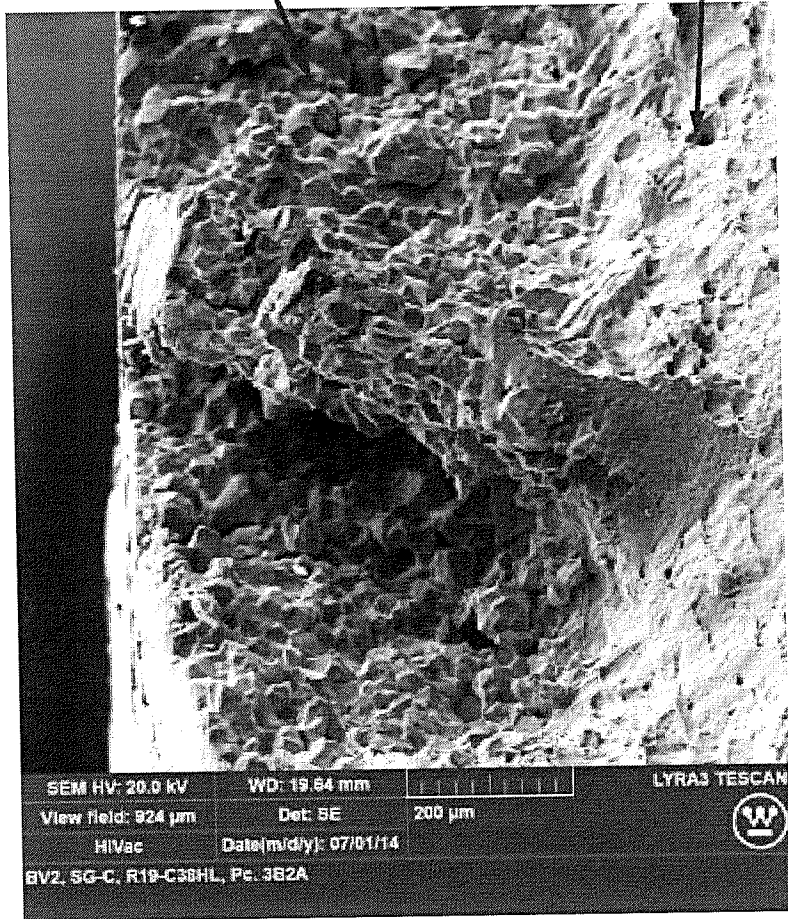


Figure 6-4: R24C41-6B (04H) Burst Opening Depth Profile

Intergranular Cracking ("Rock Candy" Surface)

Ductile Tearing



Intergranular Cracking ("Rock Candy" Surface)

Ductile Tearing

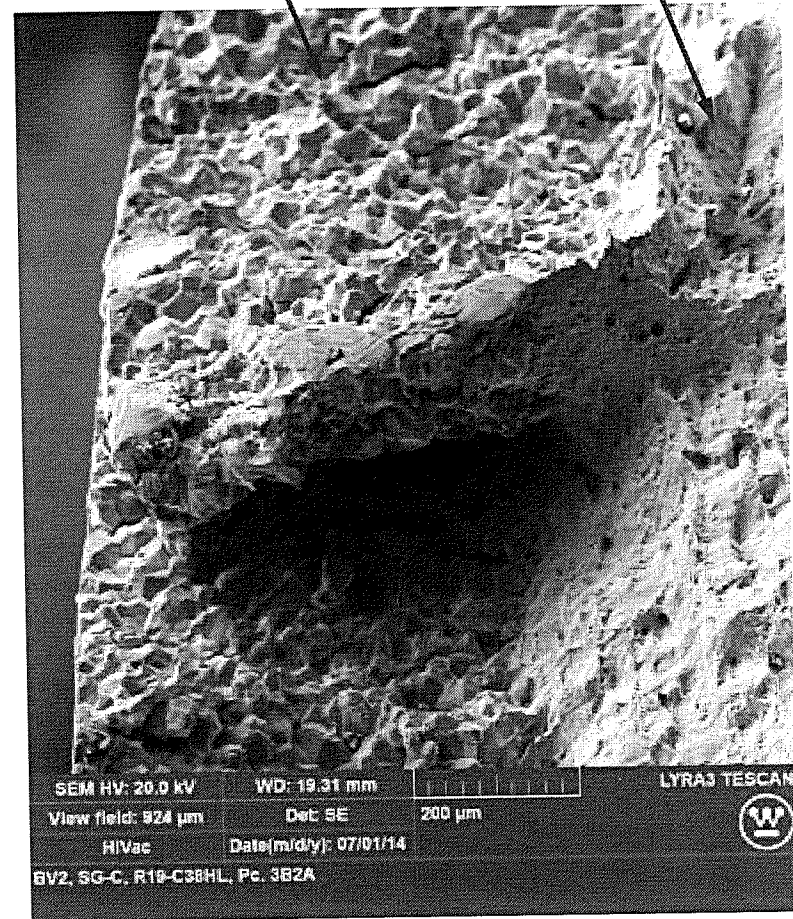


Figure 6-5: Example of R19C38-3B Burst Opening Fracture Surface (Near Top End of Crack)



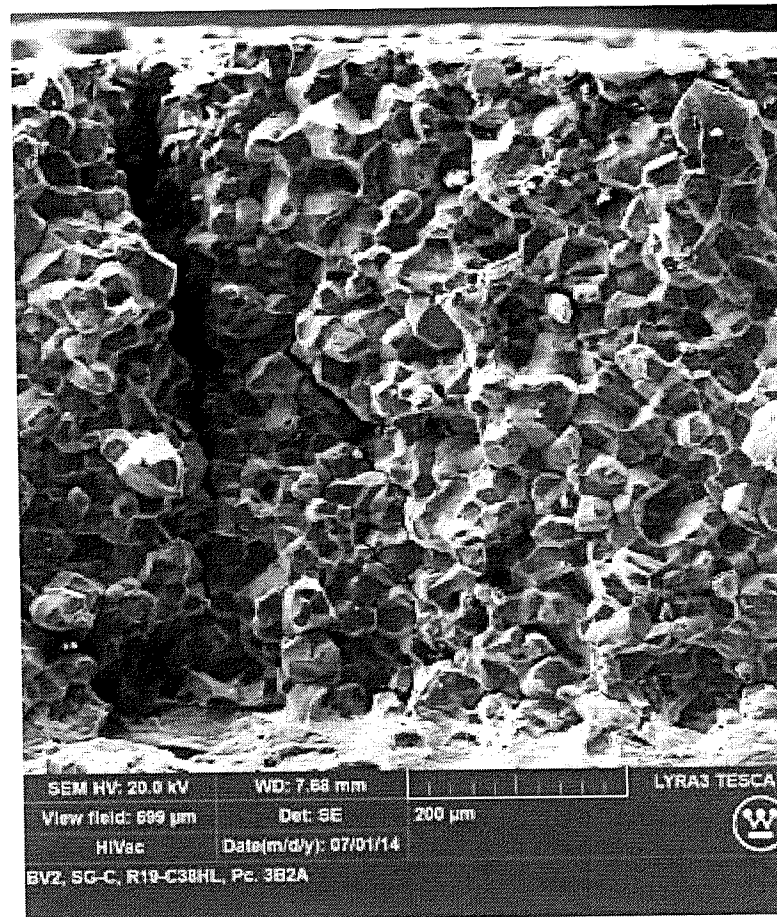


Figure 6-6: Example of R19C38-3B Burst Opening Fracture Surface (Center of Crack)

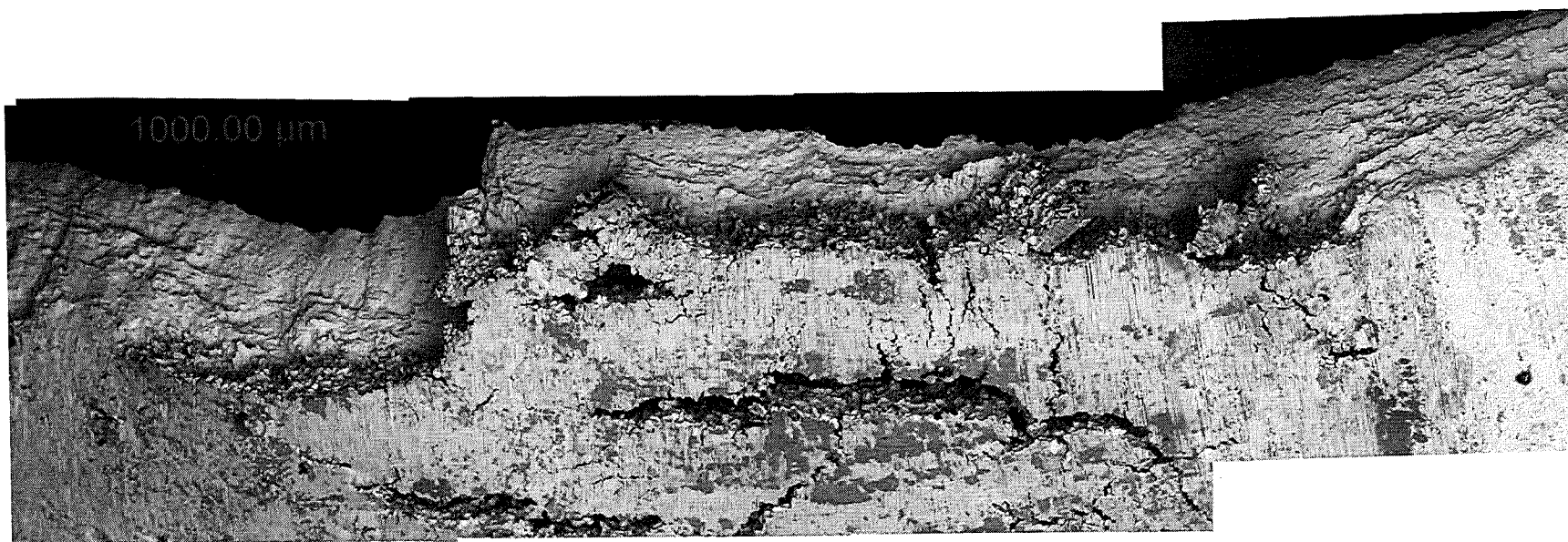


Figure 6-7: OD Surface of R19C38 02H, Adjacent to Burst Opening (Axial Direction is Horizontal)

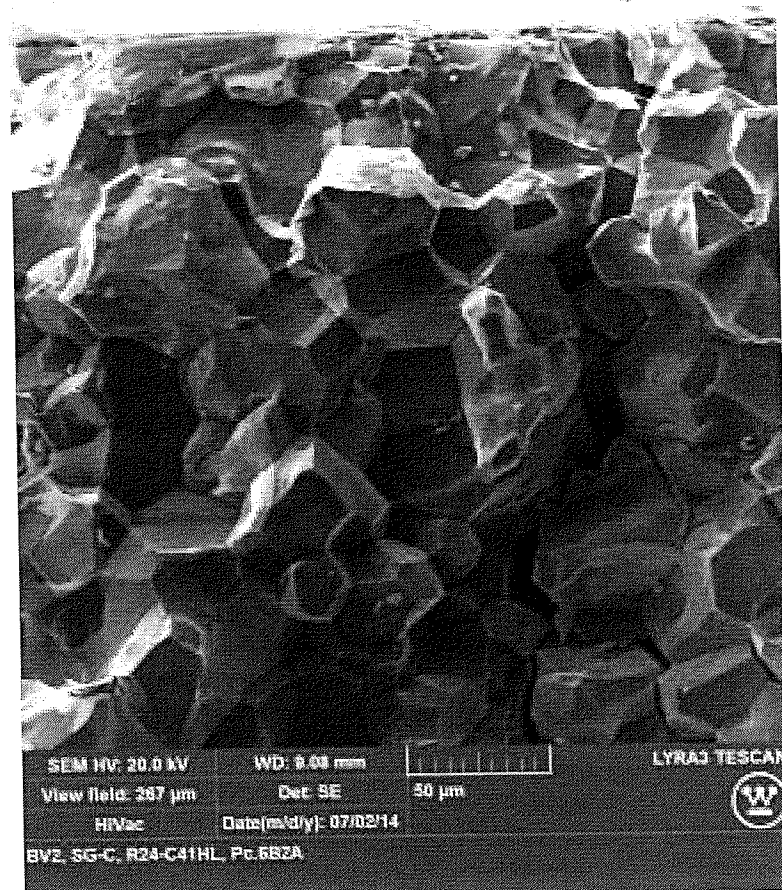
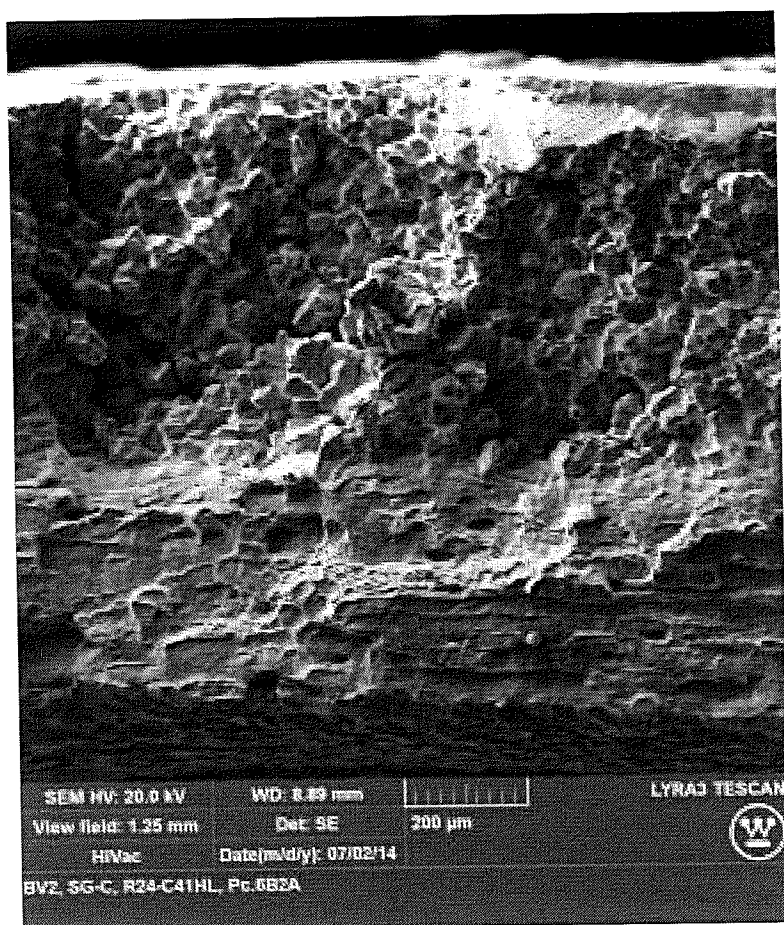


Figure 6-8: Example of R24C41-6B Burst Opening Fracture Surface

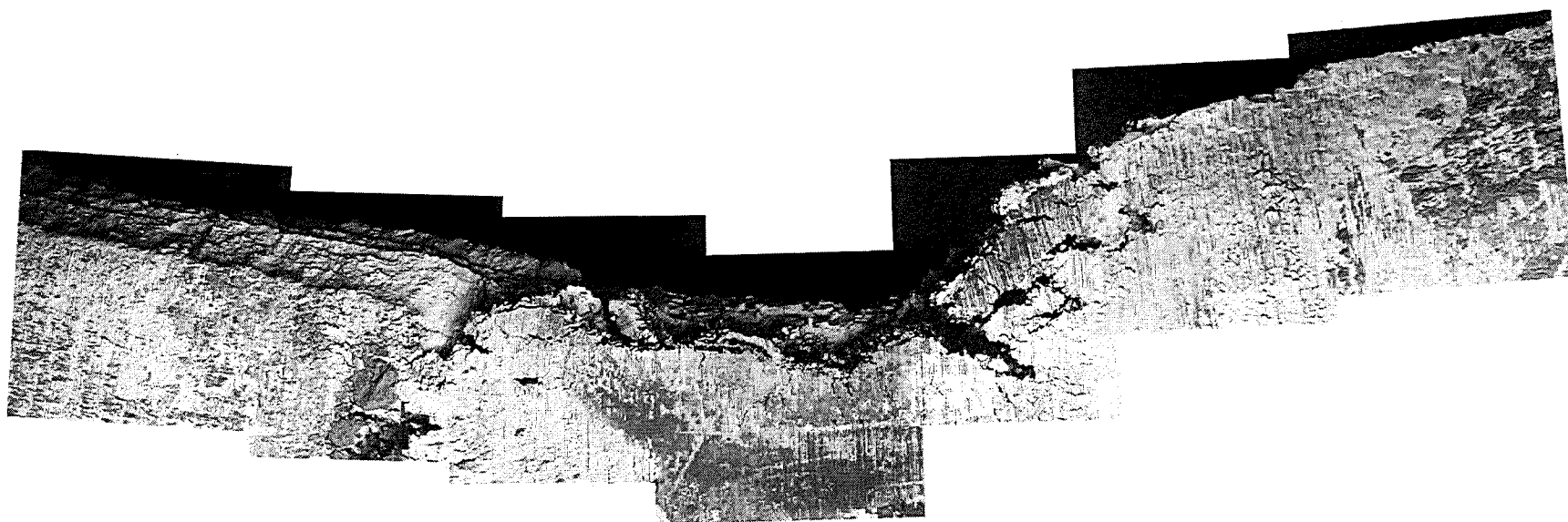


Figure 6-9: OD Surface of R24C41 04H, Adjacent to Burst Opening (Axial Direction is Horizontal)

## 7.0 METALLOGRAPHY OF CRACKS

### 7.1 Procedure

One transverse section was taken from each of the support plate regions. Table 7-1 summarizes the defect metallography samples.

The metallographic samples were mounted in epoxy to show the cracks in cross-section. Each mounted sample was ground with SiC papers, followed by diamond wheels using polishing oil, followed by diamond aerosol sprays, leaving the edge to be examined with a mirror finish. Samples were then examined and photographed after an electrolytic Nital etch. The electrolytic Nital etch was used to highlight the relationship between the cracks and the grain boundaries.

### 7.2 R19C38 02H

Figure 7-1 shows a view of a transverse cross-sectional sample (3B2B) taken from the 02H TSP of R19C38. The gap in the circumference is the SEM sample (refer to the Figure 5-1 sectioning diagram). The left side of the burst opening is just to the left of the '2' mark in the figure.

At this elevation of the TSP, there were only two areas, other than the burst opening, that showed any sign of corrosion; these are indicated by the number markers in Figure 7-1. The '1' marker is where the cracks at the 200° azimuthal location were identified (see Figure 4-14 and Figure 4-17). The number '2' marker is associated with the cracks near the 340° location (see Figure 4-14). Cracks near the 0° location are on the SEM sample and the cracks near the 280° location were very short and were not captured in this cross section.

Figure 7-2 shows a closer view of the cracks at the 200° location. The cracks have been widened by the swelling of the tube during the burst test. Cracking is intergranular without signs of IGA and are thus intergranular stress corrosion cracks (IGSCC). As these initiate from the outer surface, they are also ODSCC. The figure shows several cracks, two of which break the OD surface at this elevation and two cracks which break the OD surface at another elevation that is not shown in this view. The deepest of these (the middle crack) is 25.7%TW.

Figure 7-3 shows a crack at the 340° location, as well as the left side of the burst opening. The 340° crack is 22.9%TW and the crack depth of the burst opening is approximately 27%TW at this elevation. The figure also shows two other cracks which break the OD surface at another elevation that is not shown in this view.

### 7.3 R24C41 02H

Figure 7-4 shows a view of a transverse cross-sectional sample (3B2) taken from the 02H TSP of R24C41. As the burst occurred outside of the TSP region, the entire circumference is shown. The "O" that is inside the tube corresponds with the 0° location (since the view is in the down direction, azimuthal locations proceed in the counter-clockwise direction. This elevation was chosen to show the cracks at about the 170° location and the patch of shallow corrosion on both sides of 0° (see Figure 5-3 and Figure 4-18). The '1' marker is located at about 20°, the '2' marker is at about 160° and '3' marker is located at about the 340° location.

Figure 7-5 shows the 20° location of Marker '1'. It shows two shallow axial ODSCC, without any IGA. The maximum depth shown is 11.3%TW.

Figure 7-6 shows the 160° location of Marker '2'. It shows three shallow axial ODSCC, without any IGA. The maximum depth shown is 14.2%TW.

Figure 7-7 shows the 340° location of Marker '3'. It shows two shallow axial ODSCC, without any IGA. The maximum depth shown is 10.7%TW.

#### 7.4 R24C41 03H

Figure 7-8 shows a view of a transverse cross-sectional sample (5B2) taken from the 03H TSP of R24C41. As the burst occurred outside of the TSP region, the entire circumference is shown. The "O" that is inside the tube corresponds with the 0° location (since the view is in the down direction, azimuthal locations proceed in the counter-clockwise direction). This elevation was chosen to show the cracks at the 180° location and the patch of shallow corrosion (see Figure 5-4 and Figure 4-20). The '1' marker is located at about 180°.

Figure 7-9 shows the cracks at the 180° location. The cracks are intergranular, but are shallow. These are only 2-4 grains deep. The deepest crack in this view is 4.4%TW.

#### 7.5 R24C41 04H

Figure 7-10 shows a view of a transverse cross-sectional sample (6B2B) taken from the 04H TSP of R24C41. The gap in the circumference is the SEM sample (refer to the Figure 5-5 sectioning diagram). The left side of the burst opening is just to the right of the '1' mark in the figure, and the "O" that is inside the tube corresponds with the 0° location (since the view is in the down direction, azimuthal locations proceed in the counter-clockwise direction).

As the mid-plane of the visual observation map shows (Figure 4-23), there were several patches of cracks around the mid-plane of the 04H TSP. There were small cracks at the 80° location (Marker '1'), the 40° location (Marker '2'), and larger cracks in the 315°-360° range (Markers '3', '4' and '5').

Figure 7-11 shows the 80° location of Marker '1'. It shows several axial ODSCC cracks with a patch of shallow (<2 grains deep) IGA. The maximum crack depth shown is 16.4%TW.

Figure 7-12 shows the 40° location of Marker '2'. It shows three axial ODSCC cracks, without any IGA. The maximum crack depth shown is 23.2%TW.

Figure 7-13 shows the 350° location of Marker '3'. It shows several axial ODSCC cracks, without any IGA. The maximum crack depth shown is 35.2%TW.

Figure 7-14 shows the 335° location of Marker '4'. It shows several axial deep ODSCC cracks, without any IGA. The maximum crack depth shown is 40.8%TW.

Figure 7-15 shows the 315° location of Marker '5'. It shows several axial deep ODSCC cracks, without any IGA. The maximum crack depth shown is 45.4%TW.

Many of the cracks in the 315°-360° region approached the maximum crack depth in the burst fracture (48.6%TW). Consequently, another three levels were examined. The mounted sample was ground/polished and etched another 5 mils, 14 mils and 20 mils further down the TSP region. The 350° orientation had a maximum depth of 46%TW at the 20 mil level (Figure 7-16).

Table 7-1: Defect Metallography Samples

Tube	TSP	Section	Mount#	View	Sectioning Diagram
R19C38	02H	3B2B	M3136	Transverse - Down	Figure 5-1
R24C41	02H	3B2	M3139	Transverse - Down	Figure 5-3
R24C41	03H	5B2	M3138	Transverse - Down	Figure 5-4
R24C41	04H	6B2B	M3137	Transverse - Down	Figure 5-5



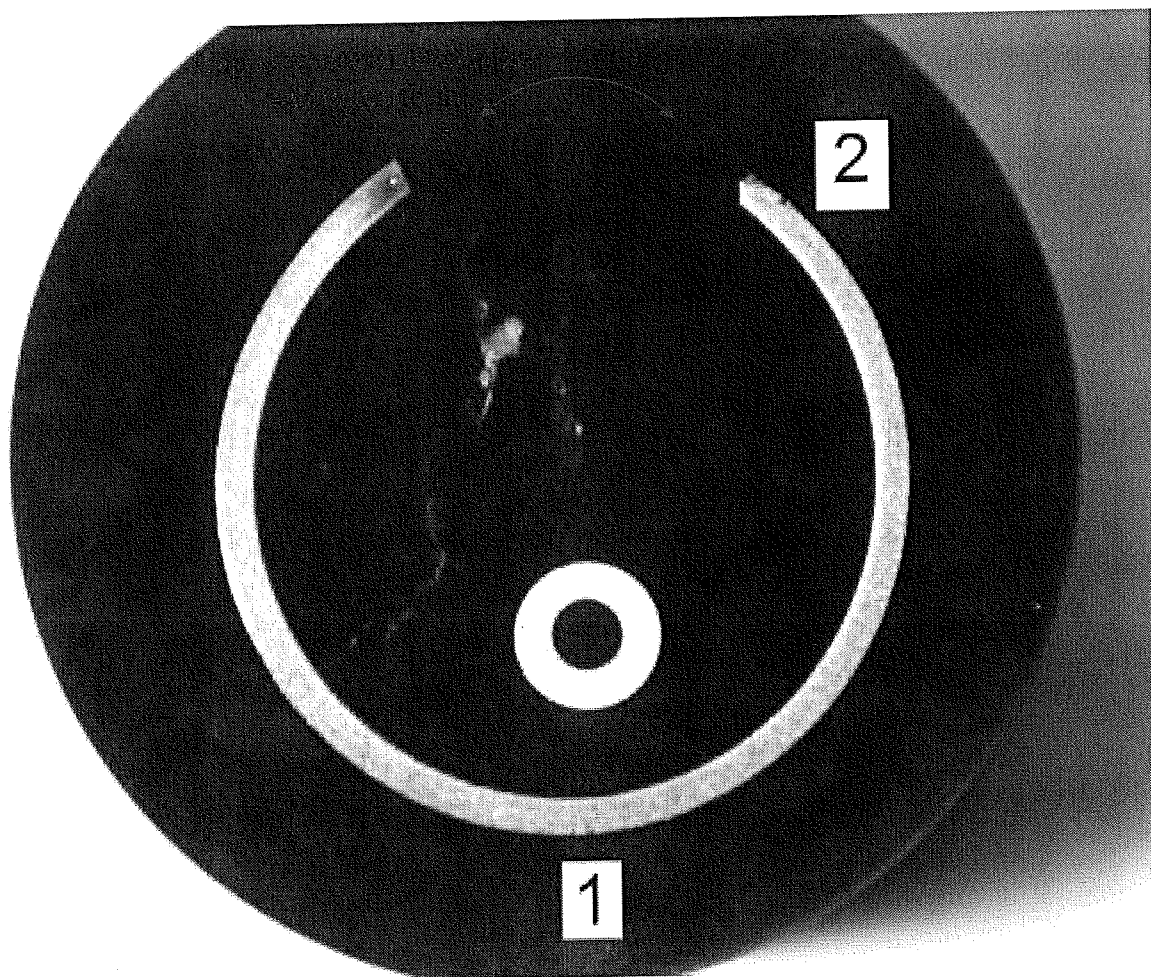


Figure 7-1: R19C38 02H - Overall View of Transverse Section

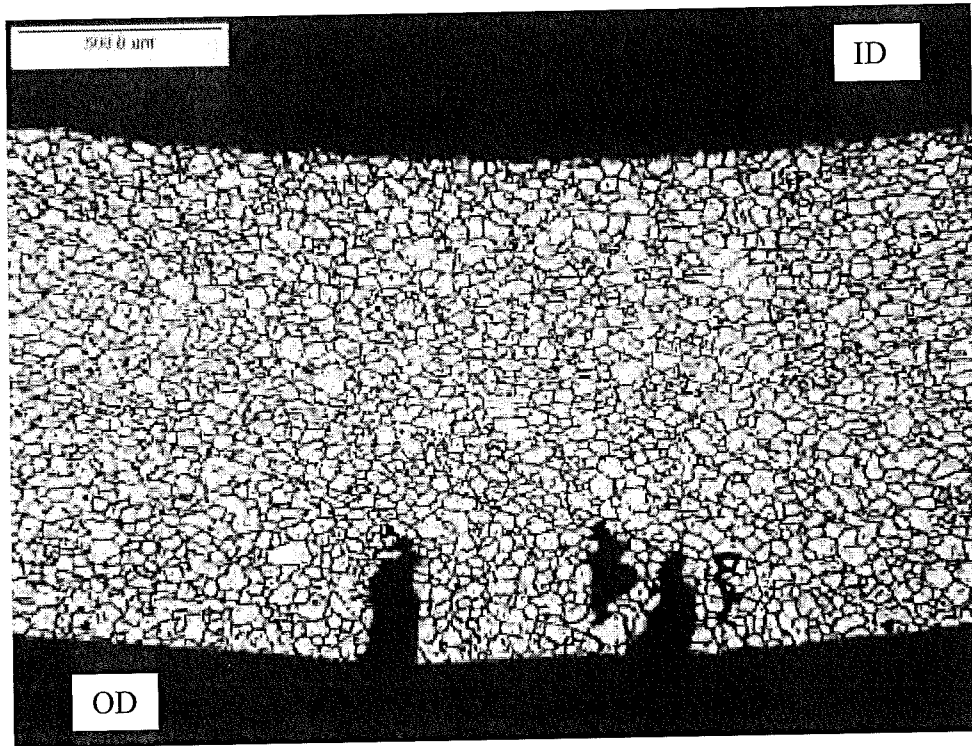


Figure 7-2: R19C38 02H Cracks at 200°

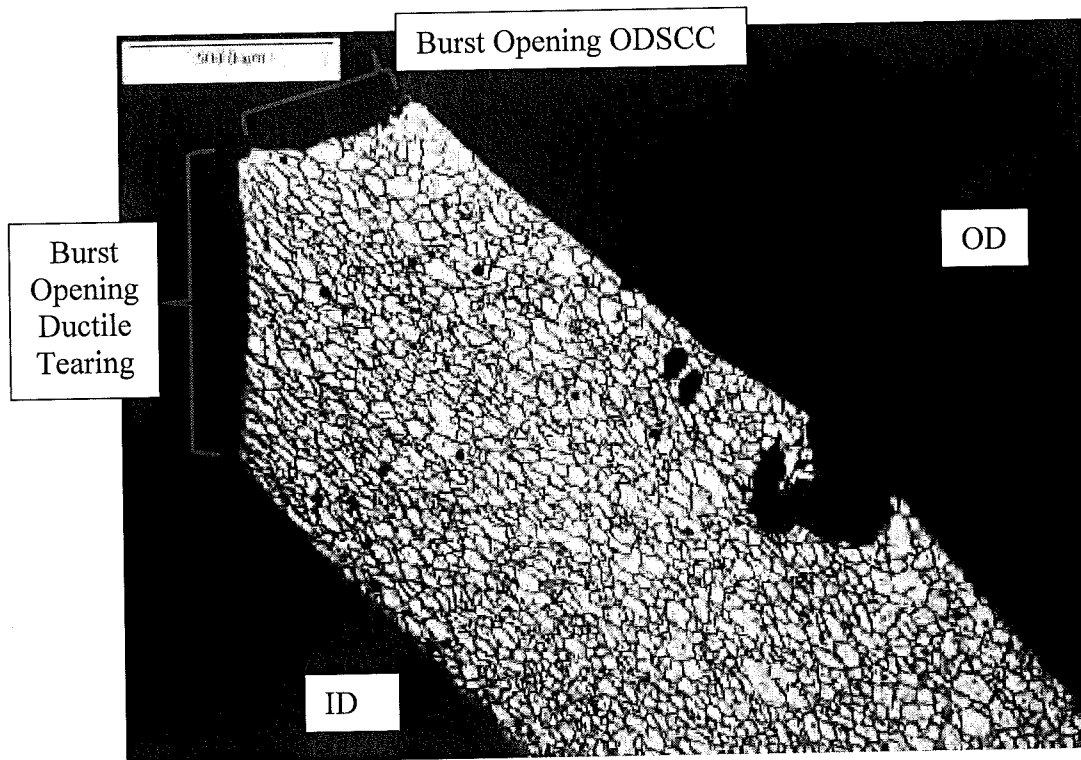


Figure 7-3: R19C38 02H Crack at 340°

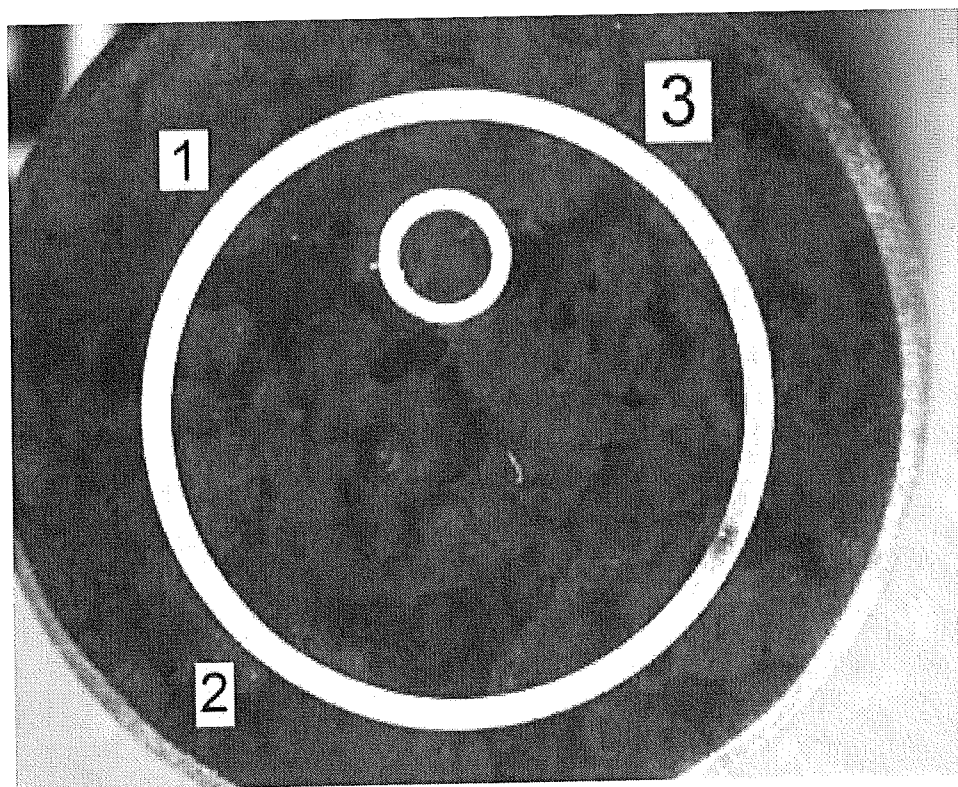


Figure 7-4: R24C41 02H - Overall View of Transverse Section

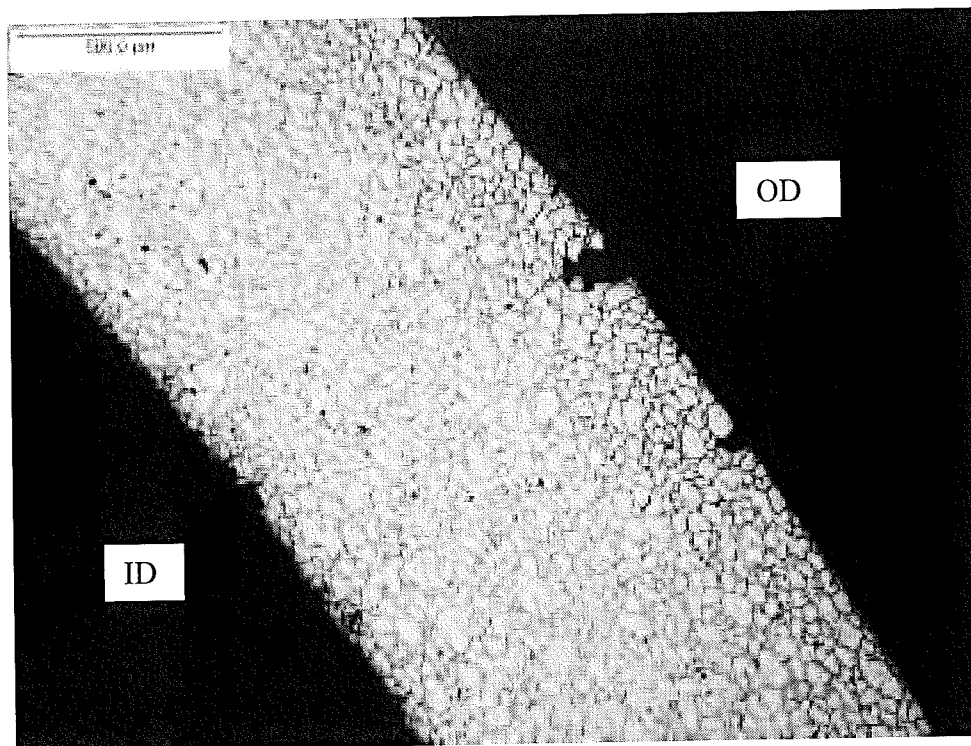


Figure 7-5: R24C41 02H Cracks at 20°

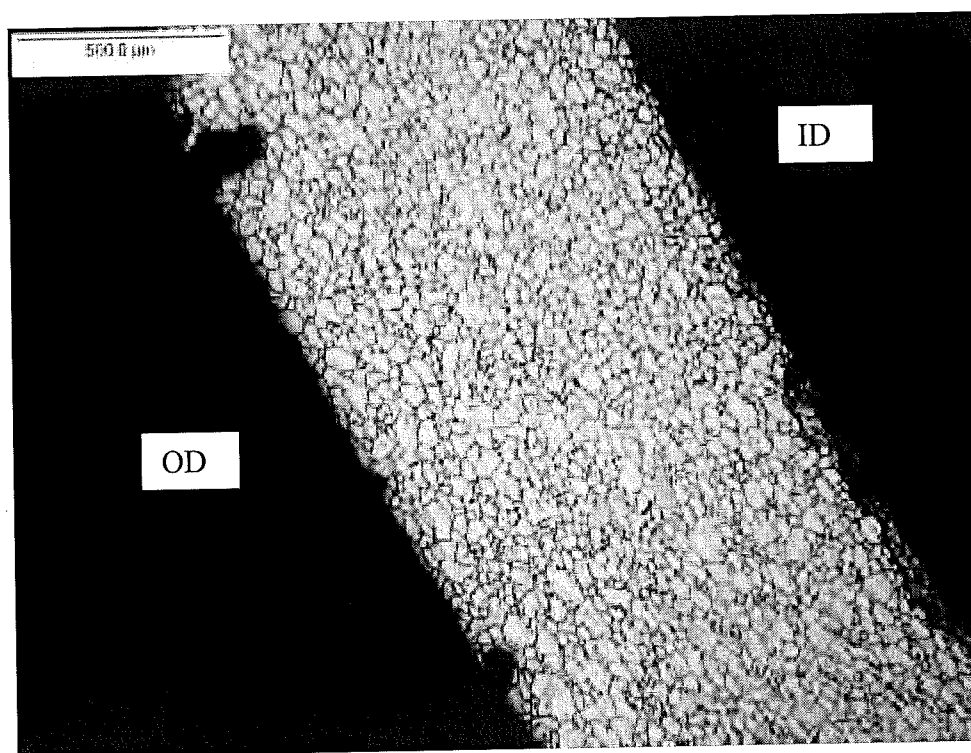


Figure 7-6: R24C41 02H Cracks at 160°

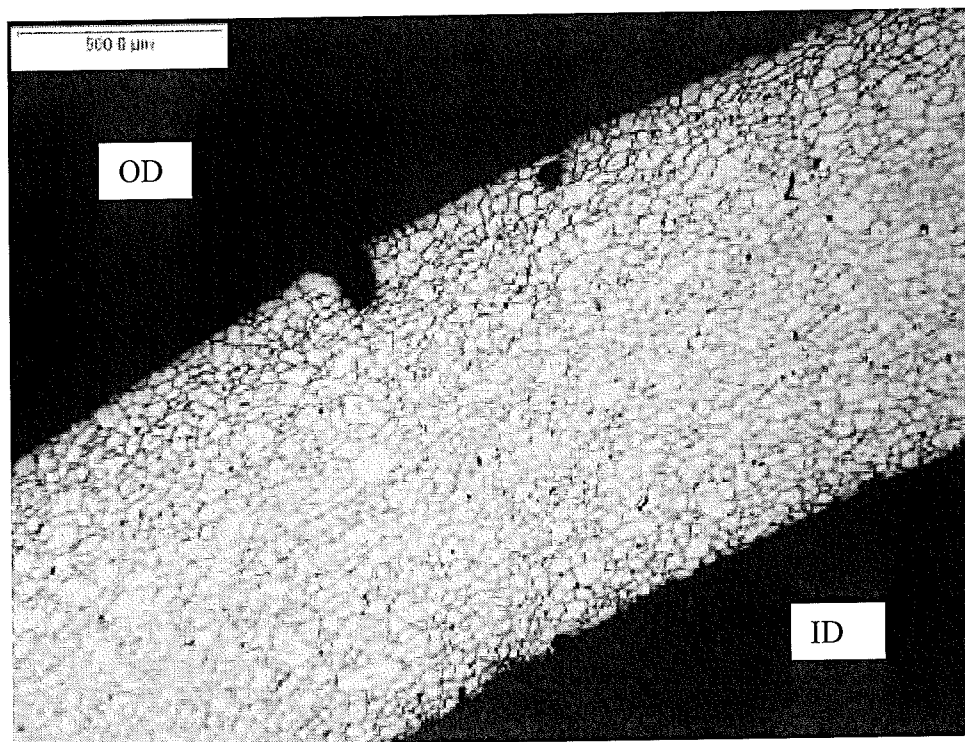


Figure 7-7: R24C41 02H Cracks at 340°

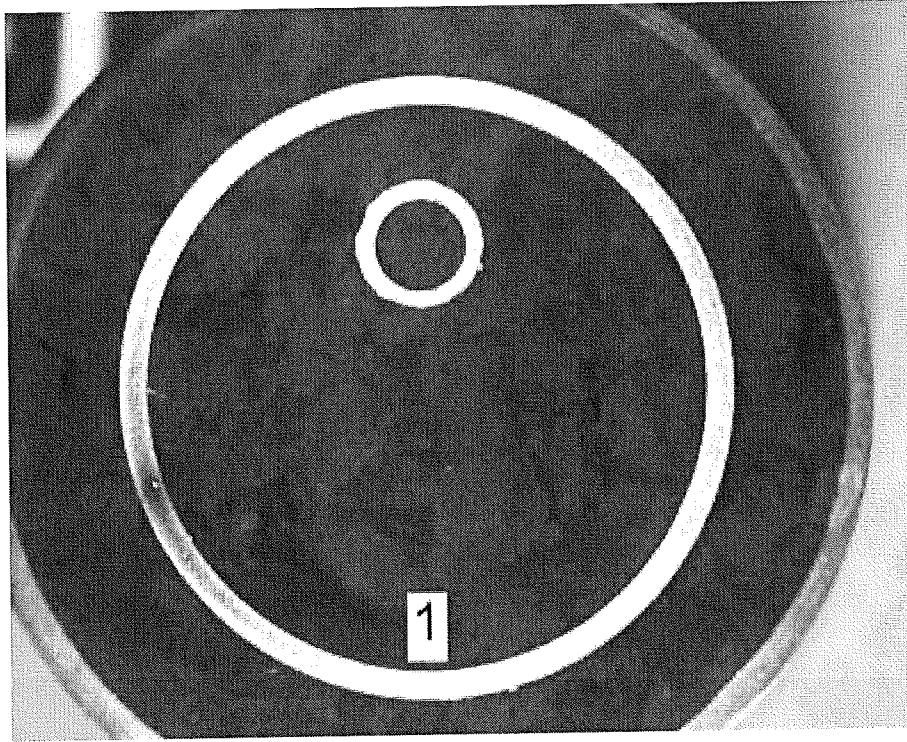


Figure 7-8: R24C41 03H - Overall View of Transverse Section

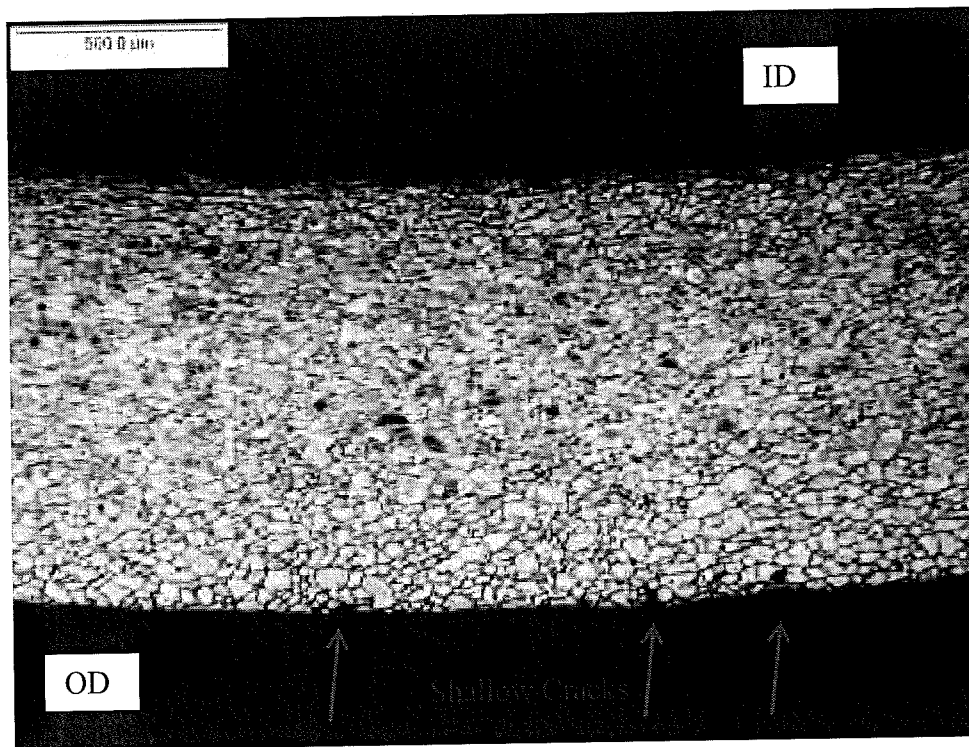


Figure 7-9: R24C41 03H Cracks at 180°



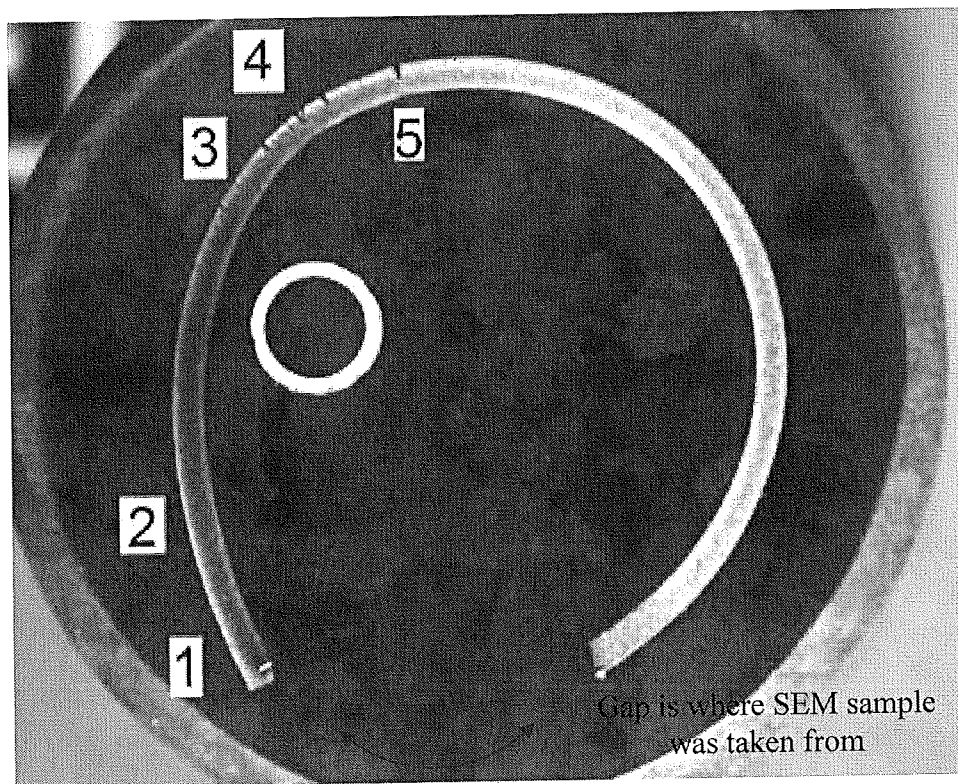


Figure 7-10: R24C41 04H - Overall View of Transverse Section

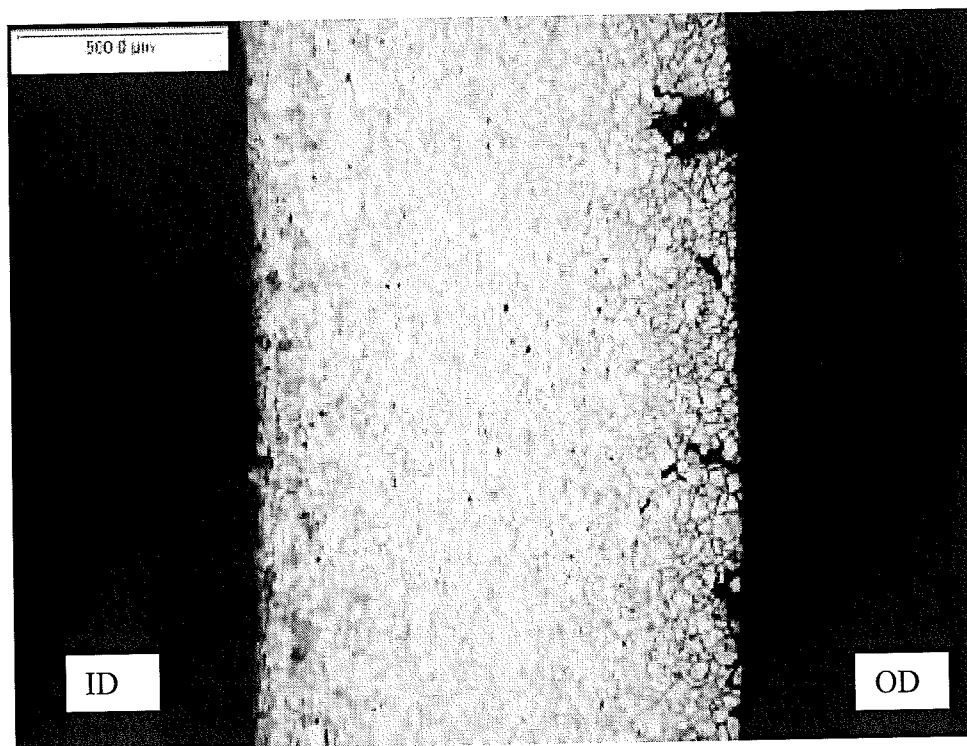


Figure 7-11: R24C41 04H Cracks at 80°

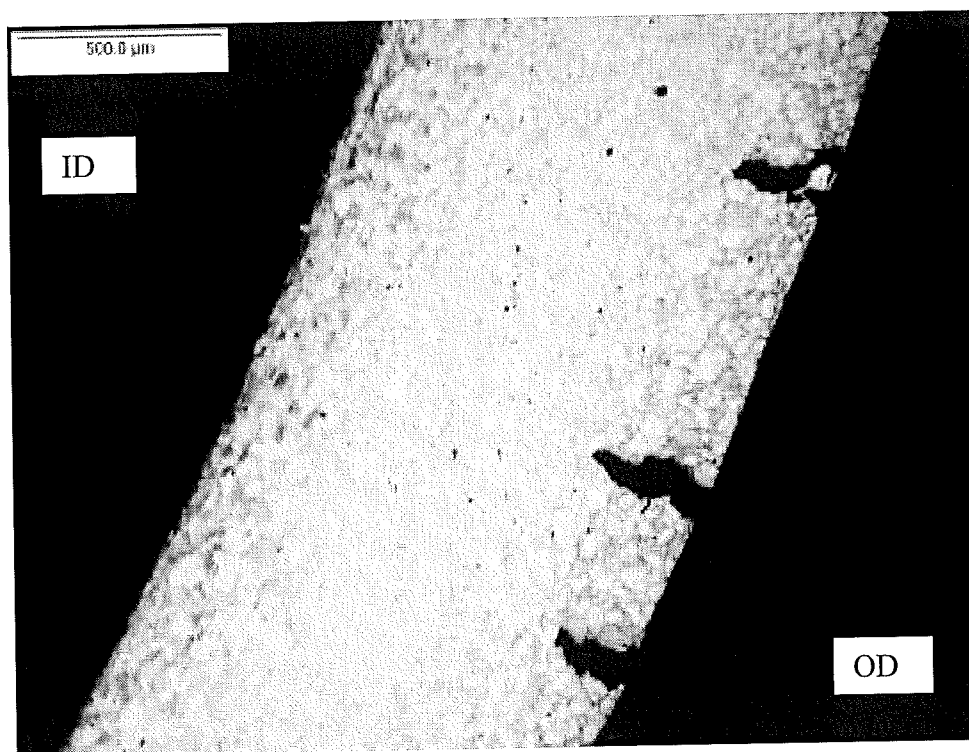


Figure 7-12: R24C41 04H Cracks at 40°



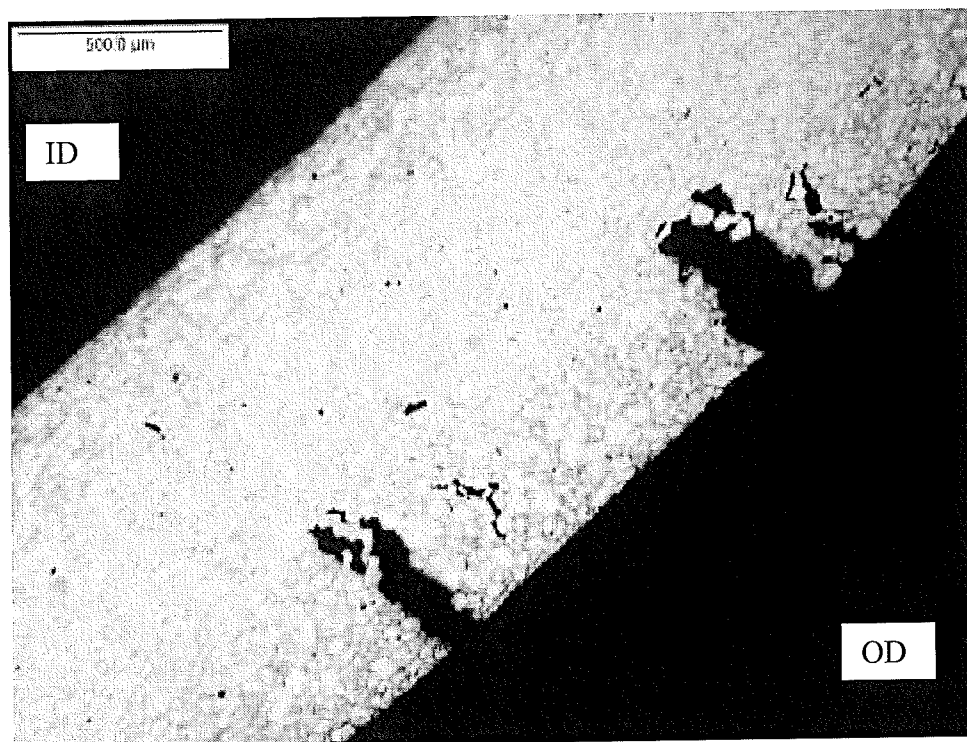


Figure 7-13: R24C41 04H Cracks at 350°

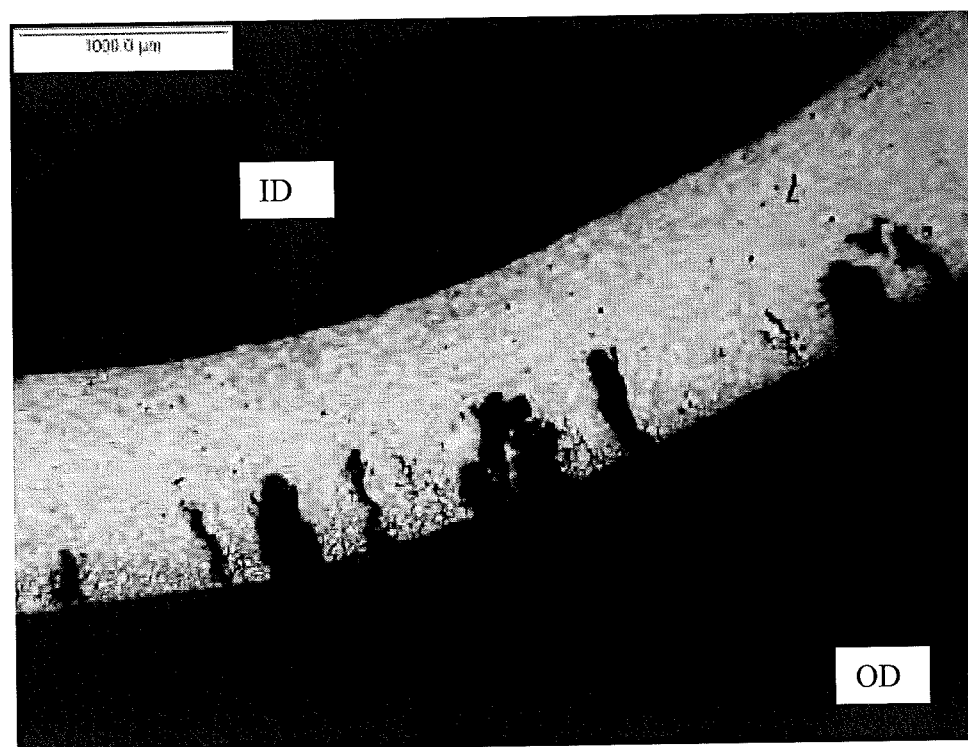


Figure 7-14: R24C41 04H Cracks at 335°

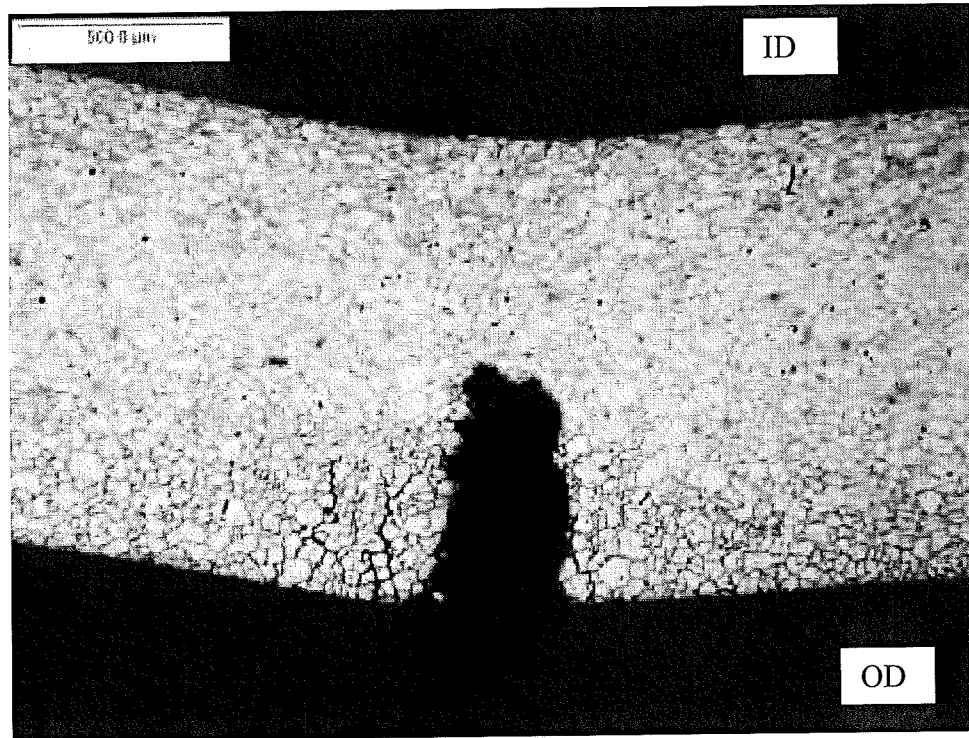


Figure 7-15: R24C41 04H Cracks at 315°

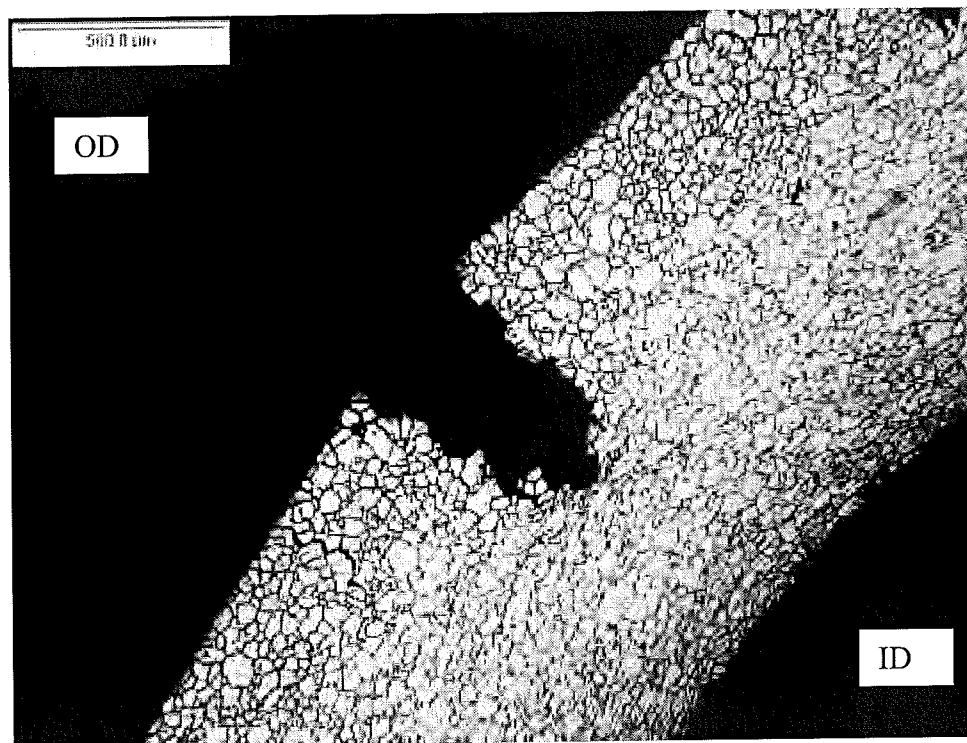


Figure 7-16: R24C41 04H Cracks at 350°, 20 mils Further Down the TSP from Figure 7-13

## 8.0 CONCLUSIONS

Hot leg TSP regions of Beaver Valley Unit 2 SG-C pulled tubes R19C38 and R24C41 were examined in the laboratory at WCS. The TSP regions were screened for leakage, were burst tested, and were examined by SEM and metallography to assess the morphology of their cracks.

Room temperature leak screening was conducted at pressures up to and including SLB pressure. None of the tubes that were pulled for laboratory examination leaked.

Room temperature burst tests were conducted on all of the TSP regions provided. All of the TSP regions had burst pressures far in excess of 3NOP. The lowest burst pressure was 9678 psig.

SEM and metallography examinations confirmed that corrosion in the TSP regions was predominantly axially orientated ODSCC with a few small and shallow patches of IGA. Cellular corrosion was not observed. There was no corrosion found outside of the TSP regions. The observed degradation is in accordance with the morphology criteria provided in Section 1.a of GL 95-05 (Reference 1). The observed degradation is consistent with the current GL 95-05 database (Reference 13).

All four TSP regions that were pulled for laboratory examination had some degree of corrosion.

The two TSP regions that had confirmed bobbin coil indications (R19C38-02H and R24C41-04H) had the deepest cracking. The R19C38-02H TSP had a maximum crack depth of 49.9%TW. The R24C41-04H TSP had a maximum crack depth of 48.6%TW located within the burst fracture, but there was another region of multiple axial cracks that were nearly as deep (maximum measured depth of 46.0%TW).

The two TSP regions that did not have confirmed bobbin coil indications (R24C41-02H and R24C41-03H) had shallower cracks. The R24C41-02H TSP had a maximum crack depth of 14.2%TW. The R24C41-03H TSP had a maximum crack depth of 4.4%TW.

## 9.0 REFERENCES

1. NRC Generic Letter 95-05, "Voltage-Based Repair Criteria for Westinghouse Steam Generator Tubes Affected by Outside Diameter Stress Corrosion Cracking," USNRC Office of Nuclear Reactor Regulation, August 3, 1995.
2. "Beaver Valley Unit 2 End-of-Cycle 17 Analysis and Prediction for End-of-Cycle 18 Voltage-Based Repair Criteria 90-Day Report," Latest Revision, SG-SGMP-14-17.
3. "Beaver Valley Unit 2 Model 51M Steam Generator Secondary Side Tube Support Plate Elevations for Eddynet Confirmation," DLC-98-768 / NSD-CPM-98-142, August 25, 1998.
4. "Transmittal of LTR-CCOE-14-54 'Pulled Tubes Receipt'," FENOC-14-41, June 3, 2014.
5. "Steam Generator Tube Sample Identification," Churchill Site Level 3 Work Instruction CS-W-9.19, Revision 0, June 2014.
6. "Beaver Valley Power Station Unit 2 2R17 Refueling Outage Steam Generator Degradation Assessment," SG-SGMP-14-4, March 2014.
7. "Leak Screening of Steam Generator Tubing," Churchill Site Level 3 Work Instruction CS-W-14.32, Revision 0, June 2014.
8. "Steam Generator Tubing Burst Testing and Leak Rate Testing Guidelines," Revision 0. EPRI, Palo Alto, CA: 2002. 1006783.
9. "Steam Generator Program Guidelines," NEI 97-06 Revision 3, March 2011.
10. "Steam Generator Management Program: Steam Generator Integrity Assessment Guidelines," Revision 3. EPRI, Palo Alto, CA: 2009. 1019038.
11. "Burst Testing of Steam Generator Tubing," Churchill Site Level 3 Work Instruction CS-W-14.31, Revision 0, June 2014.
12. "Steam Generator Information Report," LTR-SGDA-11-189, Revision 0, August 2011.
13. "Steam Generator Tubing Outside Diameter Stress Corrosion Cracking at Tube Support Plates Database for Alternate Repair Limits," Addendum 7 to NP-7480-L Database. EPRI, Palo Alto, CA: 2008. 1018047.